

Deakin University
Access to Thesis.



Peter G Mohr is the author of the thesis entitled :

**‘Absciscic acid regulation of plant defence responses
during pathogen attack’.**

This thesis may be made available for consultation, loan and limited copying for the purpose of study and/or research in accordance with the Copyright Act 1968 [Australia].

This thesis was submitted for the degree of **Doctor of Philosophy** and is the result of the authors own research, except where otherwise acknowledged, and that the thesis in whole or part has not been submitted for an award including a higher degree to any other university or institution.

**ABSCISIC ACID REGULATION OF PLANT
DEFENCE RESPONSES DURING PATHOGEN
ATTACK**

by

Peter G. Mohr

Bachelor of Science (Biological Science) (Honours)

**Submitted in fulfilment of the requirement for the degree of
Doctor of Philosophy**

Deakin University

March, 2004

Volume One

DEAKIN UNIVERSITY
CANDIDATE DECLARATION



I certify that the thesis entitled

ABSCISIC ACID REGULATION OF PLANT DEFENCE RESPONSES DURING
PATHOGEN ATTACK

submitted for the degree of

DOCTOR OF PHILOSOPHY

is the result of my own work and that where reference is made to the work of others,
due acknowledgment is given.

I also certify that any material in the thesis which has been accepted for a degree or
diploma by any other university or institution is identified in the text.

Full Name PETER GEOFFREY MOHR

Signed..... Signature Redacted by Library

Date..... 30/6/2004

Acknowledgments

I am extremely grateful and would like to thank the many people who have made the completion of this thesis possible. Firstly, I would like to thank my principal supervisor Dr. David Cahill, without your endless patience and guidance I could not have completed this research. I appreciated and benefited greatly from the ease with which we discussed and formulated solutions to the many issues that arose during this project.

I have met and formed invaluable friendships with many fellow students at Deakin University. In particular, I would like to thank Dr. James Rookes who assisted in the development of several techniques during this research and has been a great mate. Other students who have provided support in the laboratory include: Dr. Micheal Aberton, Dr. Rosalie Daniel, Dr. Maryani, Tamsyn Crowley and Andrea Young.

To my wife Maree, words do not really do justice to how much support, and encouragement you have provided throughout the entirety of this research (Thank-you!). Special thanks also to my friends and family who have supported me.

This research would not have been possible without the generous donations of seeds and pathogens from scientists across the globe: Randy Sholl of the Arabidopsis Biological Resource Centre (USA), Dr. Malcolm Ryley (Department of Primary Industries, Australia), Dr. Eric Holub (Horticulture Research International, UK) and Prof. Roger Innes (Indiana University, USA). Thanks also to the team at the Victorian Microarray Technology Consortium (Australia) who had the technology and expertise to conduct the microarray experiments.

Abstract

The plant hormone, abscisic acid (ABA), has previously been shown to have an impact on the resistance or susceptibility of plants to pathogens. In this thesis, it was shown that ABA had a regulatory effect on an extensive array of plant defence responses in three different plant and pathogen interaction combinations as well as following the application of an abiotic elicitor. In unique studies using ABA deficient mutants of *Arabidopsis*, exogenous ABA addition or ABA biosynthesis inhibitor application and simulated drought stress, ABA was shown to have a profound effect on the outcome of interactions between plants and pathogens of differing lifestyles and from different kingdoms. The systems used included a model plant and an important agricultural species: *Arabidopsis thaliana* (*Arabidopsis*) and *Peronospora parasitica* (a biotrophic Oomycete pathogen), *Arabidopsis* and *Pseudomonas syringae* pathovar *tomato* (a biotrophic bacterial pathogen) and an unrelated plant species, soybean (*Glycine max*) and *Phytophthora sojae* (a hemibiotrophic Oomycete pathogen). Generally, a higher than basal endogenous ABA concentration within plant tissues at the time of avirulent pathogen inoculation, caused an interaction shift towards what phenotypically resembled susceptibility. Conversely, a lower than basal endogenous ABA concentration in plants inoculated with a virulent pathogen caused a shift towards resistance. An extensive suppressive effect of ABA on defence responses was revealed by a range of techniques that included histochemical, biochemical and molecular approaches. A universal effect of ABA on suppression or induction of the phenylpropanoid pathway via regulation of the key entry point gene, phenylalanine ammonia-lyase (*PAL*), when stimulated by biotic or abiotic elicitors was shown. ABA also influenced a wide variety of other defence-related components such as: the development of a hypersensitive response (HR), the accumulation of the

reactive oxygen species, hydrogen peroxide and the cell wall strengthening compounds lignin and callose, accumulation of SA and the phytoalexin, glyceollin and the transcription of the SA-dependent pathogenesis-related gene (*PR-1*). The near genome-wide microarray gene expression analysis of an ABA induced susceptible interaction also revealed an as yet unprecedented insight into the great diversity of defence responses that were influenced by ABA that included: disease resistance like proteins, antimicrobial proteins as well as phenylpropanoid and tryptophan pathway enzymes. Subtle differences were found in the number and type of defence responses that were regulated by ABA in each type of plant and pathogen interaction that was studied. This thesis has clearly identified in plant / pathogen interactions previously unknown and important roles for ABA in the regulation of many defence responses.

Table of Contents

Volume One

Acknowledgments	i
Abstract	ii
CHAPTER 1: GENERAL INTRODUCTION AND LITERATURE REVIEW	1
1.1 General introduction	1
1.2 Plant disease	2
1.3 Resistance and susceptibility of plants to disease	3
1.4 Pathogen-specific resistance	4
1.4.1 Pathogen recognition	4
1.4.2 Plant resistance proteins	8
1.4.3 Pathogen elicitors	10
1.5 Signal transduction and regulation during pathogen-specific resistance.....	12
1.5.1 Ion fluxes	13
1.5.2 Reactive oxygen species.....	14
1.5.3 Signalling or regulatory protein intermediates	15
1.5.4 Phosphorylation cascades	16
1.6 Plant hormones that regulate signal transduction during pathogen-specific resistance	16
1.6.1 Salicylic acid	17
1.6.2 Jasmonic Acid / Ethylene	19
1.7 Components of plant defence during pathogen-specific resistance	20
1.7.1 Hypersensitive response	20
1.7.2 Phenylpropanoid pathway	21
1.7.3 Cell wall fortification	24
1.7.4 Phytoalexins	26
1.7.5 Pathogenesis-related proteins	27
1.8 Arabidopsis / pathogen model systems	27
1.9 The Arabidopsis / <i>Peronospora parasitica</i> plant / pathogen model system....	29
1.9.1 <i>Peronospora parasitica</i>	29
1.9.2 Arabidopsis / <i>P. parasitica</i> as a plant / pathogen model system	30
1.10 The Arabidopsis / <i>Pseudomonas syringae</i> pathovar <i>tomato</i> plant / pathogen model system	33
1.10.1 <i>Pseudomonas syringae</i> pathovar <i>tomato</i>	33
1.10.2 Arabidopsis / <i>P. syringae</i> as plant / pathogen model systems.....	34
1.11 The Soybean / <i>Phytophthora sojae</i> plant / pathogen model system	37

1.11.1 <i>Phytophthora sojae</i>	37
1.11.2 Soybean / <i>P. sojae</i> as a plant / pathogen model system	38
1.12 Abiotic elicitors of defence	40
1.13 Abscissic acid (ABA)	41
1.13.1 ABA biosynthesis.....	46
1.13.2 ABA catabolism	48
1.13.3 ABA perception.....	48
1.13.4 ABA signal transduction	49
1.13.5 ABA rapid responses (ion fluxes)	51
1.13.6 ABA slow responses (gene regulation)	52
1.14 Identification of ABA as a regulator of plant resistance or susceptibility to pathogens	53
1.14.1 Changes in ABA concentrations during plant / pathogen interactions	53
1.14.2 The impact of exogenous ABA treatment.....	54
1.14.3 The impact of ABA biosynthesis inhibitor treatment	56
1.14.4 Further evidence for ABA regulation of components of plant defence	56
1.15 Thesis aims and approaches	57
1.16 List of publications and presentations	60
CHAPTER 2: THE INFLUENCE OF ABSCISSIC ACID ON INTERACTIONS OF ARABIDOPSIS WITH THE BIOTROPHIC, OOMYCETE PATHOGEN, PERONOSPORA PARASITICA.....	62
Chapter summary.....	62
2.1 Introduction.....	63
2.2 Materials and methods	67
2.2.1 Source and background of Arabidopsis wild types and mutants.....	67
2.2.2 Growth of Arabidopsis wild type and mutant plants.....	67
2.2.3 ABA and ABA biosynthesis inhibitor treatment of Arabidopsis	68
2.2.4 ABA extraction and quantification.....	69
2.2.5 <i>P. parasitica</i> culture and maintenance	70
2.2.6 <i>P. parasitica</i> inoculum, inoculation procedure and interaction assessment...71	
2.2.7 Histochemical staining and detection of H ₂ O ₂	72
2.2.8 Thioglycolic acid derivatisation of wall bound phenolics.....	74
2.2.9 SA extraction and quantification	75
2.2.10 Total RNA isolation from plant tissues.....	76
2.2.11 Abundance of Arabidopsis <i>PAL1</i> and <i>PR-1</i> mRNA transcripts.....	77
2.2.12 Statistical analysis	79
2.3 Results.....	79
2.3.1 Characterisation of Arabidopsis / <i>P. parasitica</i> interactions.....	79
2.3.2 Treatment with ABA of Arabidopsis / <i>P. parasitica</i> interactions.....	80
2.3.3 Treatment with ABA inhibitors of Arabidopsis / <i>P. parasitica</i> interactions..85	
2.3.4 Characterisation of ABA mutant / <i>P. parasitica</i> interactions	85

2.3.5 Number of conidiophores on ABA treated ABA deficient mutants	95
2.3.6 Comparison of morphological, anatomical and biochemical defences	98
2.3.6.1 Early detection of necrosis	98
2.3.6.2 H ₂ O ₂ production	98
2.3.6.3 Lignin accumulation	101
2.3.6.4 Callose accumulation	104
2.3.6.5 AtPALI mRNA transcript accumulation	104
2.3.6.6 SA accumulation	107
2.3.6.7 AtPR-1 transcript accumulation	107
2.4 Discussion	107
CHAPTER 3: THE INFLUENCE OF ABSCISIC ACID ON INTERACTIONS OF ARABIDOPSIS WITH THE BIOTROPHIC, BACTERIAL PATHOGEN, PSEUDOMONAS SYRINGAE PATHOVAR TOMATO	120
Chapter summary	120
3.1 Introduction	121
3.2 Materials and methods	124
3.2.1 Source and growth of Arabidopsis plants	124
3.2.2 Treatment of plants with ABA and ABA biosynthesis inhibitors	124
3.2.3 Imposition of simulated drought stress	125
3.2.4 ABA extraction from leaves and quantification	125
3.2.5 <i>Pseudomonas syringae</i> pv. <i>tomato</i> cultures	125
3.2.6 Inoculation of Arabidopsis leaves with <i>P. syringae</i> pv. <i>tomato</i>	126
3.2.7 Determination of bacterial numbers within leaves	127
3.2.8 Effect of ABA or ABA biosynthesis inhibitors on <i>P. syringae</i> pv. <i>tomato</i>	128
3.2.9 Histochemical staining and detection of H ₂ O ₂	128
3.2.10 Quantification of wall bound phenolics, salicylic acid and total RNA	129
3.2.11 Abundance of Arabidopsis PALI and PR-I mRNA transcripts	131
3.2.12 Statistical analysis	131
3.3 Results	132
3.3.1 Characterisation of Arabidopsis / <i>P. syringae</i> pv. <i>tomato</i> interactions	132
3.3.2 Effect of addition of ABA or simulated drought stress on interactions	132
3.3.3 Effect of ABA biosynthesis inhibitor treatment on interactions	138
3.3.4 Development of disease in ABA deficient and ABA insensitive mutants	138
3.3.5 Comparison of morphological, anatomical and biochemical defences	145
3.3.5.1 Development of necrosis	145
3.3.5.2 H ₂ O ₂ production	145
3.3.5.3 Lignin accumulation	149
3.3.5.4 Callose accumulation	153
3.3.5.5 Accumulation of AtPALI mRNA transcripts	153
3.3.5.6 SA accumulation	153
3.3.5.7 Accumulation of AtPR-I mRNA transcripts	156
3.4 Discussion	156

Volume Two

CHAPTER 4: MICROARRAY ANALYSIS OF GENE EXPRESSION IN ARABIDOPSIS DURING INDUCED SUSCEPTIBILITY TO AN AVIRULENT STRAIN OF <i>PSEUDOMONAS SYRINGAE</i> PV. <i>TOMATO</i>.....	166
Chapter Summary	166
4.1 Introduction.....	167
4.2 Materials and methods	170
4.2.1 Germination and growth of Arabidopsis plant material	170
4.2.2 Treatment of plants with ABA	171
4.2.3 Procedure for infiltration of Arabidopsis with <i>P. syringae</i> pv. <i>tomato</i>	171
4.2.5 Collection of genome-wide gene expression data by microarray	172
4.2.6 Data analysis.....	174
4.3 Results	175
4.3.1 Preparation of treatments for microarray	175
4.3.2 Comparison of microarray data	176
4.3.3 Significant changes in gene expression.....	179
4.3.4 Defence-related gene expression changes	181
4.3.5 Expression of genes involved in signalling and regulation.....	185
4.3.6 Expression of genes involved in hormonal responses.....	185
4.3.7 Genes related to cell maintenance / development or other functions.....	188
4.3.8 Expression of unclassified genes.....	188
4.4 Discussion	191
CHAPTER 5: THE INFLUENCE OF ABSCISIC ACID ON INTERACTIONS OF SOYBEAN WITH THE HEMIBIOTROPHIC PATHOGEN <i>PHYTOPHTHORA SOJAE</i>	199
Chapter summary.....	199
5.1 Introduction.....	200
5.2 Materials and methods	204
5.2.1 Plant growth	204
5.2.2 ABA and ABA biosynthesis inhibitor treatment of soybean plants.....	205
5.2.3 ABA extraction and quantification from soybean leaves.....	206
5.2.4 Sub-culture and growth of <i>P. sojae</i>	206
5.2.5 Effect of ABA or an ABA biosynthesis inhibitor on <i>P. sojae</i> in culture	206
5.2.6 Zoospore inoculum production	207
5.2.7 Inoculation of soybean leaves with <i>P. sojae</i>	207
5.2.8 Histochemical staining and detection of H ₂ O ₂	208
5.2.9 Quantification of wall bound phenolics, SA, glyceollin and total RNA	209
5.2.10 Abundance of soybean <i>PAL1</i> mRNA transcripts	211
5.2.11 Statistical analysis	212

5.3 Results	212
5.3.1 Resistant and susceptible interactions between soybean leaves and <i>P. sojae</i>	212
5.3.2 Effect of root uptake of ABA on interactions	214
5.3.3 Effect of root uptake of ABA biosynthesis inhibitors on interactions	217
5.3.4 Comparison of morphological, anatomical and biochemical defences	220
5.3.4.1 Early detection of necrotic cell development.....	220
5.3.4.2 H ₂ O ₂ production.....	220
5.3.4.3 Accumulation of phenolic compounds	223
5.3.4.4 Callose deposition.....	228
5.3.4.5 Abundance of Gm <i>PAL1</i> mRNA transcripts.....	228
5.3.4.6 Accumulation of SA.....	228
5.3.4.7 Accumulation of glyceollin.....	232
5.4 Discussion	232
CHAPTER 6: THE INFLUENCE OF ABSCISIC ACID ON DEFENCE RESPONSES INDUCED BY AN ABIOTIC ELICITOR	241
Chapter summary	241
6.1 Introduction	242
6.2 Materials and methods	245
6.2.1 Growth of Arabidopsis and soybean plants.....	245
6.2.2 Treatment of plants with ABA	246
6.2.3 Treatment of leaves with silver nitrate	246
6.2.4 Histochemical staining of leaves.....	247
6.2.5 Extraction and quantification of wall bound phenolics, and total RNA	248
6.2.6 Abundance of <i>PAL1</i> mRNA transcripts	249
6.2.7 Statistical analysis	249
6.3 Results	249
6.3.1 Necrotic lesion development on AgNO ₃ treated leaves	249
6.3.2 Comparison of morphological, anatomical and biochemical defences	251
6.3.2.1 Accumulation of phenolics	251
6.3.2.2 Callose deposition	254
6.3.2.3 Accumulation of <i>PAL1</i> mRNA transcripts	254
6.4 Discussion	254
CHAPTER 7: GENERAL DISCUSSION	261
REFERENCES	270
APPENDICES	312
Appendix 1: Media and Solutions	312
Appendix 2: Genes in cell maintenance / development and other functions.....	313
Appendix 3: Unclassified genes.	314

Figures

Figure 1.1 Models for plant / pathogen gene-for-gene recognition.	6
Figure 1.2 A simplified scheme of the phenylpropanoid pathway of higher plants.	23
Figure 1.3 The lifecycle of <i>P. parasitic</i> .	31
Figure 1.4 The infection process of <i>P. syringae</i> pv. <i>tomato</i> .	35
Figure 1.5 The lifecycle of <i>P. sojae</i> .	39
Figure 1.6 Pathways of ABA biosynthesis and catabolism.	43
Figure 1.7 The structure of norflurazon and fluridone.	45
Figure 2.1 <i>P. parasitica</i> cultures and interactions with Arabidopsis.	81
Figure 2.2 Visualisation of interactions between Arabidopsis and <i>P. parasitica</i> .	82
Figure 2.3 The effect of ABA treatment on resistant interactions.	83
Figure 2.4 Resistant interactions treated with ABA.	84
Figure 2.5 Effect of ABA uptake on ABA concentrations and the health of plants.	86
Figure 2.6 Effect of ABA biosynthesis inhibitors on susceptible interactions.	87
Figure 2.7 <i>P. parasitica</i> conidiophores after biosynthesis inhibitor treatment.	88
Figure 2.8 Susceptible interactions treated with ABA biosynthesis inhibitors.	89
Figure 2.9 Effect of inhibitors on ABA concentrations and plant health.	90
Figure 2.10 Comparison of growth form of Arabidopsis ABA mutants.	92
Figure 2.11 Resistant interactions of ABA mutants with <i>P. parasitica</i> .	93
Figure 2.12 Interactions of ABA mutants with virulent isolates of <i>P. parasitica</i> .	94
Figure 2.13 Production of conidiophores on ABA mutants.	96
Figure 2.14 Conidiophores on ABA deficient mutants treated with ABA.	97
Figure 2.15 Early stages of hyphal spread or necrosis development.	99
Figure 2.16 DAB detection of H ₂ O ₂ production in ABA mutants.	100
Figure 2.17 Detection of lignin deposition in ABA mutants.	102
Figure 2.18 Wall bound TGA derivatives in ABA mutants.	103
Figure 2.19 Callose deposition in ABA mutants.	105
Figure 2.20 Abundance of AtPAL1 mRNA transcripts in ABA mutants.	106
Figure 2.21 SA accumulation in ABA mutants.	108
Figure 2.22 Abundance of AtPR-1 mRNA transcripts in ABA mutants.	109
Figure 3.1 Disease and <i>P. syringae</i> pv. <i>tomato</i> numbers in Arabidopsis.	133
Figure 3.2 ABA treated Arabidopsis infiltrated with <i>P. syringae</i> pv. <i>tomato</i> .	133
Figure 3.3 Effect of treatment with ABA on leaves and <i>P. syringae</i> pv. <i>tomato</i> .	135
Figure 3.4 Drought stressed Arabidopsis infiltrated with <i>P. syringae</i> pv. <i>tomato</i> .	137

Figure 3.5 Inhibitor treated leaves infiltrated with <i>P. syringae</i> pv. <i>tomato</i> .	137
Figure 3.6 Effect of inhibitors on Arabidopsis and <i>P. syringae</i> pv. <i>tomato</i> .	139
Figure 3.7 <i>P. syringae</i> pv. <i>tomato</i> vacuum infiltration of Arabidopsis plants	141
Figure 3.8 <i>P. syringae</i> pv. <i>tomato</i> vacuum infiltration of ABA mutants.	143
Figure 3.9 Comparison of growth form of ABA mutants.	143
Figure 3.10 Development of necrotic cells.	146
Figure 3.11 Necrotic cells in ABA treated Arabidopsis.	146
Figure 3.12 DAB detection of H ₂ O ₂ .	148
Figure 3.13 H ₂ O ₂ in ABA treated Arabidopsis.	148
Figure 3.14 Detection of lignin deposition.	151
Figure 3.15 Lignin deposition in ABA treated Arabidopsis.	150
Figure 3.16 Callose deposition following infiltration with <i>P. syringae</i> pv. <i>tomato</i> .	152
Figure 3.17 AtPAL1 mRNA transcripts after infiltration.	154
Figure 3.18 SA accumulation following infiltration with <i>P. syringae</i> pv. <i>tomato</i> .	155
Figure 3.19 AtPR-1 mRNA transcripts following infiltration.	157
Figure 4.1 Scheme for microarray analysis treatments.	173
Figure 4.2 Disease symptoms on ABA treated leaves following infiltration.	177
Figure 4.3 Scatter plots of microarray treatment data.	178
Figure 4.4 Significant changes in Arabidopsis gene expression.	180
Figure 4.5 Expression of genes encoding enzymes of monolignol biosynthesis.	184
Figure 4.6 Changes in expression of 389 genes with unclassified function.	190
Figure 5.1 Interactions between soybean leaves and <i>P. sojae</i> .	213
Figure 5.2 Effect of ABA treatment on resistance.	215
Figure 5.3 Effect of root uptake of ABA on ABA concentrations and <i>P. sojae</i> .	216
Figure 5.4 Effect of ABA biosynthesis inhibitor treatment on susceptibility.	218
Figure 5.5 Effect of biosynthesis inhibitors on ABA concentrations and <i>P. sojae</i> .	219
Figure 5.6 Early detection of necrotic cell development.	221
Figure 5.7 Necrotic cell development following ABA or inhibitor treatment.	222
Figure 5.8 H ₂ O ₂ production following ABA or inhibitor treatment	224
Figure 5.9 Phenolic deposition in resistant and susceptible interactions.	225
Figure 5.10 Phenolic deposition following ABA or inhibitor treatment.	226
Figure 5.11 Wall bound TGA derivatives following inoculation with <i>P. sojae</i> .	227
Figure 5.12 Callose deposition in resistant and susceptible interactions.	229
Figure 5.13 Abundance of GmPAL1 mRNA.	230

Figure 5.14 SA accumulation in resistant and susceptible interactions.	231
Figure 5.15 Glyceollin accumulation in resistant and susceptible interactions.	233
Figure 6.1 Lesion development following treatment with AgNO ₃ .	250
Figure 6.2 Wall bound phenolic accumulation following treatment with AgNO ₃ .	252
Figure 6.3 Wall bound TGA derivatives following treatment with AgNO ₃ .	253
Figure 6.4 Callose deposition following treatment with AgNO ₃ .	255
Figure 6.5 Effect of ABA application on <i>PAL1</i> mRNA transcripts.	256

Tables

Table 1.1 Examples of the six structural classes of plant resistance (R) proteins.	7
Table 1.2 Location of <i>RPP</i> genes on Arabidopsis chromosomes.	32
Table 2.1 Summary of Arabidopsis / <i>P. parasitica</i> interactions.	82
Table 2.2 Conidiophores on leaves following treatment with ABA.	83
Table 2.3 Conidiophores on leaves treated with ABA biosynthesis inhibitors.	87
Table 2.4 Summary of ABA mutant interactions with <i>P. parasitica</i> .	111
Table 2.5 Summary of defences in ABA mutants inoculated with <i>P. parasitica</i> .	112
Table 3.1 ABA treated Arabidopsis / <i>P. syringae</i> pv. <i>tomato</i> interactions.	159
Table 4.1 Description of Arabidopsis treatments prepared for microarray.	177
Table 4.2 Description of microarray treatment data comparisons.	178
Table 4.3 Significant changes in gene expression in comparison A and B.	180
Table 4.4 Genes involved in defence mechanisms.	182
Table 4.5 Genes involved in signalling and regulation.	186
Table 4.6 Genes related to hormonal responses.	187
Table 4.7 Summary of genes related to maintenance and other functions.	189
Table 5.1 Summary of treated soybean / <i>P. sojae</i> interactions.	234
Table 5.2 Summary of defences in treated soybean / <i>P. sojae</i> interactions.	236
Table 6.1 Summary of ABA treatment and application of AgNO ₃ on defences.	258

Chapter 1: General introduction and literature review

1.1 General introduction

The objective of the research presented in thesis was to better understand the role of abscisic acid (ABA) in the regulation of plant defence responses during pathogen attack. Previous studies have alluded to the importance of ABA in determining either plant resistance or susceptibility to pathogens. However, the extent to which ABA is involved and the mechanisms that underlie its influence on plant / pathogen interactions remain poorly understood. In this thesis the role of ABA was further examined through the study of resistant and susceptible interactions in three plant / pathogen model systems: *Arabidopsis thaliana* (L.) Heynh. (hereafter referred to as *Arabidopsis*) / *Peronospora parasitica* (Pers. ex Fr.) Fr. (a biotrophic Oomycete pathogen), *Arabidopsis* / *Pseudomonas syringae* pathovar (pv.) *tomato* Cuppels (a biotrophic bacterial pathogen) and *Glycine max* (L.) Merr. (soybean) / *Phytophthora sojae* Kauf. and Gerd. (a hemibiotrophic Oomycete pathogen). The role of ABA in regulation of plant responses to an abiotic elicitor, silver nitrate, was also investigated in both *Arabidopsis* and soybean. Therefore the literature review that follows in this chapter covers topics that form a basis for the research presented, including:

- Plant susceptibility or resistance to pathogens,
- Components of defence during resistance,
- Plant hormones that are involved in resistance,
- Plant / pathogen model systems,
- Abiotic elicitors,
- ABA perception, biosynthesis and signal transduction, and
- What is known about ABA in plant resistance and susceptibility?

1.2 Plant disease

Plants are sessile organisms that must survive whatever challenges they encounter in their environment. They are under a constant threat of disease from potentially pathogenic organisms such as bacteria, fungi, Oomycetes, viruses, and nematodes (Jackson and Taylor, 1996). Plant pathogens can obtain nutrition from plants by three major lifestyles; necro-, bio- or hemibiotrophy. A necrotrophic pathogen actively kills plant tissue as it colonises, obtaining nutrients from the killed cells. A biotrophic pathogen obtains nutrition from living plant cells. A hemibiotroph exhibits both necro- and biotrophic phases during disease development. Hemibiotrophs establish themselves by eluding detection and forming associations with living plant cells, much like biotrophs. Later during the infection process, these pathogens more closely resemble necrotrophs, since they may spread rapidly and actively kill host cells (Johal *et al.*, 1995). Bacterial pathogens tend to be either necro- or biotrophs, whereas Oomycetes can be necro-, bio- or hemibiotrophs (Jackson and Taylor, 1996).

Diseases of plants can have an enormous impact on the economic and social lives of the human population. For example, the 'Irish Potato Famine' in 1845 was caused by the pathogen *Phytophthora infestans* Mont. and the 'Great Bengal Famine' resulting from destruction of the 1942 rice (*Oryza sativa* (L.)) harvest by the pathogen *Helminthosporium oryzae* Breda de Haan, resulted in many human deaths (Klinkowski 1970; Schumann 1991). The potential for serious crop disease epidemics still persists today as a result of intensive agricultural practices that rely on monoculture crops planted over wide geographical areas. Studying plant / pathogen interactions is therefore important to not only contribute to our understanding of basic plant processes but also to improve agricultural productivity.

1.3 Resistance and susceptibility of plants to disease

Despite the constant threat to plants posed by pathogens, disease rarely develops. There are three main barriers that cause the failure of pathogens to multiply and spread in plant tissues. Firstly, the plant may be unable to support the niche requirements of the invading pathogen. Secondly, the plant may possess preformed structural and biochemical compounds that confine a penetrating pathogen. Thirdly, upon recognition of the attacking pathogen defence mechanisms may be triggered that localises the invasion (Hammond-Kosack and Jones, 1996). If a pathogen fails to cause disease because of the first or second barriers, the plant is considered to be a non-host species. If a pathogen successfully overcomes all three barriers and causes disease, the plant is considered to be a susceptible host species.

Throughout this thesis a number of terms are used to describe the interactions of a host with a pathogen. Resistance of a plant to a pathogen can be categorised into non-host, age-, organ- or pathogen-specific and systemic acquired resistance (SAR) (Heath 1995). Non-host resistance is the most common form of plant resistance, and is based on non-specific defence mechanisms of a non-host plant species and is also termed 'basic resistance'. Age-related resistance refers to the general phenomenon of plants becoming more resistant to pathogens as they age or mature. Organ-specific resistance is expressed when a pathogen that causes disease on one part of a host plant (eg. roots) is unsuccessful when it attempts to attack another (eg. leaves). Presumably age-related and organ-specific resistance is based on differences in components of basic resistance in differently aged plants or organs (Heath 1996). These latter forms of resistance comprise components of a potential second barrier that pathogens face during infection but are not relevant to this thesis and therefore will not be a focus.

Pathogen-specific resistance, the most commonly studied form of resistance, is expressed by a genotype of an otherwise susceptible host species that recognizes a specific isolate, race or strain of pathogen (Heath 1996). SAR refers to a distinct form of resistance that is triggered following or during pathogen-specific resistance. SAR develops in distal, uninfected parts of the plant and results in a broad-spectrum resistance to pathogens normally causing disease (Sticher *et al.*, 1997). Pathogen-specific resistance, the potential third barrier to invading pathogens will be the major focus of this thesis.

Unless otherwise stated, the term resistance will be utilised in this thesis to describe a pathogen-specific resistant interaction between a resistant plant and an avirulent pathogen, resulting in no disease (sometimes referred to as an incompatible interaction). In contrast, the term susceptibility will refer to an interaction between a susceptible plant and a virulent pathogen, resulting in disease (sometimes referred to as a compatible interaction). The terms avirulent and virulent pathogen will be described in section 1.4.1.

1.4 Pathogen-specific resistance

1.4.1 Pathogen recognition

The perception of specific pathogens by host plants that leads to induced defence responses has been postulated to follow the gene-for-gene concept. The concept infers that for every dominant gene determining resistance in a host plant, there is a matching dominant gene conditioning avirulence in the pathogen (Flor 1946). The prevailing model for explaining the biochemical basis of the gene-for-gene concept is the ‘receptor-ligand’ model (Keen 1990). According to this model, an avirulence (*Avr*) gene of a pathogen encodes an elicitor protein that is perceived by a receptor protein, encoded by a matching resistance (*R*) gene of the host plant

(Figure 1.1). Pathogen perception subsequently triggers signalling cascades that coordinate and lead to the activation of an array of defence responses that predominantly includes a rapid cell death or hypersensitive response (HR) (Hammond-Kosack and Jones, 1996). The absence or inactivation of either *R* or *Avr* genes compromises recognition and therefore downstream defence responses, resulting in disease if the invading pathogen overcomes basic resistance (Warren *et al.*, 1998). Therefore detection of an *Avr* protein by the host plant constitutes the pivotal event in successful pathogen-specific resistance.

The number of *R* proteins and matching *Avr* proteins that have been identified in plants and pathogens respectively is increasing (Table 1.1). However, in only a few cases has the physical interaction between *R* and *Avr* proteins been able to be demonstrated, for example, *Pto* a *R* protein of tomato (*Lycopersicon esculentum* Mill.) with *AvrPto* an *Avr* protein of *P. syringae* pv. *tomato* (Tang *et al.*, 1996). This has stimulated debate over the possible existence of at least a third component (plant) protein required for pathogen-specific recognition of an *Avr* protein by a resistant host.

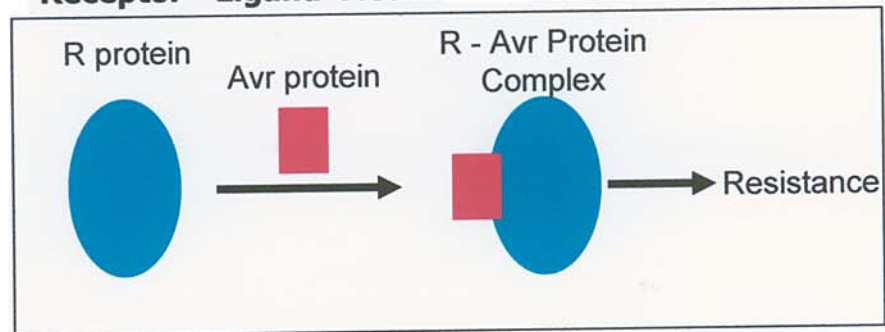
A third component protein could simply be a plant co-receptor (Luderer and Joosten, 2001). Another possibility is the ‘guard hypothesis’ that proposes the third component protein is represented by a plant virulence target of the *Avr* protein (Van Der Biezen and Jones, 1998). Binding of the *Avr* protein to its virulence target is perceived by the matching *R* protein, which is ‘guarding’ this virulence target and results in the initiation of defence responses (Figure 1.1). In the case of the *R* protein being absent, binding will result in enhanced susceptibility. Possible third components have already been identified in many gene-for-gene plant / pathogen interactions (Table 1.1). For example, the requirement for the third component

Figure 1.1 Models for protein-protein interactions that underlie plant / pathogen gene-for-gene recognition.

In the 'receptor-ligand' model, a plant R protein and a pathogen Avr protein interact directly to activate defence signalling, resulting in resistance. In the 'guard hypothesis', a plant R protein, a pathogen Avr protein and a third (plant) protein interact with one another to activate defence signalling, resulting in resistance.

Figure modified from Martin *et al.* (2003).

'Receptor - Ligand' Model



'Guard Hypothesis' Model

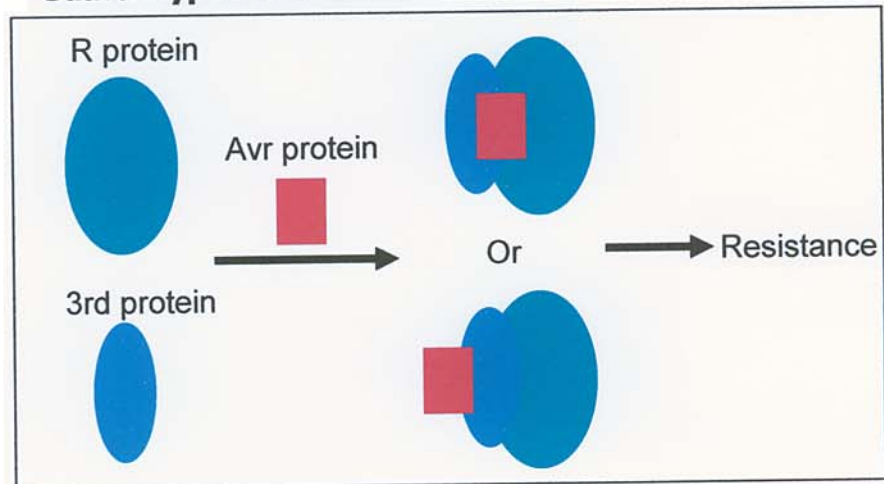


Table 1.1 Examples of the six structural classes of plant resistance (R) proteins and possible third protein components, involved in recognition of pathogen avirulence (Avr) proteins.

Structure Class	R Protein (s)	Third Component	Plant	Pathogen	Avr Protein(s)
1 STK-MM	Pto	Prf	Tomato	<i>Pseudomonas syringae</i> (B)	AvrPto; AvrPtoB
2 LRR-NBS-CC	Bs2		Pepper	<i>Xanthomonas campestris</i> (B)	AvrBs2
	HRT	TIP	Arabidopsis	Turnip Crinkle Virus	Coat protein
	Mi		Tomato	<i>Meloidogyne incognita</i> (N)	
	Pi-ta	No	Rice	<i>Magnaporthe grisea</i> (F)	Avr-Pita
	RPP8, RPP13		Arabidopsis	<i>Peronospora parasitica</i> (O)	
	RPS2, RPS5, RPM1*	p75, PBS1, RIN4*	Arabidopsis	<i>P. syringae</i> (B)	AvrRpt2, AvrPphB, AvrRpm1; AvrB
3 LRR-NBS-TIR	L, M, P		Flax	<i>Melampsora lini</i> (F)	AL, AM, AP
	N		Tobacco	Tobacco Mosaic Virus	Replicase Protein
	RPP1, RPP4, RPP5		Arabidopsis	<i>P. parasitica</i> (O)	
	RPS4		Arabidopsis	<i>P. syringae</i> (B)	AvrRps4
4 LRR-TM	Cf-2, Cf-9	Rcr3, HABS	Tomato	<i>Cladosporium fulvum</i> (F)	Avr2, Avr9
5 LRR-TM-STK	Xa21		Rice	<i>Xanthomonas oryzae</i> (B)	
6 Unknown	Hm1		Maize	<i>Cochliobolus carbonum</i> (F)	
	HS1 ^{pro-1}		Beet	<i>Heterodera schachtii</i> (N)	
	RRS1-R		Arabidopsis	<i>Ralstonia solanacearum</i> (B)	
	RTM1, RTM2		Arabidopsis	Tobacco Etch Virus	

Structure Class abbreviations: CC, coiled-coil domain; LRR, leucine rich repeat; MM, myristylation motif; NBS, nucleotide binding site; STK, serine / threonine protein kinase; TIR, similarity to N terminus of the Toll and Interleukin 1 receptor protein; TM, transmembrane domain. Except for viruses, pathogens are abbreviated: B, bacterium; F, fungus; N, nematode; O, Oomycete. Only cloned Avr proteins and identified third component proteins are listed. * Denotes that RPM1 recognizes two Avr proteins (AvrRPM1 and AvrB) from two different *P. syringae* pathovars and RIN4 may act as a third component for each. Table is a compilation of information from Luderer and Joosten (2001), Van't Slot and Knogge (2002) and Martin *et al.* (2003).

protein Prf in Pto / AvrPto recognition (Salmeron *et al.*, 1996). The exact mechanism underlying the involvement of a third component protein in perception of an Avr protein by a matching R protein remains to be elucidated.

It should also be noted that some R proteins recognise more than one pathogen signal. For example, Pto also recognises AvrPtoB an Avr protein three times the mass of AvrPto but from the same pathogen (Kim *et al.*, 2002). Therefore the narrowly defined version of the gene-for-gene concept appears to breakdown. Katagiri *et al.* (2002) highlight that the gene-for-gene concept was put forward by Flor based on the study of flax (*Linum usitatissimum* (L.)) / flax rust fungus (*Melampsora lini* (Pers.) H. Lev.) interactions in the 1940's and 1950's, when knowledge of gene function at the molecular level was almost non-existent. Also with the current knowledge of molecular interaction mechanisms, the gene-for-gene concept could be interpreted more broadly, to include the possibility of multiple protein recognition complexes and recognition of multiple Avr proteins by a single R protein. For example, a plant has pathogen recognition mechanism(s) composed of a repertoire of genetically definable recognition specificities and that pathogen recognition by these mechanism(s) leads to a successful deployment of defence responses in the plant.

1.4.2 Plant resistance proteins

Many structural and functional domains and regions have been identified that in various combinations form R proteins, but as yet little is known of their immediate roles. The leucine-rich repeat (LRR) domain appears to play a central role in protein-protein interactions, particularly Avr protein binding (Kobe and Deisenhofer, 1994; Jia *et al.*, 2000). The nucleotide binding site (NBS) region has a critical role potentially through either nucleotide binding or hydrolysis (Martin *et al.*, 2003). The

coiled-coil (CC) domain, for example, a leucine zipper (LZ) has been implicated in protein-protein interactions that involve signal transduction but also pathogen recognition. Regions with similarity to the N terminus of the Toll and Interleukin 1 receptor protein (TIR) domains are also implicated in signalling and pathogen recognition (Martin *et al.*, 2003). The serine / threonine protein kinase (STK) domains play a central role as catalytic domains in signal transduction, for example, in Pto via modulation of phosphorylation state (Zhou *et al.*, 1995). The myristylation motif (MM) may be involved in the localisation of R proteins to a membrane (Martin *et al.*, 2003).

The R proteins identified so far can be categorized into six classes based on their structural and functional domains and regions (Table 1.1). Class one consists of just one member Pto, with a STK domain and a MM at its N terminus. Class two comprises a large number of proteins having a region of LRR, a NBS, and an N-terminal LZ or other CC sequence. Class three is similar to class two but instead of the CC sequence these proteins have a TIR region. The R proteins belonging to the first three classes lack transmembrane (TM) domains and all are likely to be localised intracellularly. The Cf proteins from tomato form class four with a TM domain, an extracellular LRR, and a small cytoplasmic tail. Class five consists of just the Xa21 protein from rice, which in addition to an extracellular LRR and a TM domain, has a cytoplasmic STK region. These two classes encode R proteins that are thought to span membranes. Class six comprises of R proteins that have not been as well characterised and do not fit into these five classes. Although Arabidopsis RRS1-R gene, that confers resistance to *Ralstonia solanacearum* Smith contains a structure similar to a class three R protein but with a nuclear localisation signal (Lahaye 2002). The localisation of R proteins has proved difficult experimentally due to their low

abundance in cells and rapid degradation upon Avr protein binding (Boyce *et al.*, 1998).

1.4.3 Pathogen elicitors

Elicitors of pathogen origin that trigger plant defence responses consist of an extremely diverse array of surface localised or secreted carbohydrates, lipids, and proteins. The wide variety of elicitors that plants recognise is structurally distinct, without the presence of a common motif (Knogge 2002). However, pathogen elicitors can be classified into two groups: general or race-specific elicitors. While general elicitors are able to trigger defence both in host and non-host plants, race-specific elicitors induce defence responses leading to resistance only in specific host cultivars (Montesano *et al.*, 2003). General and race-specific elicitors are recognised by membrane associated receptors whereas only race-specific elicitors are recognised by intracellular receptors (Nurnberger 1999; Mithofer *et al.*, 2000). The majority of receptors (R proteins) that have been cloned and characterised recognise race-specific elicitor proteins encoded by *Avr* genes.

The *Avr* proteins that have been cloned and characterised from viruses, bacteria, fungi, Oomycetes and nematodes are extremely diverse in structure and function (Van't Slot and Knogge, 2002). The largest number and best understanding of *Avr* genes and their encoded proteins has come from the study of bacterial pathogens. Since the first bacterial *Avr* gene was cloned from *Pseudomonas syringae* (Staskawicz *et al.*, 1984), more than 40 *Avr* genes from gram-negative bacteria of genera *Pseudomonas*, *Xanthomonas*, *Erwinia* and *Ralstonia* have been identified (Leach and White, 1996). These pathogens require a highly specialised type III protein secretion system to deliver *Avr* proteins into plant cells (Buttner and Bonas, 2002). Production and delivery of the type III secretion system is under the control of

the hrp (hypersensitivite response and pathogenicity) pilus, a filamentous surface appendage encoded by the hrp gene locus (Roine *et al.*, 1997; Galan and Collmer, 1999).

Avr proteins can promote disease, as first identified for *AvrBs2* from the bacterium *Xanthomonas campestris* pv. *vesicatoria* Doidge (Kearney and Staskawicz, 1990). The deletion or mutation of several different bacterial *Avr* genes results not only in the loss of avirulence in the presence of the respective plant *R* genes but simultaneously in a reduction of virulence on susceptible plants (White *et al.*, 2000). Furthermore, several *Avr* genes when expressed in the host lacking the corresponding *R* gene induce disease-like symptoms, suggesting their products to be directly involved in promoting virulence (Kjemtrup *et al.*, 2000). The expression of *Avr* genes is therefore not only disadvantageous from host recognition leading to resistance but can also play a dual role that is advantageous in promoting virulence, indicating why these genes are maintained by pathogens. However, the mechanisms underlying the impact of *Avr* proteins on plants as well as their targets within host cells remain elusive.

Compared with bacterial *Avr* genes the number of characterised *Avr* genes from fungi has remained low due to substantially larger genomes and the frequency of strict biotrophic lifestyles making fungi not easily amenable to molecular genetic approaches (Van't Slot and Knogge, 2002). However, since the interaction of *Cladosporium fulvum* Cke. with tomato was identified as the first plant / fungal model system to comply at the molecular level with the gene-for-gene hypothesis (De Wit 1992), many *C. fulvum* *Avr* genes have been cloned and characterised (Rivas and Thomas, 2002). Interestingly, many necrotrophic fungi also secrete host-selective toxin (HST) proteins that can function as essential determinants of

pathogenicity, involved in killing plant cells to gain access to the host nutrients. Investigations into plant molecular and biochemical responses to HST proteins has revealed responses typically associated with pathogen-specific resistance induced by Avr proteins (Wolpert *et al.*, 2002). For example, the Victoria blight of oats (*Avena sativa* (L.) Thell.) is caused by the necrotrophic fungus *Cochliobolus victoriae* Nelson and its pathogenicity strictly results from its ability to produce the HST, victorin (Scheffer *et al.*, 1967). The signalling events, cell death and other defence responses induced by victorin share many of the characteristics of an avirulence-elicited defence response and may be conferred through a single dominant *R*-like gene (Wolpert *et al.*, 2002).

In contrast to bacteria and fungi, viral genomes are extremely small and encode only a limited number of proteins expressed from within the plant cell. Each of the proteins (replicase, coat and movement) involved in the life cycle of one of the most extensively studied plant viruses, tobacco mosaic virus (TMV), act as Avr proteins (Van't Slot and Knogge, 2002). To date only the MAP-1 Avr protein from the root-knot nematode *Meloidogyne incognita* Kof. et White of tomato has been cloned (Williamson 1998; Semblat *et al.*, 2001). The only Oomycete Avr protein to be cloned to date is Avr1b of *P. sojae* (Tyler 2002).

1.5 Signal transduction and regulation during pathogen-specific resistance

For pathogen-specific resistance to be effective plant defence components must be deployed rapidly following pathogen recognition. However, the defence components cannot be unleashed with impunity, as they are resource-intensive and can inflict substantial collateral damage on plant tissue. Therefore signal transduction and regulation must confine deployment of defence components to the appropriate

place and time (McDowell and Dangl, 2000). Despite major advances in our understanding of the molecular mechanisms (*R* / *Avr* genes) of recognition in pathogen-specific resistance, the precise signalling pathways that initiate and regulate components of defence remain elusive. It is likely the difficulties encountered deciphering pathogen-specific resistant signalling results from the complexity of signalling hierarchies and crosstalk between common pathways in response to various stimuli (Genoud and Metraux, 1999). Despite these difficulties, several important signalling components for *R* gene mediated resistance have been identified: ion fluxes, reactive oxygen species (ROS), specific protein intermediates and phosphorylation cascades.

1.5.1 Ion fluxes

One of the earliest responses downstream of pathogen recognition is a rapid change in ion fluxes at the cellular membrane. Influxes have been observed of both hydrogen (H^+) and calcium (Ca^{2+}) as well as effluxes of potassium (K^+) and chloride (Cl^-) (Jabs *et al.*, 1997). Changes in ion fluxes can occur within 10 minutes and cause membrane depolarisation and acidification of plant cells (Nurnberger *et al.*, 1994; Pike *et al.*, 1998). Ion fluxes are believed to be a consequence of H^+ -ATPases, and plasma membrane-bound ion-channels activated by dephosphorylation (Atkinson and Baker, 1989; Blumwald *et al.*, 1998). The importance of Cl^- efflux has been revealed by its inhibitors that also prevent K^+ efflux, the oxidative burst and phytoalexin accumulation (Jabs *et al.*, 1997). Ca^{2+} influx has also proven crucial in membrane depolarisation, electrolyte leakage, the oxidative burst and the HR (Marre *et al.*, 1998; Grant *et al.*, 2000). Ca^{2+} fluxes are believed to trigger the oxidative burst via signalling involving calmodulin (Harding and Roberts, 1998).

1.5.2 Reactive oxygen species

Another rapid response to pathogen recognition is the oxidative burst producing ROS; in particular superoxide (O_2^-), hydrogen peroxide (H_2O_2) and nitric oxide (NO). O_2^- was the first ROS identified in pathogen-specific resistance of potato (*Solanum tuberosum* (L.) Kartoffel) to *P. infestans* (Doke 1983). However, O_2^- is poorly diffusible and unstable and therefore in most plants is rapidly dismutated to H_2O_2 (Lamb and Dixon, 1997). H_2O_2 is the most stable ROS and is highly permeable to membranes and therefore has been identified as a potential defence signal molecule (Yamasaki *et al.*, 1997). In *R* gene mediated resistance H_2O_2 production is prolonged and biphasic whereas in susceptible interactions leading to plant disease it is short and monophasic (Lamb and Dixon, 1997). O_2^- and therefore H_2O_2 production is likely to occur through membrane bound NADPH oxidases and / or peroxidases regulated by Ca^{2+} (Bolwell *et al.*, 1995; Mithofer *et al.*, 1997; Keller *et al.*, 1998; Torres *et al.*, 2002). The production of H_2O_2 has been implicated in HR induction, direct antimicrobial activity and activation of the phenylpropanoid pathway, depending on the plant and pathogen combination (Lamb and Dixon, 1997; Guo *et al.*, 1998; Overmyer *et al.*, 2003).

Nitric oxide has also been identified as a potential signal molecule in *R* gene mediated resistance. Inhibitors of NO synthesis compromise Arabidopsis pathogen-specific resistance to *P. syringae* (Delledonne *et al.*, 1998), whereas addition of NO donors induce phytoalexin production and synthesis of defence related genes in potato and tobacco (*Nicotiana tabacum* (L.)) respectively (Noritake *et al.*, 1996; Durner *et al.*, 1998). The recent discovery of an induced nitric oxide synthase in tobacco resistance to TMV (Chandok *et al.*, 2003) has opened the possibility for rapid determination of NO synthesis and signalling in plant resistance.

1.5.3 Signalling or regulatory protein intermediates

Mutational dissection of pathogen-specific resistance in plants such as tomato, barley (*Hordeum vulgare* (L.)) and Arabidopsis, has identified a limited number of signalling and regulatory proteins. These protein intermediates act downstream of pathogen recognition and give initial insights into the complex and diverse genetic framework of defence signalling pathways (Feys and Parker, 2000). Lethality, redundancy and the existence of parallel and additive pathways could account for the limited number of protein intermediates identified to date (Martin *et al.*, 2003).

A small number of mutants impaired in *R* gene mediated resistance have been used to identify genes that are specifically required for the function of individual *R* genes. For example, the tomato *rcr3* (required for *Cladosporium* resistance 3) mutant specifically compromise the function of *R* gene *Cf-2* but not *Cf-5*. These two *R* genes recognise different *C. fulvum* races although the respective *R* proteins are 93% similar at the amino acid level (Dixon *et al.*, 2000). Also an Arabidopsis *pbs1* (*AvrPphB* susceptible 1) mutant suppresses resistance to the bacterial pathogen *P. syringae* mediated by the *R* gene *RPS5*, but not other Arabidopsis *R* genes (Warren *et al.*, 1999).

In contrast, many of the protein intermediates identified so far are necessary for the function of multiple *R* genes reinforcing the notion that common processes operate downstream of plant recognition of pathogens (Feys and Parker, 2000). For example, RAR1 (non-race-specific resistance 1) is a zinc-binding protein that was identified in barley and when mutated compromised the function of many *R* genes that recognised powdery mildew isolates such as *Erysiphe graminis* DC. f.sp. *hordei* Em. Marchal (Peterhansel *et al.*, 1997; Shirasu *et al.*, 1999). When mutated

the PBS2 and PBS3 proteins of *Arabidopsis* affect the function of multiple *R* genes that recognise *P. syringae* races (Warren *et al.*, 1999).

A correlation has been identified between particular *Arabidopsis* R protein structural classes and the indispensable function of proteins EDS1 (enhanced disease susceptibility 1) or NDR1 (nonrace-specific disease resistance 1) in pathogen-specific resistance. Mutations in the lipase-like protein EDS1 (Falk *et al.*, 1999) abolished resistance mediated by class three R proteins. Whereas mutations of the NDR1 protein suppressed resistance conferred by class two R proteins (Aarts *et al.*, 1998). However exceptions do exist, such as *RPP8* that encodes a class two R protein and requires neither EDS1 or NDR1 proteins to confer pathogen-specific resistance (McDowell *et al.*, 2000).

1.5.4 Phosphorylation cascades

A major role for phosphorylation in *R* gene mediated signalling has been identified for *R* genes *Pto*, *Xa21*, and *Rpg1* (Martin *et al.*, 2003). The role of signal transduction through phosphorylation that is initiated by the STK of *Pto* and that involves another STK, *Pti1* and transcription factors *Pti4*, *Pti5*, and *Pti6* is crucial for resistance (Zhou *et al.*, 1995; Zhou *et al.*, 1997). Calcium-dependent protein kinases (CDPK) and mitogen-activated protein kinases (MAPK) have also been identified for specific phosphorylation events in *R* gene mediated resistance (Romeis *et al.*, 2001; Zhang and Liu, 2001).

1.6 Plant hormones that regulate signal transduction during pathogen-specific resistance

Plant hormones regulate many developmental and physiological processes in plants and more recently roles in signal transduction and regulation of pathogen-specific resistance have been identified. The number of hormones implicated in

pathogen-specific resistance is growing rapidly and includes salicylic acid (SA), jasmonic acid (JA), ethylene (Et), ABA and brassinolide (Thomma *et al.*, 2001b; Audenaert *et al.*, 2002; Nakashita *et al.*, 2003). The potential role(s) for the hormone ABA in pathogen-specific resistance will be discussed in more detail in section 1.14. The roles of plant hormones SA, JA and Et in signal transduction and regulation of pathogen-specific resistance are the best characterised to date. Rather than operating independently in pathogen-specific resistance, the three hormones are linked together in a complex web of interactions, as indicated by the *Arabidopsis hrl1* (HR like lesion 1) mutant (Devadas *et al.*, 2002) and global expression phenotyping of hormone-defective *Arabidopsis* mutants (Glazebrook *et al.*, 2003).

1.6.1 Salicylic acid

SA is important in both signal transduction and regulation of pathogen-specific resistance and SAR (Sticher *et al.*, 1997; Shirasu and Schulze-Lefert, 2000; Metraux 2001). SA was originally identified as being involved in plant resistance following measurement of increased endogenous levels after pathogen infection initially at the site of inoculation, and later in distal parts of the plant (Malamy *et al.*, 1990). It appears unlikely that SA is itself the mobile signal responsible for SAR (Vernooij *et al.*, 1994). A large body of evidence that supports the notion that SA is a critical regulator in a number of plant defence responses has recently come from transgenic and mutant plant analysis (Dixon *et al.*, 2002).

Analysis of transgenic *Arabidopsis* and tobacco plants expressing the bacterial *nahG* gene (that encodes the enzyme, salicylate hydroxylase that inactivates SA) have shown that in response to some pathogens depletion of SA causes the breakdown of both pathogen-specific resistance and SAR (Gaffney *et al.*, 1993; Delaney *et al.*, 1994; Friedrich *et al.*, 1995). Caution should be exercised when using

NahG plants, however, as they accumulate catechol, a derivative of SA that affects resistance to the non-host pathogen *Pseudomonas syringae* pv. *phaseolicola* (Van Wees and Glazebrook, 2003). The expression patterns of defence-related genes in pathogen challenged NahG plants also differ when compared to SA deficient mutants such as *sid2* (SA induction-deficient 2) (Glazebrook *et al.*, 2003).

What factor or factors stimulate increased SA concentration *in planta* and how those increases in turn regulate resistance remain largely unknown. However, accumulation of the defence protein pathogenesis-related protein 1 (PR-1) has been observed following increases in SA and is a commonly used indicator of SA-dependent defence responses (Yalpani *et al.*, 1991; Xie *et al.*, 1998). Analysis of the lesion mimic mutants of Arabidopsis *lsd1* (lesions stimulating disease response 1) and *acd6* (accelerated cell death 6) suggest that SA, in conjunction with ROS, are intimately associated with the regulation of cell death during a HR (Rate *et al.*, 1999; Alvarez 2000; Aviv *et al.*, 2002). Scrutiny of the NPR1 (non-expressor of pathogenesis-related proteins) protein that operates downstream of SA accumulation in Arabidopsis, has also highlighted the importance of SA and NPR1 in HR and callose accumulation, another potential defence component (Rate and Greenberg, 2001).

SA is not necessary for the induction of resistance to all pathogens (Huckelhoven *et al.*, 1999; Pieterse and Van Loon, 1999). NPR1 can also function downstream of JA / Et independent of SA and SA can function independently of NPR1 in different resistance pathways (Pieterse *et al.*, 1998; Reuber *et al.*, 1998; Rairdan and Delaney, 2002). This indicates the complexity and interplay between hormones in the regulation of plant resistance to pathogens. The potential biosynthetic pathways for SA will be discussed in section 1.7.2.

1.6.2 Jasmonic Acid / Ethylene

JA and other jasmonates such as methyl-JA are synthesised via the octadecanoid pathway from linolenic acid (Leon and Sanchez-Serrano, 1999). Stresses such as herbivore damage or desiccation trigger the elevation of endogenous JA or other jasmonates that induce the expression of specific jasmonate responsive genes to combat the stress (Wasternak and Parthier, 1997; Berger 2001). Et is a gaseous molecule that has been implicated in many physiological and developmental processes including fruit ripening and seed germination (Abeles *et al.*, 1992). Unlike that for SA and JA, many elements in Et signal transduction have been described using genetic and biochemical approaches. Specific receptors bind ethylene and trigger a phosphorelay through two-component signal transducers that activate downstream protein kinase cascades, ending in stimulation of either gene transcriptional activators or repressors (McGrath and Ecker, 1998; Fluhr 1998; Fujimoto *et al.*, 2000).

Interestingly JA and Et, two very different molecules, with differing roles during a plant's life cycle interact in similar ways and often require concomitant activation during pathogen-specific resistance. For example, during the resistance response of *Arabidopsis* to *Alternaria brassicicola* (Schwein) Wiltshire increased concentrations of both JA and Et correlated with the induction of PDF1.2 (a common marker of JA / Et-dependent defence responses) independently of SA (Penninckx *et al.*, 1998; Thomma *et al.*, 1998). Analysis of *Arabidopsis* mutants blocked in JA or Et biosynthesis or sensitivity confirmed such observations but have also highlighted the importance of these two molecules in non-host resistance, susceptibility and induced systemic resistance (ISR) (Knoester *et al.*, 1998; Pieterse *et al.*, 1998; Vijayan *et al.*, 1998; Ton *et al.*, 2002; O'Donnell *et al.*, 2003). Both JA and Et may

act in resistance through regulation of ROS, HR, defence genes and the phenylpropanoid pathway, however, much remains unknown (Knoester *et al.*, 1998; Overmyer *et al.*, 2003).

1.7 Components of plant defence during pathogen-specific resistance

How components of defence initiated by *R* gene recognition and regulated by various signalling pathways, mediate pathogen-specific resistance remains poorly understood. The study of mutants (particularly of *Arabidopsis*) that are defective in various components of defence have revealed that each component has an additive effect and the loss of one does not necessarily result in resistance being completely compromised (Slusarenko and Schlaich, 2003). Therefore rather than there being a straightforward linear pathway from recognition to resistance, the pathway is more likely to be a complicated ‘lattice’ or ‘grid-like’ network of interconnecting signals and defensive components (Martin *et al.*, 2003). The better studied components found to be important in pathogen-specific resistance include; a HR, activation of the phenylpropanoid pathway, cell wall fortification, accumulation of phytoalexins and PR proteins (Hammond-Kosack and Jones, 1996).

1.7.1 Hypersensitive response

The HR is defined as rapid death of plant cells in association with the restriction of pathogen growth (Goodman and Novacky, 1994). The number of cells that die during a HR depends on the pathogen, and may not be restricted to cells having direct contact with the pathogen. The HR is often associated with, but not always required, for pathogen-specific resistance affective against biotrophic pathogens that require living host cells for survival (Yu *et al.*, 1998; Heath 2000). For non-biotrophic pathogens that do not require live host cells to survive, a role for the HR in pathogen-specific resistance is not obvious (Mayer *et al.*, 2001). However,

a role for HR cell death releasing signals that induce defensive responses in surrounding cells have been identified (Dangl *et al.*, 1996; Graham and Graham, 1999). The exact role that HR plays in pathogen-specific resistance is somewhat controversial and remains unclear (Heath 2000).

Several cellular changes that occur during a HR include, nuclear migration and alteration, cytoskeletal rearrangement and cytoplasmic shrinkage have been studied in detail (Heath *et al.*, 1997; Skalamera and Heath, 1998; Mould and Heath, 1999). Other changes often associated with a HR such as, cell wall alterations in the form of callose and wall bound phenolics are not as well studied (Hutcheson 1998). Key signals in the activation and development of HR appear to be ion fluxes, ROS and SA (Alvarez 2000; Heath 2000). The expression of HR is believed to be under strict molecular control as a form of programmed cell death (PCD), and in many ways resembles animal cell apoptosis (Jones 2001). However, the molecular components that control HR remain to be determined. Molecular analysis of lesion mimic mutants such as the Arabidopsis *lsd* mutants are providing the first insights into the complex positive and negative interplay that regulate cell death (Shirasu and Schulze-Lefert, 2000).

1.7.2 Phenylpropanoid pathway

The phenylpropanoid pathway is responsible for the production of a wide range of protective compounds for UV resistance, wounding and pathogen resistance (Dixon and Paiva, 1995). The rate-limiting enzyme that controls the extent of phenylpropanoid synthesis is phenylalanine ammonia-lyase (PAL) which converts L-

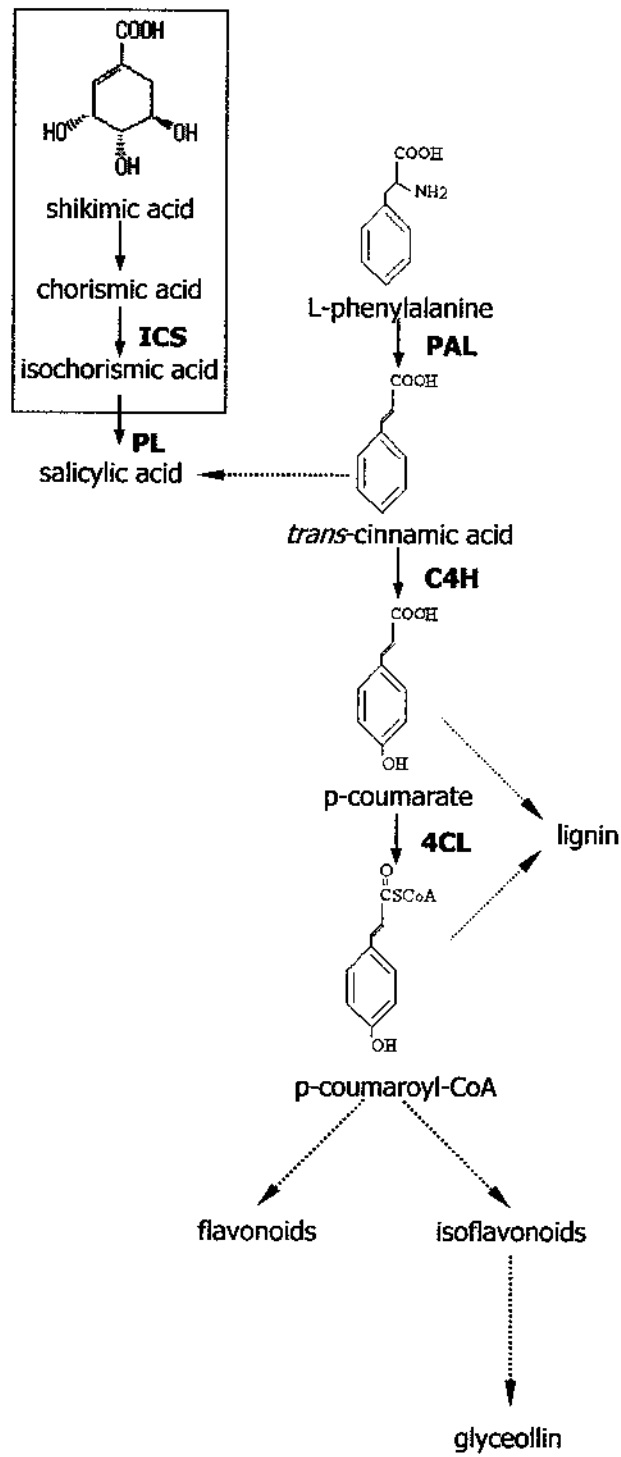
phenylalanine to *trans*-cinnamic acid (Figure 1.2). After this enzymatic event a number of specific branch pathways are possible for the formation of a variety of compounds, such as coumarins, benzoic acids, hydroxycinnamic acids, stilbenes, and flavonoids / isoflavonoids (Dixon *et al.*, 2002). However, all classes of phenylpropanoid compounds are not present in all species. For example, the isoflavonoids are limited to leguminous species eg. soybeans and have thus not been found in *Arabidopsis* (Dixon *et al.*, 2002).

The enzymatic steps that are involved in biosynthesis of the major classes of phenylpropanoid compounds are now well established, and many of the corresponding genes have been cloned. However, many of the biosynthetic enzymes are encoded by large gene families and the function of many individual family members remains unknown (Dixon *et al.*, 2002). One exception is the small *PAL* gene family of *Arabidopsis* with only three members. The first member cloned, *PAL1*, has high similarity in its amino acid sequence and expression pattern with *PAL* from other plant species (Ohl *et al.*, 1990). *PAL2* has a high degree of similarity to *PAL1* in both sequence and expression pattern, in contrast to *PAL3*, that has an additional intron (Wanner *et al.*, 1995). Less well understood is the regulatory genes and feedback mechanisms that orchestrate rapid, coordinated induction of phenylpropanoid defences in response to pathogen recognition (Blount *et al.*, 2000; Dixon *et al.*, 2002).

Phenylpropanoid biosynthetic pathways are among the most frequently observed metabolic activities that are transcriptionally induced upon infection of plants with pathogens (Hagemeier *et al.*, 2001). Rapid increases in the expression and enzyme activity of *PAL* and other phenylpropanoid genes is often associated

Figure 1.2 A simplified scheme of the phenylpropanoid pathway of higher plants.

The core reactions that form the backbone of the phenylpropanoid pathway are shown. Initially L-phenylalanine is converted to *trans*-cinnamic acid, that is converted to p-coumarate and then finally to p-coumaroyl-CoA. Phenylpropanoid defence compounds such as salicylic acid (SA), lignin, flavonoids and isoflavonoids (eg. glyceollin) are derived via multi-step conversions of these core reaction products (represented by dashed arrows). SA may also be formed by a phenylpropanoid independent pathway, via a shikimic acid multi-step conversion to isochorismic acid (black box) and then SA. Abbreviations: C4H, cinnamate 4-hydroxylase; 4CL, 4-coumarate:CoA ligase; ICS, isochorismate synthase; PAL, phenylalanine ammonia-lyase; PL, pyruvate lyase. Figure is a compilation of information from Dixon and Paiva (1995), Wildermuth *et al.* (2001) and Dixon *et al.* (2002).



with plant resistance (Bhattacharyya and Ward, 1988; Haberer *et al.*, 1989). Three phenylpropanoid-derived compounds of particular importance in pathogen-specific resistance are SA, lignin (cell wall fortification) and some phytoalexins (antimicrobial activity) (Dixon and Paiva, 1995) (Figure 1.2). However, in addition to the biosynthesis of SA by the phenylpropanoid pathway it is likely that SA is also synthesised via isochorismate synthase (Wildermuth *et al.*, 2001) (Figure 1.2).

1.7.3 Cell wall fortification

Microbes must negotiate the cell wall of plants to reach the nutrient rich cytoplasm. Fortification of the cell wall could increase resistance against biotrophic pathogens by impeding the leakage of cytoplasmic contents and therefore reduce nutrient availability. For necrotrophs that actively break down the cell wall, fortification could reduce the effectiveness of degrading enzymes and also prevent toxins from reaching the plant cell (Hammond-Kosack and Jones, 1996). At the point of contact with a pathogen and in cells surrounding a HR there is usually an accumulation of cell wall fortification compounds, such as glycoproteins, lignin, suberin and callose (Hammond-Kosack and Jones, 1996; Benhamou and Nicole, 1999).

Protein cross linking within the wall via basic hydroxyproline-rich glycoproteins (HRGP) is thought to play a key role in the organisation of the primary cell wall architecture and may act as foci for initiation of lignin and suberin polymerisation (Showalter 1993). Both lignin and suberin have a number of roles during plant growth and development and as cell wall fortification compounds during plant resistance to pathogens (Sherf and Kolattukudy, 1993; Franke *et al.*, 2002). Lignin and suberin form a physical barrier against penetration by an invading pathogen and also prevent water loss from plant cells (Moershbacher *et al.*, 1990;

Whetten and Sederoff, 1995; Bolwell *et al.*, 1997). The deposition of lignin and suberin may in part be under the control of ROS (Graham and Graham, 1991; Facchini *et al.*, 2002).

Lignins are complex aromatic heteropolymers composed mainly of three phenylpropanoid-derived hydroxycinnamyl alcohol monomers (monolignols), *p*-coumaryl, coniferyl, and sinapyl alcohols (Boerjan *et al.*, 2003). Although researchers have studied lignin for more than a century, many aspects of monolignol biosynthesis and its formation into lignin remain unresolved (Lewis 1999; Boudet 2000). The aromatic domain of suberin is unique and distinct from lignin, comprised of primarily (poly)hydroxycinnamates while the aliphatic domain is distinct from cutin in terms of its chemical composition and cellular location. Similarly to lignin, controversy still remains over the biosynthesis and assembly of suberin (Bernards and Lewis, 1998; Bernards 2002).

Callose is a heterogeneous β -1,3-glucan that is deposited in many specialised plant cell walls or wall-associated structures, acting as a permeability barrier and strengthening or sealing agent during growth and development (Stone and Clarke, 1992). Callose deposition can be induced by pathogens as a major component of inducible plant cell wall appositions (papillae) or around HR cells as part of the complex cell wall strengthening process that halts pathogen invasion (Aist 1976; Skou *et al.*, 1984). Callose may also provide a medium for the deposition of toxic compounds to pathogens, impede nutrient transfer from plant cells to pathogen, or delay pathogen growth long enough for other plant defences to become active (Stone and Clarke, 1992).

1.7.4 Phytoalexins

Plants can employ chemical defence either as pre-formed anti-microbial substances (phytoanticipins) generally correlated with non-host resistance, or as induced antimicrobial substances (phytoalexins) which accumulate after contact with a pathogen (Van Etten *et al.*, 1994). Phytoalexins are therefore defined as low-molecular-weight secondary plant metabolites with antimicrobial properties that are absent in healthy tissue and accumulate rapidly at the site of attempted pathogen infection (Smith 1996). Strong correlative evidence exists for phytoalexin involvement in pathogen-specific resistance. For example, 1) localisation and timing of phytoalexin accumulation in infected tissue in relation to pathogen development, 2) rapid phytoalexin production in pathogen-specific resistance interactions, 3) use of metabolic inhibitors that enhance susceptibility and block phytoalexin production, 4) a positive relationship between pathogen virulence and tolerance of phytoalexins, and 5) an increase of plant tissue resistance by stimulation of phytoalexin production prior to inoculation (Keen 1981).

Extensive research on phytoalexins has provided insight into the biosynthesis and chemical diversity of these molecules as well as their role in defence (Hammerschmidt 1999). For example, glyceollin, a phytoalexin of soybeans (Ayers *et al.*, 1976), is synthesised via the phenylpropanoid pathway (Figure 1.2), whereas camalexin, a phytoalexin of *Arabidopsis* (Tsuji *et al.*, 1992), is synthesised via the tryptophan pathway (Hammerschmidt 1999). Both phytoalexins are induced following pathogen recognition and have direct inhibitory effects on certain pathogens *in vitro* (Bhattacharyya and Ward, 1987b; Tsuji *et al.*, 1992). However, *Arabidopsis* mutants deficient in camalexin are the only plants in which phytoalexin-deficient (*pad*) mutants have been reported (Glazebrook and Ausubel, 1994). The use

of *pad* mutants has not as yet clarified the role of camalexin in resistance or how its deposition is regulated (Thomma *et al.*, 1999b). Therefore substantial information on phytoalexins has been generated indicating their importance in resistance, but some doubt remains due to the correlative nature of the research conducted thus far.

1.7.5 Pathogenesis-related proteins

The term PR protein was first used to describe numerous extracellular proteins that accumulated in response to TMV infection of tobacco and have since been identified in a number of pathogen-specific interactions (Linthorst 1991). The definition of a PR protein has subsequently been broadened to include intra- and extracellularly localised proteins that accumulate in plant tissue after pathogen attack (Bowles 1990). PR proteins comprise low-molecular-weight proteins (eg. acidic and basic chitinases and glucanases) that accumulate at the site of infection and during SAR, in distal tissues (Ward *et al.*, 1991). The role of PR proteins in resistance has been supported by transgenic studies where high expression of PR proteins leads to increased resistance to certain pathogens (Alexander *et al.*, 1993; Lui *et al.*, 1994). Many PR proteins have been identified in Arabidopsis such as PR-1, PR-2, PR-3, PR-4, PR-5 and PDF1.2 (Uknes *et al.*, 1993; Samac *et al.*, 1990; Potter *et al.*, 1993; Penninckx *et al.*, 1996). The synthesis of PR proteins can be grouped into two, those dependent on SA (PR-1, PR-2 and PR-5) and those dependent on JA / Et (PR-3, PR-4 and PDF1.2) (Clarke *et al.*, 1998, Penninckx *et al.*, 1998). However, the signals responsible for the induction of PR proteins appear to be more complex than simple SA or JA / Et dependency (Nawrath and Metraux, 1999; Tierens *et al.*, 2002).

1.8 Arabidopsis / pathogen model systems

Arabidopsis is a small flowering cruciferous plant, distributed across Europe, Asia and North America (Al-Shehbaz and O’Kane, 2002). It was introduced as an

experimental system in the 1940's (Langridge 1955) and has become important for investigating many aspects of higher plant biology (Meinke *et al.*, 1998). It has a number of experimental advantages, including its small size, short life cycle, self-fertility, and the production of large amounts of seed. These attributes allow for rapid growth and analysis of a large number of individuals in a minimum of space over a relatively short time. *Arabidopsis* also has a compact genome with a low percentage of repetitive DNA, making it an ideal organism for genetic and molecular studies such as mutant analysis, cloning of genes, and detailed mapping of its genome. It can be easily genetically engineered (eg. *Agrobacterium*-mediated transformation) allowing for detailed analysis of gene function and expression (Davis 1993). The *Arabidopsis* genome has also been sequenced and consists of over 25,000 genes on five chromosomes, which encode proteins from 11,000 families (The *Arabidopsis* Genome Initiative 2000).

Despite the advantages of *Arabidopsis* as an experimental plant, it took until the late 1980's before the first *Arabidopsis* / pathogen model systems emerged (Koch and Slusarenko, 1990). In the last decade many examples of *Arabidopsis* / pathogen (fungal, bacterial, viral, Oomycete and nematode) model systems with *R* gene mediated resistance or susceptibility have been characterised (Baker *et al.*, 1997). Well characterised *Arabidopsis* / pathogen model systems and the development of mutagenic and transgenic techniques has lead to systematic attempts to dissect the molecular and genetic basis of plant disease resistance (Buell 1998). This type of approach was previously difficult in many plant host species due to the relative intractability of genetic analysis, caused by long generation times and large, polyploid, or repetitive genomes (Glazebrook *et al.*, 1997). Therefore some of the most extensive studies in plant pathology have been conducted in the last decade

utilising Arabidopsis / pathogen model systems (Shapiro 2000). Two of the most commonly studied Arabidopsis / pathogen model systems are those of Arabidopsis with the pathogens *P. parasitica* or *P. syringae* pv. *tomato*.

1.9 The Arabidopsis / *Peronospora parasitica* plant / pathogen model system

1.9.1 *Peronospora parasitica*

The class Oomycetes in the kingdom Chromista contains organisms that are fungal-like in appearance but are completely different from the true fungi in their morphology, physiology, biochemistry and molecular characteristics (Kumar and Rzhetsky, 1996). Many important Oomycete plant pathogens belong to the orders Pythiales (genera *Phytophthora* and *Pythium*) and Peronosporales (genus *Peronospora*) (Hall 1996). Oomycete plant pathogens have a variety of parasitic lifestyles including necro-, bio- and hemibiotrophy (Drenth and Goodwin, 1999). The obligate biotrophic parasitism in the order Peronosporales, family Peronosporaceae is considered to be derived from *Phytophthora* lineages that lost the ability to produce zoospores (Cooke *et al.*, 2000). It involves the development of hyphal networks within host tissue and the production of haustoria that penetrate plant cell walls and invaginate the host cell plasma membrane (Sargent 1981). These pathogens are prevalent in cool, damp conditions, establishing intimate relationships with a wide range of plants, and cause significant damage to many crop species (Channon 1981).

P. parasitica is an obligate biotroph of the family Peronosporaceae that was originally described as a group of organisms that caused 'downy mildew' of Brassicas. Recently *P. parasitica* and five other downy mildew species have been placed in a new subgroup, renaming the species *Hyaloperonospora* Constant. *parasitica* (Pers.:Fr) Fr. (Constantinescu and Fatehi, 2002). However, for consistency and to minimise confusion with previous research the organism will be referred to hereafter in this thesis as *Peronospora parasitica*.

1.9.2 Arabidopsis / *P. parasitica* as a plant / pathogen model system

Isolates of *P. parasitica* occur naturally on wild populations of Arabidopsis, and the infection process has been well documented (Koch and Slusarenko, 1990; Uknes *et al.*, 1992) (Figure 1.3). A range of resistant interactions has also been observed that are dependent on the specific *P. parasitica* isolates used and Arabidopsis genotype (Holub *et al.*, 1994). The pathogen-specific resistant Arabidopsis / *P. parasitica* interactions have been utilised to the greatest extent to identify, map and clone specific *RPP* (recognition of *P. parasitica*) genes. To date 27 *RPP* genes have been postulated on the basis of differential interactions, but only a minority have been cloned (Slusarenko and Schlaich, 2003) (Table 1.2). The *RPP* genes are not randomly distributed on the Arabidopsis chromosomes, but most reside in major recognition gene complexes (MRC), interspersed with resistance genes that are active against other pathogens (Holub 1997).

The structures of *RPP* proteins (Table 1.2) that have been identified so far fall into either class two or three, as described in Table 1.1. However, an unexpected complexity and diversity beyond these two structural classes in requirements for various signal transduction pathways and defence components has been revealed by studies of Arabidopsis mutants (Parker *et al.*, 2000). For example, *RPP8* and *RPP13*-

Figure 1.3 The lifecycle of *P. parasitica* during susceptible interactions with Arabidopsis.

Sexual, homothallic oospores are capable of persisting in infected tissue or soil for a number of years. Infections arise initially from oospores that germinate and the subsequent mycelium penetrates Arabidopsis seedlings. Intercellular hyphae bearing haustoria that penetrate and feed on host cells, colonise the entire plant. After 1 wk conidiophores grow out of stomata and release spherical asexual conidiospores by movement of air currents. On contact with an Arabidopsis leaf the conidia germinate and initiate the next round of infection. Also at 1 wk further oospores are produced within the Arabidopsis tissue. Figure modified from Shusarenko and Schlaich (2003)

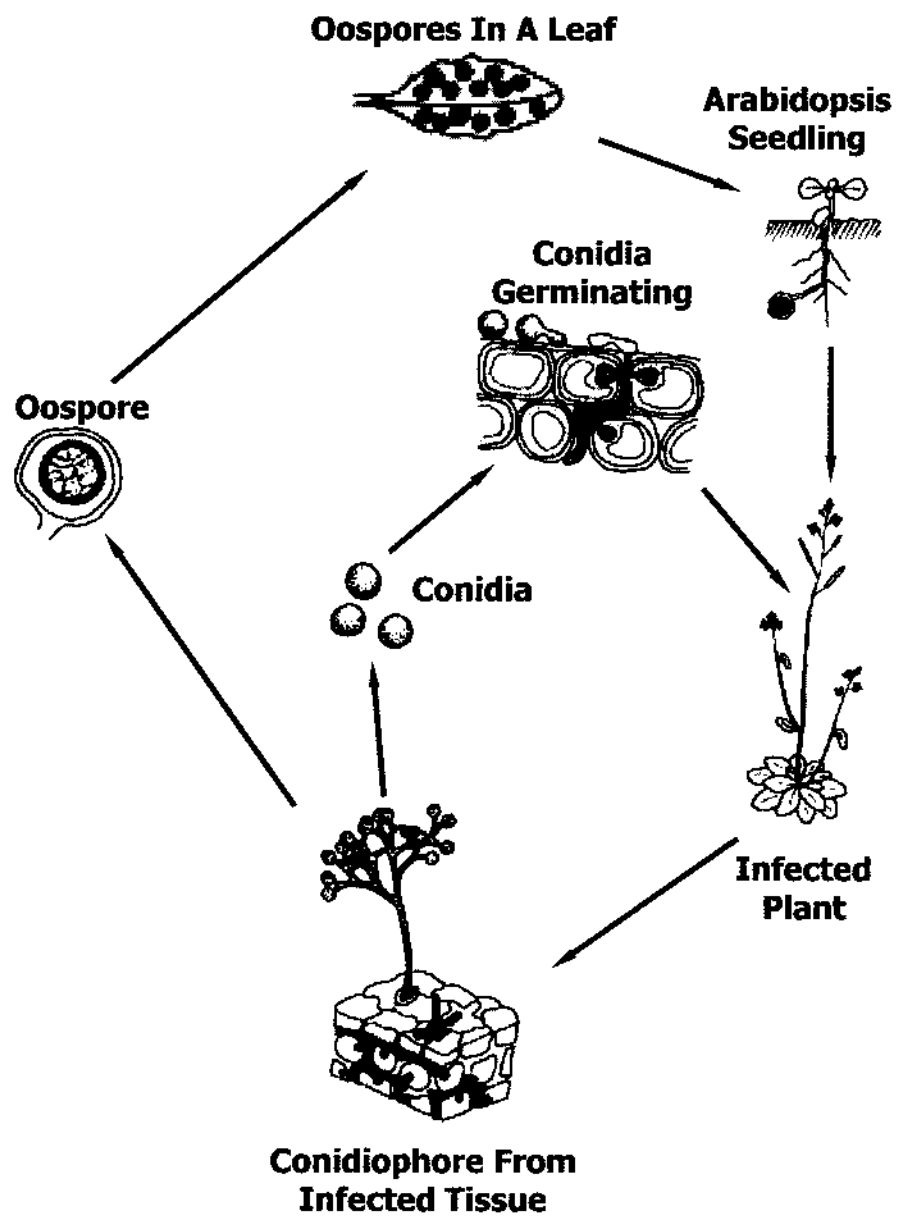


Table 1.2 Location of *RPP* genes in major recognition gene complexes (MRC) on *Arabidopsis* chromosomes.

If cloned the structure of the RPP protein encoded by the *RPP* gene is shown.

MRC	Chromosomal Location	RPP gene	RPP Structure
MRC-A	One	No <i>RPP</i> genes	
MRC-B	One	<i>RPP6</i> <i>RPP7</i> <i>RPP25</i> <i>RPP27</i>	
MRC-F	Three	<i>RPP1-WsA</i> formerly <i>RPP10*</i> <i>RPP1-WsB</i> formerly <i>RPP14*</i> <i>RPP1-WsC</i> formerly <i>RPP1*</i> <i>RPP1-Nd</i> <i>P1-Nd</i> formerly <i>RPP26</i> <i>RPP13-Nd</i> formerly <i>RPP16</i> <i>RPP13-Nd</i> formerly <i>RPP17</i> <i>RPP13-Nd*</i> <i>RPP13-RLD</i> formerly <i>RPP11</i>	TIR-NBS-LRR TIR-NBS-LRR TIR-NBS-LRR CC-NBS-LRR
MRC-H	Four	<i>RPP2</i> <i>RPP4*</i> <i>RPP5*</i> <i>RPP12</i> <i>RPP18</i>	 TIR-NBS-LRR TIR-NBS-LRR
MRC-J	Five	<i>RPP8*</i> <i>RPP8</i> formerly <i>RPP23</i> <i>RPP21</i> <i>RPP22</i> <i>RPP24</i>	 CC-NBS-LRR
Not in MRCs	Not mapped	<i>RPP3</i>	
	One	<i>RPP9</i>	
	Two	<i>RPP19</i>	
	Two	<i>RPP20</i>	
	Two	<i>RPP28</i>	

* Denotes *RPP* genes that have been cloned. Table modified from Slusarenko and Schlaich (2003).

RLD both encode RPP proteins from class two, with *RPP13-RLD* requiring a functional EDS1 protein whereas *RPP8* does not (Aarts *et al.*, 1998). Coupled with limited correlative biochemical data, much still remains unknown about *RPP* gene mediated resistance (Slusarenko and Schlaich, 2003). Also little progress has been made in the process of characterising the products of *Avr* genes from *P. parasitica*. Only a recent map-based cloning of genes from *P. parasitica* has identified a region containing the *Avr* gene, *ATR1Nd* (*Arabidopsis thaliana*-recognised *Avr* gene by *RPP1-Nd* R gene) (Rehmany *et al.*, 2003).

1.10 The *Arabidopsis* / *Pseudomonas syringae* pathovar *tomato* plant / pathogen model system

1.10.1 *Pseudomonas syringae* pathovar *tomato*

Bacterial pathogens of plants are derived from genera belonging to the kingdom Monera (Bacteria). The genus *Pseudomonas* of phylum Gracilicutes consists of a very diverse assemblage of bacterial organisms. Phytopathogenic *Pseudomonas* species cause an array of diseases in plants ranging from necrotic lesions and spots on fruit, stems, and leaves, to galls, scabs, rots, cankers, blights and wilting. *Pseudomonas* induced plant diseases are worldwide in distribution and involve representatives of most major groups of higher plants (Schroth *et al.*, 1981). The *P. syringae* group is principally known as an assemblage of foliar pathogens, consisting of at least 40 pathovars based on host range, among different plant species (Gardan *et al.*, 1999).

P. syringae pv. *tomato* is a Gram-negative, rod-shaped, biotrophic bacterium that is the casual agent of leaf 'bacterial speck' diseases in many crop species, but especially in tomato (Davis *et al.*, 1991). Serious outbreaks of disease caused by *P. syringae* pv. *tomato* are relatively infrequent, but are favoured by high leaf wetness,

cool temperatures and cultural practices that allow bacteria to be disseminated between plant hosts (Preston 2000). *P. syringae* pv. *tomato* first flourishes on the surface of tomatoes as an epiphyte before it enters into the intercellular space of leaves through stomata or wounds (Hirano and Upper, 2000) (Figure 1.4). In susceptible interactions a rapid multiplication in numbers results in necrotic lesion formation whereas resistant interactions have low numbers and a HR (Bashan *et al.*, 1981). The first plant *R* gene was cloned from tomato with the isolation of the *Pto* gene that confers resistance against *P. syringae* pv. *tomato* strains carrying the *AvrPto* gene (Martin *et al.*, 1993) and the complete genome of *P. syringae* pv. *tomato* strain DC3000 was recently sequenced (Buell *et al.*, 2003).

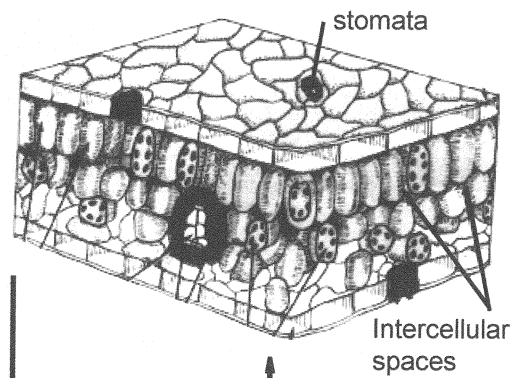
1.10.2 Arabidopsis / *P. syringae* as plant / pathogen model systems

P. syringae is easily cultured and amenable to a wide range of molecular, genetic and cell biology techniques. Many *P. syringae* pathovars (*atropurpurea*, *glycinea*, *maculicola*, *phaseolicola*, *pisi* and *tomato*) produce susceptible or resistant interactions on Arabidopsis leaves when artificially infiltrated into intracellular spaces (Dong *et al.*, 1991; Crute *et al.*, 1994). In particular, Arabidopsis exhibits pathogen-specific resistance or susceptibility to strains of *P. syringae* pv. *tomato* that are similar to those observed on naturally infected tomato (Whalen *et al.*, 1991). Despite concerns about the lack of natural infection and artificial inoculation methods, the Arabidopsis / *P. syringae* systems have flourished as recognised model plant / pathogen systems (Preston 2000; Katagiri *et al.*, 2002). These systems have been especially beneficial in investigations of *R* and *Avr* genes.

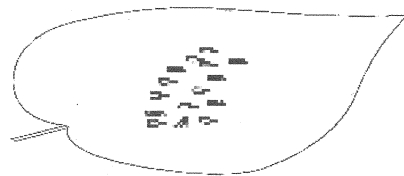
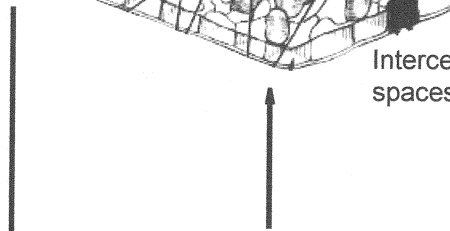
The product of the *AvrPphB* gene of *P. syringae* pv. *phaseolicola* is perceived in Arabidopsis by at least two *R* proteins, *RPS5* and *PBS1*. *RPS5* encodes a class two *R* protein and *PBS1* encodes a functional protein kinase with similarity to

Figure 1.4 The infection process of *P. syringae* pv. *tomato* during susceptible interactions.

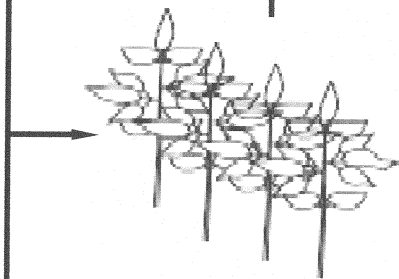
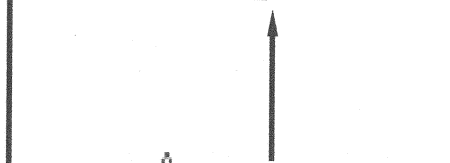
An immigrant bacterium arrives on a leaf either through the air or from growth on a seedling that has germinated in soil containing infected tissue. If conditions are favourable the bacteria will multiply epiphytically and finally enter stomata or wounds. *P. syringae* pv. *tomato* continue to multiply intercellularly and often emerge out of stomata onto the leaf surface. Bacteria will again be spread by air or in diseased leaves on the soil. Figure modified from Hirano and Upper (2000).



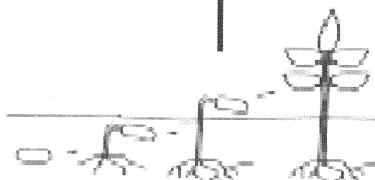
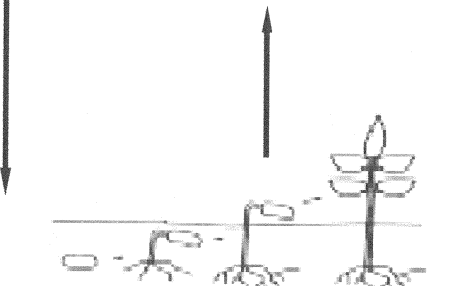
Bacteria also multiply within the intercellular spaces of leaves and emerge out of stomata



Epiphytic bacterial multiplication on the surface of leaves



Bacteria immigrate to plants by seedling germination or the air



Seedlings germinating in soil containing infected tissue

the Pto class one R protein (Warren *et al.*, 1998; Swiderski and Innes, 2001). RPS5, PBS1 and AvrPphB proteins all contain a MM, suggesting a common localisation of the three proteins at the plasma membrane (Luderer and Joosten, 2001). The AvrRps4 protein of *Pseudomonas syringae* pv. *psidi* is perceived by the Arabidopsis RPS4 protein. The AvrRps4 protein is hydrophobic and the *RPS4* gene encodes a class three R protein that is predicted to be cytosolic (Gassmann *et al.*, 1999).

The products of the *AvrRpm1* gene of *Pseudomonas syringae* pv. *maculicola* and *AvrB* gene of *Pseudomonas syringae* pv. *glycinea* are both perceived by the Arabidopsis RPM1 protein (Bisgrove *et al.*, 1994). The RPM1 protein encodes a class two R protein that is likely to reside at the cytoplasmic face of the plasma membrane (Boyes *et al.*, 1998). The proteins encoded by AvrRpm1 and AvrB do not share homology except for a MM that localises the proteins at the plasma membrane of the host plant (Nimchuk *et al.*, 2000). The perception of AvrRpm1 and AvrB by RPM1 is believed to be indirect, with the third component RIN4 a possible virulence target required for perception (Eckardt *et al.*, 2001).

The AvrRpt2 protein of *P. syringae* pv. *tomato* is perceived by the Arabidopsis RPS2 protein (Kunkel *et al.*, 1993). AvrRpt2 encodes a protein that is secreted and promotes virulence in the absence of RPS2 in the host (Chen *et al.*, 2000). RPS2 is a cytoplasmic class two R protein (Bent *et al.*, 1994) and might be indirectly perceived after AvrRpt2 initially binds to a third protein component, p75, a potential virulence target (Leister and Katagiri, 2000). Direct evidence for type III-dependent translocation of AvrRpt2 from *P. syringae* pv. *tomato* has been shown and all Avr proteins from *P. syringae* that are specific to Arabidopsis are believed to be delivered to the plant cells via this protein secretion system (Mudgett and Staskawicz, 1999; Preston 2000).

As with pathogen-specific resistance to *P. parasitica*, there is still limited knowledge on the particular signal transduction pathways and defence components that are important for resistance against *P. syringae*. Studies of *Arabidopsis* mutants and limited biochemical studies have also revealed that resistance is complex and as yet not fully understood.

1.11 The soybean / *Phytophthora sojae* plant / pathogen model system

1.11.1 *Phytophthora sojae*

The *Phytophthora* genus (kingdom Chromista, class Oomycetes, order Pythiales) comprises some 60 species of destructive Oomycete plant pathogens of bio-, necro- and hemibiotrophic lifestyles, that cause rots of roots, crowns, stems, leaves, and fruits of an enormous range of plants (Erwin and Ribeiro, 1996; Cooke *et al.*, 2000). The economic damage to crops caused by *Phytophthora* species in the USA alone runs into billions of dollars annually, and worldwide the cost is many times this amount (Erwin and Ribeiro, 1996). *P. sojae* is an aggressive hemibiotroph that has a very narrow host range, only causing root and stem rot of soybeans and a few related leguminous species (Erwin and Ribeiro, 1996). *P. sojae* races are morphologically indistinguishable but can be determined by soybean cultivar specific infection (Laviolette and Athow, 1977). Greater than forty races of *P. sojae* have been identified and are believed to have arisen by clonal evolution and rare outcrosses (Forster *et al.*, 1994). Disease caused by *P. sojae* is an ongoing problem in soybean growing areas around the world (Anderson and Buzzell, 1992a; Yanchun and Chongyao, 1993; Ryley *et al.*, 1998). In the state of Ohio (USA) alone, *P. sojae* root rot of soybeans causes a \$120 million annual loss to growers (The Department of Plant Pathology at the Ohio State University, <http://plantpath.osu.edu/highlights->

1999.php). At least six races of *P. sojae* have been isolated from soybean-growing regions of eastern Australia (Ryley *et al.*, 1998). In Australia, these races of *P. sojae* have previously caused up to 90% soybean plant losses (Rose *et al.*, 1982).

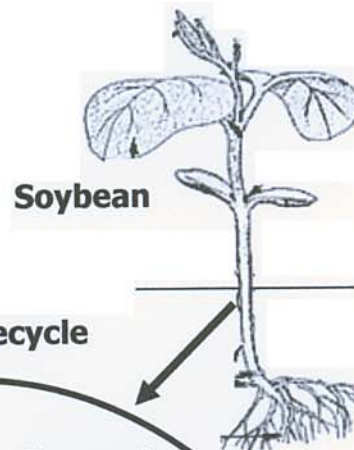
1.11.2 Soybean / *P. sojae* as a plant / pathogen model system

One of the most thoroughly investigated plant / Oomycete model systems is the soybean / *P. sojae* system (Judelson 1996). The life cycle of *P. sojae* during susceptible interactions with soybeans has been described in detail (Erwin and Ribeiro, 1996) (Figure 1.5). Resistant and susceptible interactions at the ultrastructural level between soybean / *P. sojae* have also been thoroughly examined (Ward *et al.*, 1979; Ward *et al.*, 1989b; Enkerli *et al.*, 1997). The complex exchange of signalling cues between the pathogen and the host are not well understood (Qutob *et al.*, 2002). Many *P. sojae* molecules (not encoded by *Avr* genes) such as hepta- β -glucans, glycoproteins and elicitors have been described that elicit non pathogen-specific defence responses, (Sharp *et al.*, 1984; Dorey *et al.*, 1997; Qutob *et al.*, 2003). A *P. sojae* protein has also been identified that induces necrosis as the pathogen changes from biotrophy to necrotrophy in soybean tissues (Qutob *et al.*, 2002).

The *Phytophthora* Genome Consortium (PGC) (<http://xgi.ncgr.org/pgc>) that superseded the *Phytophthora* Genome Initiative is a collaboration that aims to sequence the genomes of plant pathogenic Oomycetes, including *P. sojae*. Genetic analysis of *P. sojae* has defined ten out of the 13 or more *Avr* genes *Avr1a*, *Avr1b*, *Avr1d*, *Avr1k*, *Avr3a*, *Avr3b*, *Avr3c*, *Avr4*, *Avr5* and *Avr6* (Whisson *et al.*, 1995; May *et al.*, 2002). Positional cloning has identified *Avr1a*, *Avr1b*, *Avr1k*, *Avr4* and *Avr6* loci and allowed the first *P. sojae* *Avr* protein *Avr1b*, to be cloned and characterised (Tyler 2001; MacGregor *et al.*, 2002). The *Avr1b* protein is a hydrophilic protein

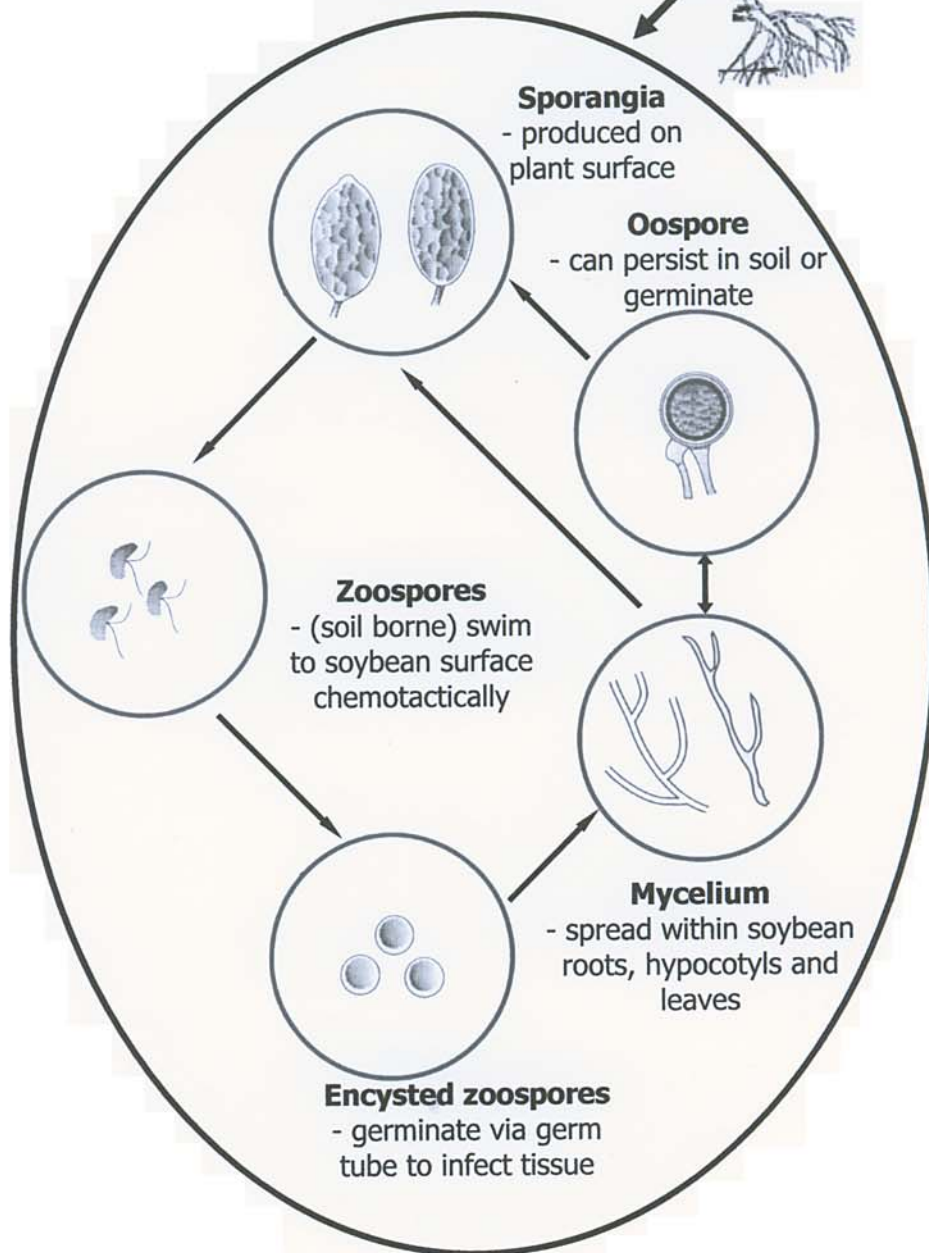
Figure 1.5 Components of the lifecycle of *P. sojae* during susceptible interactions with soybeans.

Sexual, homothallic, paragynous oospores are capable of persisting in infected tissue or soil for a number of years. Oospores can germinate producing hyphae that directly penetrate soybean roots or stems, or via asexual, nonpapillate, ovoid and obpyriform sporangia. Mycelium also produce oospores and sporangia within soybean tissue. Upon flooding of the soil, sporangia release uninucleate, biflagellate zoospores. The zoospores swim within the free water and are chemotactically attracted to soybeans. When *P. sojae* zoospores reach soybean tissue they encyst and then penetrate the tissue via germ tubes. In the early hours of infection hyphae spread intercellularly, obtaining nutrients biotrophically via haustoria, before spreading intracellularly and feeding necrotrophically. A few days after penetration oospores are again produced within the soybean tissue. Figure modified from Erwin and Ribeiro (1996).



Soybean

***P. sojae* Lifecycle**



specifically expressed during infection and triggers a vigorous defence response in soybean plants containing the *R* gene, *Rps1b* (Tyler 2002).

At least 14 soybean *R* genes (*Rps* genes) have been described that protect soybeans against *P. sojae* through recognition of specific *Avr* gene products that trigger resistance (Anderson and Buzzell, 1992b; Buzzell and Anderson, 1992; Burnham *et al.*, 2003). Six *Rps* genes are clustered at the *Rps1* locus (*Rps1a*, *Rps1b*, *Rps1c*, *Rps1d*, *Rps1e* and *Rps1k*) and three at the *Rps3* locus (*Rps3a*, *Rps3b*, and *Rps3c*). There has been a number of efforts to clone *Rps* genes, for example, *Rps2* (Kanazin *et al.*, 1996) and *Rps1k* (Salimath and Bhattacharyya, 1999; Gardner *et al.*, 2001). In both cases a BAC contig spanning the *Rps* gene has been isolated.

Due to the lack of cloned *Rps* and *Avr* genes of soybean and *P. sojae* respectively, understanding of pathogen-specific recognition events, signal transduction and defence components important for resistance is poor. Examination of a small number of soybean mutants (for example, Kossak *et al.*, 1996; Hoffman *et al.*, 1999) and biochemical studies (for example, Bhattacharyya and Ward, 1987a; Graham *et al.*, 1990) represent the limited knowledge of pathogen-specific resistance in soybeans to *P. sojae*.

1.12 Abiotic elicitors of defence

Apart from general and race-specific (biotic) elicitors of pathogen origin, abiotic elicitors such as the air pollutant ozone, and heavy metals eg. silver nitrate also trigger plant defence components. Ozone stimulated plant defence components have been documented in plant species such as *Arabidopsis* (Sharma and Davis, 1994), tobacco (Bahl *et al.*, 1995) and soybean (Booker and Miller, 1998). Silver nitrate-stimulated plant defence components have been documented in plant species such as *Arabidopsis* (Hammerschmidt *et al.*, 1993) and soybeans (Cahill and Ward,

1989b). Abiotic elicitors have been found to be useful for analysing defence induction in the absence of a pathogen. The system is thus simplified.

Receptors that trigger plant defence responses to race-specific elicitors have been cloned and described in section 1.4.2. Receptors for general elicitors have also been cloned, for example, a protein with affinity for a *P. sojae* cell wall hepta glucan (Mithofer *et al.*, 2000). It remains unknown how abiotic elicitors trigger plant defence components, but membrane degradation may be a stimulus (Mishra and Choudhuri, 1999). Downstream of abiotic elicitation a number of signal transduction pathways and induced defence components are similar to those activated during race-specific resistance, particularly those that involve the phenylpropanoid pathway (Kervinen *et al.*, 1998; Rossetti and Bonatti, 2001). However, with a limited number of studies into abiotic elicitor induced plant defence signals and components, much still remains to be determined.

1.13 Absciscic acid (ABA)

There is compelling evidence that in addition to SA, JA and Et, ABA is a regulator of the interaction of plants with pathogens, but this possibility has not been explored to any great extent. Firstly discovered in the early 1960's as a growth inhibitor that accumulated in abscising cotton fruit ('abscisin II') (Okhuma *et al.*, 1963) and that promoted bud dormancy in leaves of sycamore trees ('dormin'), was subsequently renamed as absciscic acid (ABA) (Addicott and Carns, 1983). The synthesis of ABA has been identified in all higher and lower plants, as well as several phytopathogenic fungi (Hartung and Gimmler, 1994; Wu and Shi, 1998). ABA is known to have numerous roles in plants and indeed one study (Hoth *et al.*, 2002) has ABA as a regulator of more than 1300 *Arabidopsis* genes. Regulatory roles for ABA during seed development, primary dormancy and in response to

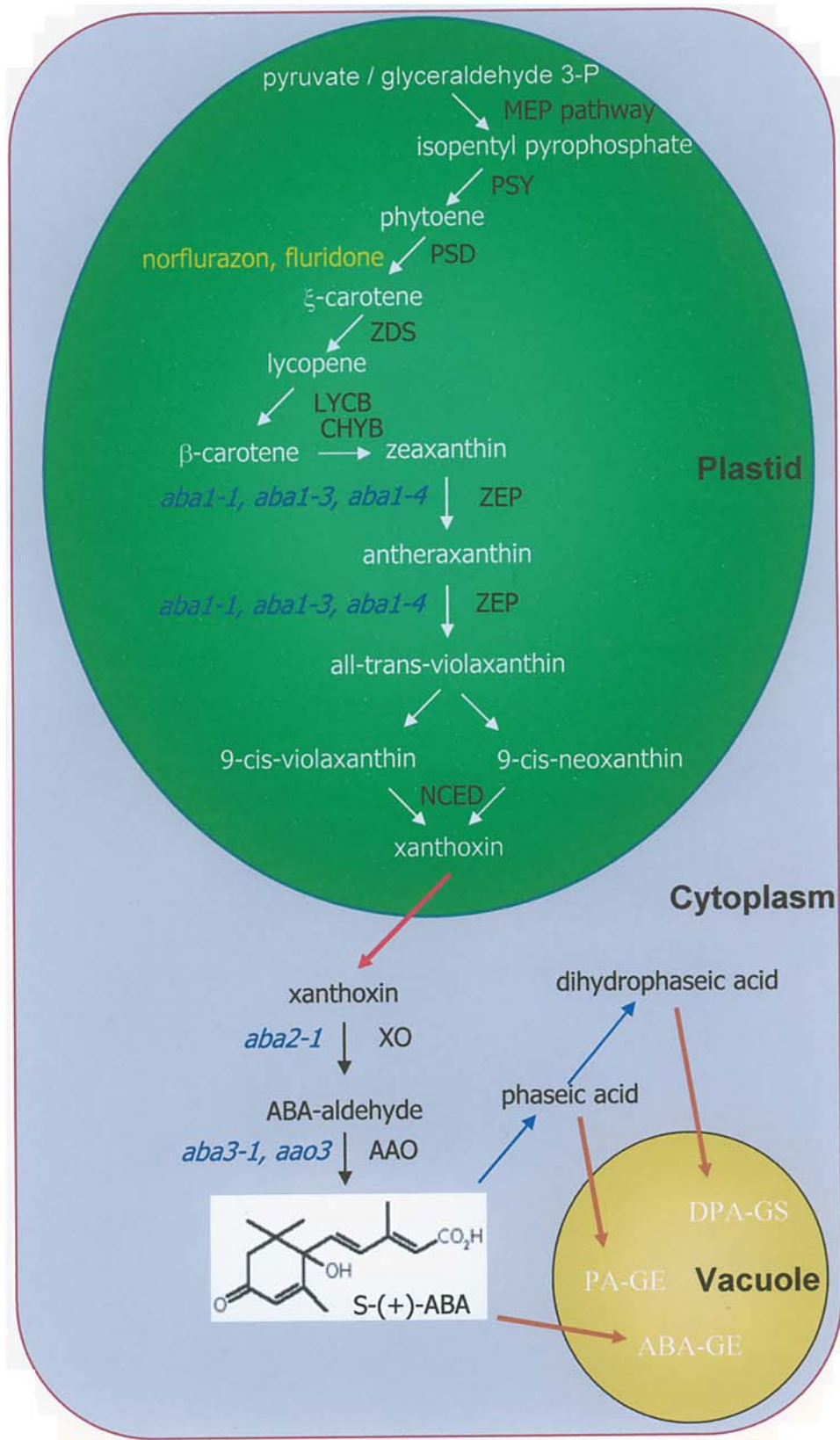
environmental stresses such as drought, salinity and cold are well documented (Davies 1995). ABA has also been implicated in the regulation of the cell cycle, cell division and elongation, cell death and responses to UV radiation and pathogen attack (Leung and Giraudat, 1998; Albinsky *et al.*, 1999; Fath *et al.*, 1999; Rock 2000; Yang *et al.*, 2002).

ABA is a sesquiterpenoid ($C_{15}H_{20}O_4$) with the naturally occurring form S-(+)-ABA, having a 2-cis,-4-trans side chain (Finkelstein and Rock, 2002) (Figure 1.6). In contrast with other plant hormones, endogenous concentrations of ABA can rise and fall dramatically during its action (Zeevart and Creelman, 1988). The regulation of processes controlled by ABA is primarily at the level of ABA biosynthesis and catabolism. ABA action requires synthesis of the relevant enzymes rather than redistribution of existing ABA pools (Zeevart and Creelman, 1988; Millborrow 2001). There is also good evidence that ABA is a drought signal that is transported via xylem from roots to shoots (Hartung *et al.*, 2002).

Cellular ABA concentrations are influenced by transport, the movement of ABA by protein carriers and passive uptake (Cutler and Krochko, 1999). As a weak acid (pKa-4.8), ABA is mostly uncharged when present in the relatively acidic apoplastic compartment of plants and can easily enter cells across the plasma membrane. The major control of ABA distribution among plant cell compartments follows the “anion trap” concept: the dissociated (anion) form of this weak acid accumulates in alkaline compartments (eg. illuminated chloroplasts) and may redistribute according to the steepness of the pH gradient across membranes. In addition to partitioning according to the relative pH of compartments, specific uptake carriers contribute to maintaining a low apoplastic ABA concentration in unstressed plants (Finkelstein and Rock, 2002).

Figure 1.6 Pathways of ABA biosynthesis and catabolism in a simplified higher plant cell.

The first biosynthetic steps take place in the plastid (white arrows), with multi-step conversions of pyruvate and glyceraldehyde 3-P to isopentyl pyrophosphate (IPP), IPP to β -carotene, β -carotene to zeaxanthin and zeaxanthin to xanthoxin. Xanthoxin is transported into the cytoplasm (red arrow) where the final steps of biosynthesis occur, conversion to S-(+)-abscisic acid (S-(+)-ABA). Catabolism can occur in the cytoplasm (blue arrows) to phaseic acid (PA) and dihydrophaseic acid (DPA), or via conjugation to glucose esters (GE) or glucosides (GS) that are stored within a vacuole (brown arrows). Carotenoid biosynthesis inhibitors (yellow text) and Arabidopsis deficient mutants (blue text) are listed at the biosynthetic steps they inhibit. Note that organelles are not to scale. Abbreviations: ABA-aldehyde, abscisic acid aldehyde; AAO, ABA-aldehyde oxidase; CHYB, β -carotene hydroxylase; LCYB, lycopene β -cyclase; MEP pathway, 2C-methyl-D-ery-thritol-4-phosphate pathway; PSD, phytoene desaturase; PSY, phytoene synthase; NCED, 9-cis-epoxy-carotenoid dioxygenase; XO, xanthoxal oxidase; ZDS, ξ -carotene desaturase; ZEP, zeaxanthin epoxidase. Figure modified from Cutler and Krochko (1999), Liotenberg *et al.* (1999) and Finkelstein and Rock (2002).



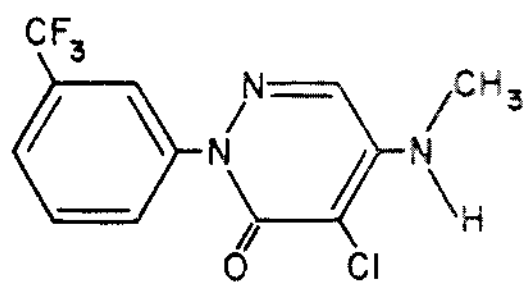
The role of ABA has been analysed in the past by monitoring the effects of the application of either ABA itself or by applying inhibitors of carotenoid biosynthesis and by relating changes in ABA content with physiological and developmental changes. For example, the application of ABA to *Arabidopsis* increased ABA concentrations and caused a reduction in leaf gas exchange related to inducing stomatal closure (Assmann *et al.*, 2000). Norflurazon a pyridazinone herbicide and fluridone a pyridinone herbicide (Figure 1.7) both inhibit carotenoid biosynthesis and therefore ABA biosynthesis by preventing the desaturation of phytoene to ξ -carotene (Figure 1.6) (Bartels and Watson, 1978). Both norflurazon and fluridone treatments of plants effectively reduce endogenous ABA levels (Popova 1998; Mohr and Cahill, 2001). However, complications with exogenous applications of chemical compounds to modify endogenous ABA levels include problems of uptake, rapid metabolism and effects on other pathways apart from those involving ABA (Koornneef *et al.*, 1998). Nevertheless they form an important and useful tool for dissecting ABA regulated responses.

The use of mutants defective in either ABA biosynthesis or ABA action has been an effective alternative approach to chemical inhibitor treatments. The ABA mutants have become an essential tool for the study of ABA biosynthesis and signal transduction and for the cloning of the respective genes (Koornneef *et al.*, 1998). The identification of a wide range of ABA mutants particularly in *Arabidopsis* has accelerated and generated much of what is currently known about ABA and its action. However, many gaps still exist in what we know about ABA, especially its role in plant / pathogen interactions.

Figure 1.7 The structure of ABA biosynthesis inhibitors norflurazon and fluridone.

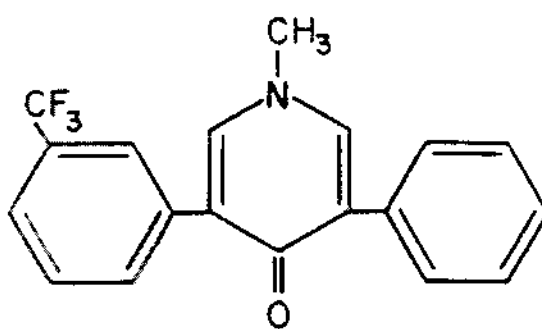
(a) Norflurazon, a pyridazinone herbicide and (b) fluridone, a pyridinone herbicide. Both contain a ring with a trifluoromethyl substitution of the phenyl ring and an oxygen on the nitrogen containing ring thought to be important for the activity of both herbicides. The structures vary in the number of rings (norflurazon 2, fluridone 3) and the position of the monomethyl substitution of the amine group (norflurazon not on a ring, fluridone on the nitrogen containing ring). Figure modified from Bartels and Watson (1978).

a



norflurazon

b



fluridone

1.13.1 ABA biosynthesis

Iso-pentenyl diphosphate (IPP) formed within plastids from pyruvate and glyceraldehyde is the immediate precursor to all carotenoids, including zeaxanthin which is required for ABA biosynthesis (Figure 1.6). IPP for ABA biosynthesis was originally believed to be derived from the mevalonic acid (MVA) pathway within the cytoplasm, however, recently it has been established that it is instead formed by the 2C-methyl-D-ery-thritol-4-phosphate (MEP) pathway within plastids (Cutler and Krochko, 1999). Many of the genes that encode enzymes of the MEP pathway have been cloned (Lichtenthaler 1999). However, the final steps that result in IPP and how the pathway is regulated remain unknown.

The enzymes that convert IPP to zeaxanthin have been cloned and are encoded by nuclear genes possessing transit peptides that allow their importation into plastids (Lichtenberg *et al.*, 1999) (Figure 1.6). By head-to-tail additions and the subsequent action of phytoene synthase (PSY), the first tetraterpene carotenoid, phytoene, is formed from IPP. The following four desaturation steps leading to ξ -carotene are catalysed by phytoene desaturase (PSD) and thus the formation of lycopene is catalysed by ξ -carotene desaturase (ZSD). By the action of lycopene β -cyclase (LCYB), lycopene is converted into β -carotene and subsequently into zeaxanthin, by β -carotene hydroxylase (CHYB) (Cunningham and Gantt, 1998).

Zeaxanthin is converted by a multi-step process to xanthoxin (Figure 1.6). Zeaxanthin is first converted by zeaxanthin epoxidase (ZEP) into all-*trans*-violaxanthin by a two step epoxidation involving an antheraxanthin intermediate that is reversible utilising violaxanthin de-epoxidase (VDE) (Demmig-Adams and Adams, 1996). The first committed step in ABA biosynthesis appears to be the oxidative cleavage of an epoxy-carotenoid precursor (either 9-*cis*-violaxanthin or 9-

cis-neoxanthin) to form xanthoxin by 9-cis-epoxy-carotenoid dioxygenase (NCED) (Tan *et al.*, 1997). However, it remains unclear how all-*trans*-violaxanthin is isomerised into both or only one of 9-cis-violaxanthin or 9-cis-neoxanthin (Liotenberg *et al.*, 1999; Taylor *et al.*, 2000).

Xanthoxin (that has recently been re-named xanthoxal) is transported to the cytoplasm from the plastid where it is converted into ABA (Finkelstein and Rock, 2002) (Figure 1.6). By a series of three ring modifications involving xanthoxin oxidase (XO), xanthoxin is converted into ABA-aldehyde. The final step in ABA biosynthesis is the oxidation of the ABA-aldehyde to S-(+)-ABA by ABA-aldehyde oxidase (AAO). This oxidative step requires a functional molybdenum cofactor (Liotenberg *et al.*, 1999). It has also been identified that two other possible intermediates xanthoxic acid and ABA-alcohol may be alternate substrates for S-(+)-ABA formation, particularly if ABA-aldehyde oxidation is blocked (Cutler and Krochko, 1999).

The availability of ABA biosynthetic mutants has allowed many of genes involved in ABA biosynthesis to be cloned and therefore much of the pathway is now known (Liotenberg *et al.*, 1999). For example, *Arabidopsis aba1* mutants impaired in functional ZEP, *aba2* mutants impaired in functional XO, *aba3* mutants impaired in the molybdenum cofactor required for AAO activity and *ao3* impaired in functional AAO (Finkelstein and Rock, 2002) (Figure 1.6). Further ABA mutant analysis, transgenic and more specific biochemical studies should not only greatly enhance our understanding of ABA biosynthesis but also that of ABA action in plants.

1.13.2 ABA catabolism

ABA degradation can be very rapid, reducing the concentration of ABA in some experiments within an hour (Jia *et al.*, 1996; Ribaut *et al.*, 1996). Little is known about the enzymes that catalyse ABA breakdown and no genes have been cloned that encode these activities. However, several metabolic pathways have been identified that degrade ABA in plant tissues (Cutler and Krochko, 1999) (Figure 1.6). In the majority of plant tissues the catabolic inactivation of ABA proceeds with hydroxylation via 8'-hydroxylase to 8'-hydroxy ABA. 8'-hydroxy ABA is unstable and rearranges spontaneously into phaseic acid (PA) and then is further reduced in some species to dihydrophaseic acid (DPA) (Krochko *et al.*, 1998). The other major pathway for ABA inactivation is esterification of ABA to an ABA-glucose ester (ABA-GE) (Zeevaart and Creelman, 1988). Both PA and DPA can also be conjugated to glucose esters or glucosides and accumulate in vacuoles along with ABA-GE (Cutler and Krochko, 1999). The glucose conjugates have little or no biological activity and are not considered to be a reserve or storage form of ABA (Zeevaart and Creelman, 1988). Several minor metabolites and conjugates of ABA have also been reported and it should also be noted that ABA can simply be exported by passive or carrier mediated efflux from cells (Cutler and Krochko, 1999).

1.13.3 ABA perception

To date genetic approaches have failed to identify ABA receptor mutants, an approach that has been successful with other hormone receptors (eg. Et) (McGrath and Ecker, 1998). No ABA receptor has yet been cloned and only indirect evidence that either or both extracellular and intracellular ABA receptors exist. Indirect evidence for the site of ABA perception to be extracellular has been based on several studies of manipulation of extracellular pH, ABA-protein conjugates and indirect

biochemical assays (Anderson *et al.*, 1994; MacRobbie 1995; Schultz and Quatrano, 1997; Jeannette *et al.*, 1999; Desikan *et al.*, 1999; Ritchie and Gilroy, 2000). However, the possibility of intracellular perception also exists as observed by microinjection, photolysable caged ABA and patch clamp studies (Allan *et al.*, 1994; Schwartz *et al.*, 1994; Hamilton *et al.*, 2000). ABA-binding proteins have been identified in several studies, but their action as receptors that trigger the initial events in ABA signal transduction during a biological response, remain to be elucidated (Zhang *et al.*, 2001; Zhang *et al.*, 2002).

ABA has direct effects on membrane fluidity and thermal behaviour suggesting that some ABA activities may not require interaction with a receptor (Shripathi *et al.*, 1997). It is therefore plausible that ABA may interact directly with some transport proteins or other metabolic factors such that enzymes or complexes may have sites for ABA binding. It is also possible that ABA may have different and or multiple sites of perception depending on the plant material, growth conditions or the physiological response measured (Assmann 1994). Currently much remains unknown of ABA perception in plants.

1.13.4 ABA signal transduction

Until recently very little was known of ABA signal transduction cascades downstream of ABA perception and upstream of physiological and developmental responses. A greater understanding has followed the characterisation of mutants that are changed in their response to ABA (in particular Arabidopsis ABA insensitive and sensitive mutants) and studies that have tested the roles of candidate secondary messengers and signalling intermediates in regulating cellular responses, regulated by ABA. For example, the Arabidopsis ABA insensitive (*abi*) and enhanced response (*era*) mutants affect ABA sensitivity in both seeds and vegetative tissues to varying

degrees (Bonetta and McCourt, 1998). The *abi1* and *abi2* genes have been cloned and both encode type 2C serine / threonine phosphatases, that when expressed in the wild type act as negative regulators of ABA responses (Gosti *et al.*, 1999; Merlot *et al.*, 2001). However, whether these proteins have a positive or negative role remains controversial. The *abi3*, *abi4*, *abi5* genes encode putative transcription factors of the B3 domain, AP2 domain and bZIP classes respectively (Giraudat *et al.*, 1992; Finkelstein *et al.*, 1998; Finkelstein and Lynch, 2000). The *eral* gene encodes the β sub-unit of a protein farnesyl transferase and may also be a negative regulator of ABA action (Cutler *et al.*, 1996). A complicating factor when studying mutants with changed responses to ABA is whether the mutant actually provides insight into the process being investigated. For example, it has been shown that ABA-dependent and ABA-independent pathways interact and converge to activate genes involved in stress responses (Ishitani *et al.*, 1997). Therefore the degree of pleiotrophy of phenotypes seen in some mutants might reflect communication between signalling pathways (Bonetta and McCourt, 1998).

Biochemical studies have also recently identified possible intermediates in ABA signal transduction. ABA activates phospholipase D (PLD) possibly at the plasma membrane and this activation is required for ABA response (Ritchie and Gilroy, 2000). MAPK and several other protein kinases have also been identified as important in ABA signal transduction (Campalans *et al.*, 1999). Protein phosphatases other than those encoded by *abi1* and *abi2* such as type 1, 2A, 2B and a protein tyrosine phosphatase function in ABA signal transduction (Luan 1998). Cyclic ADP-ribose (cADPR) has also been suggested to act as a central mediator of abscisic acid responses by stimulating the release of Ca^{2+} in both stomatal response and pathways

leading to differential gene regulation (Wu *et al.*, 1997; Grill and Himmelbach, 1998).

In conjunction, genetic and biochemical studies are beginning to fill the gaps in ABA signal transduction. At this point, questions remain with respect to the extent of common steps in ABA-signalling. The relationships between the various identified signalling intermediates so far remains largely unclear but a single pathway of signal transfer that finally branches out to the individual ABA evoked response seems unlikely (Bonetta and McCourt, 1998). The existence of several signalling pathways with some crosstalk even with other hormonal pathways appears more likely (Shinozaki and Yamaguchi-Shinozaki, 2000). It is not surprising that ABA signalling may act on targets shared with other hormonal response pathways, for plant hormones as growth regulators must integrate diverse and even antagonistic signals.

1.13.5 ABA rapid responses (ion fluxes)

Rapid responses to ABA (not relying on gene regulation) occur within minutes and involve signalling systems that target ion channels (Grill and Himmelbach, 1998). The most detailed studies of a rapid response to ABA have been conducted during stomatal closure (Blatt and Grabov, 1997). Increases in ABA concentrations during responses to drought reduce stomatal aperture by inducing changes in the turgor of its two surrounding guard cells (Trejo *et al.*, 1993). ABA increases initially depolarise membrane potential that subsequently results in ion and solute redistribution from the vacuole to the apoplast of stomatal guard cells. In particular large increases in cytosolic free Ca^{2+} inactivates the inward rectifying K^+ channel and stimulates outward rectifying K^+ and anion channels resulting in effluxes of both from guard cells, lowering their turgor and volume, resulting in closure (Schroeder *et al.*, 2001). Cytosolic Ca^{2+} increases have been shown to

involve signalling intermediates such as inositol trisphosphate (IP₃), cADPR, NO and other ROS (Gilroy *et al.*, 1990; Leckie *et al.*, 1998; Pei *et al.*, 2000; Neill *et al.*, 2002). ABA has also been shown in guard cells to function through at least two rapid pathways, calcium dependent and independent (Schroeder *et al.*, 2001).

1.13.6 ABA slow responses (gene regulation)

ABA mediated slow responses to developmental and physiological processes often involve within hours, the inducement or repression of gene expression (Skriver and Mundy, 1990; Weatherwax *et al.*, 1996). A variety of genes have been reported to be ABA regulated during water deficiency, some encode for proteins of known function related to counteracting water loss and to repairing the cellular damage caused during dehydration and others have unknown functions. For example, metabolism, transport, repair, degradation, detoxifying, cell wall altering, lipid transfer, histone and late embryogenesis abundant (LEA) proteins are all up-regulated by ABA in response to water deficiency (Campalans *et al.*, 1999). ABA regulation of genes occurs by controlled gene transcription via *cis*-elements in promoter sequences. ABA-responsive elements (ABREs) are *cis*-elements that have been identified in ABA-regulated genes. Many ABREs share ACGT or GCGT core sequences but these are not found in ABA inducible genes alone (Busk and Pages, 1998). Therefore cues other than the core sequences determine signal specificity and several coupling elements important to ABA specific gene induction have been identified (Shen *et al.*, 1996). ABRE binding factors (ABFs) are continually being discovered, including a distinct subfamily of bZIP proteins that have the potential to activate ABA-responsive genes (Choi *et al.*, 2000).

1.14 Identification of ABA as a regulator of plant resistance or susceptibility to pathogens

In the past three decades an enormous amount of plant research has taken place, but only a relatively small fraction of studies have focused on or identified ABA as a molecule that influences plant / pathogen interactions. It is becoming evident that ABA plays a significant role in the determination of plant resistance or susceptibility to pathogens. However, the extent and complexity of its role is far from clear. Below is a collation of studies that utilise a wide range of plants and pathogens, forming the basis of what is currently known on this topic.

1.14.1 Changes in endogenous ABA concentrations during plant / pathogen interactions

Rapid decreases in endogenous ABA concentrations have been detected in the initial hours following inoculation in several studies. In soybean hypocotyls ABA concentrations decline significantly between 2 and 4 h after avirulent *P. sojae* inoculations and 8 h after virulent inoculations (Cahill and Ward, 1989a; Mohr and Cahill, 2001). In the leaf tissue of French bean (*Phaseolus vulgaris* (L.)) a dramatic drop in ABA has also been detected 6 h after inoculation with a pathogenic bean rust fungus (*Uromyces appendiculatus* (Pers.) Unger var. *appendiculatus*) and a non-pathogenic cowpea rust fungus (*Uromyces vignae* Barclay) (Ryerson *et al.*, 1993). From the rapid change in concentration demonstrated in these studies, it is likely that ABA has an early initiated role in disease development.

In contrast, other studies have documented increases in ABA, but days after inoculation. ABA concentrations increased 2 d after tomato leaves were infected with virulent strains of *Botrytis cinerea* Pers.:Fr (Kettner and Dorffling, 1995). It should be noted that some strains of *B. cinerea* are able to synthesise ABA, as was

the case with one of the strains studied by Kettner and Dorffling (1995). In tobacco plants ABA increased 4 d after inoculation with the wilt-inducing bacterium *Pseudomonas solanacearum* Smith, and 16 d after inoculation with TMV (Steadman and Sequeira, 1970; Whenham *et al.*, 1986). ABA was also higher in maize 40 d after infection with the *Glomus* vesicular-arbuscular mycorrhizal (VAM) compared with control plants (Danneberg *et al.*, 1992). The time of initial infection was unknown in leaves of three *Salix* (willow) species infected with the molds *B. cinerea*, *Cladosporium cladosporioides* (Fres.) de Vries and the yeast *Aureobasidium pullulans* (de Bary) Arnaud but they generally had higher ABA concentrations than uninfected leaves (Tuomi *et al.*, 1993). Due to the extended times that were analysed in these studies, it is unclear whether ABA changes were a cause or consequence of disease expression or whether it had any role to play.

1.14.2 The impact of exogenous ABA treatment on plant resistance or susceptibility

The addition of ABA exogenously to many plant species immediately prior to or during infection has increased susceptibility to various pathogens. Soybeans became susceptible to avirulent races of *P. sojae* when the plants were treated prior to inoculation with ABA. Susceptibility was expressed by increased lesion sizes and decreased accumulation of glyceollin and its pre-cursors, as well as decreased activity and accumulation of mRNA for PAL (Ward *et al.*, 1989a; Graham and Graham, 1996; McDonald and Cahill, 1999; Mohr and Cahill, 2001). A line of barley resistant to *E. graminis* f.sp. *hordei* also had increased susceptibility when treated with ABA during infection (Edwards 1983).

Treatment of potato tuber slices with ABA prior to inoculation induced avirulent races of *P. infestans* to grow and sporulate in interactions indistinguishable

from virulent races (Henfling *et al.*, 1980). ABA treatment had also inhibited accumulation of the phytoalexins rishitin and lubimin. In the same study *Cladosporium cucumerinum* Ellis et Arthur, a pathogen of cucumber (*Cucumis sativus* (L.)) but not of potato grew and sporulated abundantly on potato tuber slices treated with ABA prior to inoculation. However, ABA treatment increased the accumulation of rishitin and lubimin in this interaction (Henfling *et al.*, 1980). Application of ABA prior to and at the time of inoculation of tomato leaves with virulent strains of *B. cinerea* increased the extent and speed of the susceptible necrotic leaf areas compared with control leaves (Kettner and Dorffling, 1995; Audenaert *et al.*, 2002). However, ABA application did not induce susceptibility of tomato leaves to non-virulent strains of *B. cinerea* (Kettner and Dorffling, 1995).

In some plant species the effect of ABA treatment on susceptibility or resistance has been pathogen dependent. ABA treatment of French bean prior to elicitation by a preparation from the fungus *Rhizoctonia solani* Kuhn., reduced the accumulation of the phytoalexins phaseollin and kievitone (Goossens *et al.*, 1987). In contrast, ABA treatment prior to and during the infection process of French bean with a compatible fungal pathogen *Colletotrichum lindemuthianum* Sac. et Magnus, decreased susceptibility (Dunn *et al.*, 1990). Also tobacco plants treated with ABA prior to and during the infection process displayed generally increased susceptibility to *Peronospora tabacina* Adam the blue mold pathogen, but decreased susceptibility to infection with TMV (Fraser 1982; Salt *et al.*, 1986). Clearly application of ABA to different plant / pathogen interactions can have differing consequences.

1.14.3 The impact of ABA biosynthesis inhibitor treatment and ABA deficient mutations on plant resistance or susceptibility

The addition of ABA biosynthesis inhibitors at various concentrations to soybean and French bean prior to infection increased resistance and susceptibility respectively. Norflurazon treatment of soybeans prior to inoculation with virulent races of *P. sojae* restricted pathogen spread, increased PAL activity and glyceollin accumulation (McDonald and Cahill, 1999; Mohr and Cahill, 2001). In contrast, application of fluridone to resistant French bean hypocotyls increased *C. lindemuthianum* symptom severity (Dunn *et al.*, 1990).

Inoculation of ABA deficient mutant and wild type tomato plants with *B. cinerea* in two independent studies has revealed different levels of resistance dependent on the mutation and inoculation procedure. The *sitiens* ABA deficient tomato plants were found to be more resistant to *B. cinerea* with increased PAL activity compared with wild type plants. Treatment with ABA restored susceptibility of *sitiens* plants to *B. cinerea* (Audenaert *et al.*, 2002). The *flacca* ABA deficient tomato plants did not show a decline in susceptibility toward *B. cinerea* compared to wild type plants. However, ABA treatment of *flacca* caused necrotic areas to increase faster but their final size was the same and the effect of exogenous ABA resembled that of wild type (Kettner and Dorffling, 1995). With a different inoculation protocol for *B. cinerea* Audenaert *et al.* (2002) found the same level of resistance in *flacca* as *sitiens* plants.

1.14.4 Further evidence for ABA regulation of components of plant defence

A number of further observations also provide evidence for ABA regulation of components of plant defence. For example, the application of ABA to wheat (*Triticum aestivum* (L.) Em. Thell.) reduced PAL and deposition of cell wall

hardening phenylpropanoid compounds (diferulic and ferulic acids) without pathogen inoculation (Wakabayashi *et al.*, 1997). Treatment of French bean plants with ABA markedly reduced the deposition of phenolic compounds in the cell walls inoculated with *U. vignae* (Li and Heath, 1990). The application of ABA to tobacco suspension cell cultures down regulated expression of β -1,3-glucanase, an enzyme known to be induced during resistance to pathogens (Rezzonico *et al.*, 1998). In contrast, ABA treatment of *Brassica carinata* (A.) Braun leaves increased the expression of *BcJAS1*, a gene expressed in response to *Alternaria brassicae* (Berk.) Sacc. inoculation (Zheng *et al.*, 2001).

To date, only two studies suggest possible interactions between ABA and other hormones implicated in plant resistance to pathogens. JA treatment of faba beans (*Vicia faba* (L.)) caused a dramatic drop in ABA and increases in phenolics following germination in soil infested with *Fusarium oxysporum* Schlacht. Ex Fr. f.sp. *fabae* (Ahmed *et al.*, 2002). Ahmed *et al.* (2002) concluded that ABA was involved in cross talk with JA-induced defence in faba bean plants against *Fusarium* wilt. The *sitiens* mutants of tomato were more sensitive to benzo(1,2,3)thiadiazole-7-carbothioic acid (a SA analog and plant defence activator) treatment, with lower levels required to induce *PR1a* expression compared with wild type plants (Audenaert *et al.*, 2002). From their results Audenaert *et al.* (2002) conclude that ABA may negatively modulate the SA-dependent defence pathway in tomato.

1.15 Thesis aims and approaches

It is clear from the research conducted thus far that ABA influences the resistance or susceptibility of many plant / pathogen interactions. However, analysing the effect that increased or decreased ABA concentrations have on these interactions has rarely progressed beyond the identification of changed lesion

phenotypes or expression of a single plant defence gene or biochemical response. The aim of the research detailed in this thesis was to greatly expand the current understanding of plant defence responses regulated by ABA and therefore how ABA influences plant / pathogen interactions. Five major approaches were undertaken to achieve this aim and each of these is detailed in a research chapter presented in this thesis (chapters 2-6).

The understanding of pathogen-specific resistance has rapidly increased in the past decade with the development of *Arabidopsis* / pathogen model systems. For the first time, the influence of ABA was investigated in *Arabidopsis* / *P. parasitica* (Oomycete) (chapter 2) and *Arabidopsis* / *P. syringae* pv. *tomato* (bacteria) (chapter 3) resistant and susceptible interactions. In these two chapters the regulatory effects of ABA concentration changes were examined utilising *Arabidopsis* deficient and insensitive mutants, addition of exogenous ABA, simulated drought stress (chapter 2 only) and ABA biosynthesis inhibitor treatments. To establish a broader role for ABA pathogens from differing evolutionary backgrounds and pathogenic habits were also used.

In both chapters 2 and 3 the influence of ABA on a wide range of *Arabidopsis* defence components was investigated. Defence components of the phenylpropanoid pathway that were examined include the abundance of the mRNA transcripts of the rate limiting enzyme PAL, accumulation of the defence hormone SA and deposition of the cell wall reinforcing compounds, lignin and suberin. Accumulation of the defence signal H_2O_2 , development of the HR (a common indicator of pathogen-specific resistance), another cell wall reinforcing compound callose and the expression of a *PR-1* gene (an indicator of SA-dependent responses)

were also investigated. The important role of each of these defence components during pathogen-specific resistance has been detailed in the above literature review.

A further advantage of studying ABA regulation in Arabidopsis / pathogen interactions was the availability of commercial Arabidopsis genome arrays. The microarrays allowed rapid analysis of global changes in gene expression during an ABA regulated Arabidopsis / pathogen interaction (chapter 4). The unbiased genome arrays permitted identification of ABA regulated defence genes as well as genes not previously associated with defence or those with unknown function. Therefore, providing unprecedented insight into the regulatory role that ABA plays in a plant / pathogen interaction.

The influence of ABA on resistant and susceptible interactions has previously been examined in the soybean / *P. sojae*, plant / pathogen model system. The influence of ABA was further investigated utilising this complimentary system and analysis of defence components including the influence of ABA on the phytoalexin, glyceollin production (chapter 5). Finally, treatment with the abiotic elicitor, silver nitrate, that had previously been effective in inducing both Arabidopsis and soybean defence responses similar to those during resistance to pathogens, form the basis for the final research chapter (chapter 6). The influence of ABA on defence responses induced by silver nitrate was investigated in a similar approach to chapters 2, 3 and 5 (chapter 6). This provided unique insight into ABA regulation of defence components that are important during pathogen-specific resistance but induced by a non gene-for-gene recognition event.

In summary, the regulatory role of ABA during plant defence was extensively examined in this thesis to a level not previously attempted via analysis of two

different plant species in interactions with three different pathogens and an abiotic agent.

1.16 List of publications and presentations

A paper that describes some of the results from chapters 2 and 3, has been published:

Mohr PG, Cahill DM (2003) Absciscic acid influences the susceptibility of *Arabidopsis thaliana* to *Pseudomonas syringae* pv. *tomato* and *Peronospora parasitica*. *Functional Plant Biology* **30**, 461-469.

A paper that describes preliminary data on the soybean / *P. sojae* interaction and formed a basis for chapter 5, has been published:

Mohr PG, Cahill DM (2001) Relative roles of glyceollin, lignin and the hypersensitive response and the influence of ABA in compatible and incompatible interactions of soybeans with *Phytophthora sojae*. *Physiological and Molecular Plant Pathology* **58**, 31-41.

This work was also presented as two oral presentations at conferences (primary author):

- 1) 'The influence of absciscic acid on plant / pathogen interactions utilising soybean and Arabidopsis model systems' at the 13th Biennial Conference of the Australasian Plant Pathology Society, Cairns, Australia, 24th-27th September 2001.
- 2) 'Absciscic acid regulation of bacterial and Oomycete pathogen interactions with Arabidopsis' at Combio2003, Melbourne, Australia, 28th September to 2nd October, 2003.

Two poster presentations at conferences (primary author):

- 1) Mohr PG, Cahill DM 'The influence of abscisic acid (ABA) on plant / pathogen interactions utilising soybean and Arabidopsis model systems' at Combio2000, Wellington, New Zealand, 11th-14th December, 2000.
- 2) Mohr PG, Cahill DM 'Direct evidence for a regulatory role of abscisic acid in Arabidopsis defence responses' at the 8th International Congress of Plant Pathology, Christchurch, New Zealand, 2nd-7th February, 2003.

A poster presentation (co-author):

- 1) Rookes JE, Mohr PG, Cahill DM 'Roles for the phenylpropanoid pathway in defence of Arabidopsis against *Peronospora parasitica* and *Pseudomonas syringae* pv. *tomato*' at Combio2003, Melbourne, Australia, 28th September to 2nd October, 2003.

Chapter 2: The influence of abscisic acid on interactions of Arabidopsis with the biotrophic, Oomycete pathogen, *Peronospora parasitica*

Chapter summary

The plant hormone abscisic acid (ABA) plays an important role in the outcome of many plant / pathogen interactions. However, the mechanisms by which concentrations of ABA influence plant resistance or susceptibility to pathogens, remain largely undiscovered. The molecular and biochemical basis for interactions between Arabidopsis and the obligate biotrophic Oomycete *Peronospora parasitica*, have previously been extensively investigated. In the present study, a suppressive role for ABA was identified for the first time in the regulation of Arabidopsis defence components following inoculation with *P. parasitica*. In particular, low concentrations of ABA within the ABA deficient mutant *aba1-1* resulted in hydrogen peroxide production, development of a hypersensitive like response and changed callose distribution when challenged with a virulent isolate of *P. parasitica*. In the same interaction the phenylpropanoid pathway was also activated with increased *PAL1* mRNA transcript abundance by 13% and lignin accumulation by 131%. Several Arabidopsis ABA deficient mutants, including *aba1-1*, therefore had increased resistance to virulent isolates of *P. parasitica*.

Part of the research detailed in this chapter has been published. The primary author contributed 100% of the research.

Mohr PG, Cahill DM (2003) Abscisic acid influences the susceptibility of *Arabidopsis thaliana* to *Pseudomonas syringae* pv. *tomato* and *Peronospora parasitica*. *Functional Plant Biology* **30**, 461-469.

2.1 Introduction

Peronospora parasitica (Pers. ex Fr.) Fr. is an obligate biotrophic Oomycete that establishes intimate relationships with its cruciferous plant hosts, resulting in 'downy mildew' disease (Channon 1981). *P. parasitica* isolates have been identified that naturally infect and proliferate in susceptible *Arabidopsis* ecotypes, but infections are rapidly localised to the site of penetration in resistant ecotypes (Koch and Slusarenko, 1990). Development of susceptibility or resistance is determined by the genetic backgrounds of both the plant and pathogen (Holub *et al.*, 1994). The clear molecular basis for the outcome of *Arabidopsis* / *P. parasitica* interactions has meant that it is now an important plant / pathogen model system.

Resistant *Arabidopsis* / *P. parasitica* interactions are initiated by the recognition of *P. parasitica* ATR (*Arabidopsis thaliana* recognised) proteins by *Arabidopsis* RPP (recognition of *P. parasitica*) proteins (Holub and Beynon, 1997). To date the molecular position of only one *P. parasitica* ATR gene, *ATRIND*, has been mapped (Rehmany *et al.*, 2003). In contrast, 27 RPP genes have been either cloned or characterised (Slusarenko and Schlaich, 2003). The structure of RPP proteins include a region of leucine-rich repeats (LRR) and a nucleotide binding site (NBS), but variation at the N-terminus with either a leucine-zipper (LZ) or similarity to a Toll and Interleukin 1 receptor (TIR) protein (Martin *et al.*, 2003).

The signal transduction pathways triggered by RPP proteins, are not completely understood but important components have been identified (Slusarenko and Schlaich, 2003). It appears that the majority of TIR-NBS-LRR RPP proteins require a functional EDS1 (enhanced disease susceptibility 1) protein for resistant signalling, whereas LZ-NBS-LRR RPP proteins require NDR1 (nonrace-specific disease resistance 1) (Aarts *et al.*, 1998; Warren *et al.*, 1999). It has been postulated

that signalling pathways involving EDS1 or NDR1 are parallel but converge downstream to stimulate the same components of defence (Parker *et al.*, 2000). The plant hormone salicylic acid (SA) plays a key role in disease resistance signalling of many plants (Alvarez 2000) and several *RPP* gene mediated resistant interactions are SA dependent (Delaney *et al.*, 1994; McDowell *et al.*, 2000). The two hormones jasmonic acid (JA) and ethylene (Et) have also been identified as important signals during resistant interactions of many plants (Penninckx *et al.*, 1996) but *RPP* protein signalling appears to be JA / Et independent (Thomma *et al.*, 1998). In contrast, the accumulation of reactive oxygen species (ROS) and especially hydrogen peroxide (H_2O_2), have previously been identified as important diffusible defence signals in many resistant interactions (Lamb and Dixon, 1997) including those mediated by *RPP* genes (Aviv *et al.*, 2002).

Several components that comprise an effective defence response against *P. parasitica*, have been correlated with resistance. The development of a hypersensitive response (HR) in the form of necrotic flecks, cavities or pits adjacent to penetrating *P. parasitica* hyphae, are common characteristics of resistant interactions (Holub *et al.*, 1993; Holub *et al.*, 1994). Deposition of the cell wall reinforcing compounds callose and lignin in association with the HR, also contribute to resistance (Parker *et al.*, 1993; Mauch-Mani and Slusarenko, 1996). Accumulation of the phenylpropanoid pathway rate limiting enzyme, phenylalanine ammonia-lyase (PAL) (Mauch-Mani and Slusarenko, 1996; Rookes and Cahill, 2003), as well as, the pathogenesis-related gene 1 (*PR-1*) (Nawrath and Metraux, 1999) both increase during resistance. The accumulation of camalexin, a phytoalexin derived from the tryptophan pathway, is similar in both resistant and susceptible interactions and therefore is believed not to be a determinant of resistance (Mert-Turk *et al.*, 2003).

A regulatory role has been identified for ABA in plant / pathogen interactions, particularly soybean (*Glycine max* (L.) Merr.) / *Phytophthora sojae* Kauf. and Gerd. (Mohr and Cahill, 2001) and tomato (*Lycopersicon esculentum* Mill.) / *Botrytis cinerea* Pers.:Fr (Audenaert *et al.*, 2002). A higher than basal concentration of ABA within plant tissues at the time of avirulent pathogen inoculation, has previously been shown to cause an interaction shift towards what phenotypically resembled susceptibility (McDonald and Cahill, 1999). Conversely, a lower than basal concentration of ABA in plants inoculated with a virulent pathogen caused a shift towards resistance (Mohr and Cahill, 2001; Audenaert *et al.*, 2002).

Despite the dramatic influence of ABA on plant / pathogen interactions, little is known of the mechanisms that cause interaction phenotype shifts. When the findings of studies conducted thus far are combined, it appears that a common mechanism is that ABA negatively regulates the production of defence components derived from the phenylpropanoid pathway: SA (Audenaert *et al.*, 2002), isoflavonoid phytoalexins and their pre-cursors (Goossens *et al.*, 1987; Graham and Graham, 1996; Mohr and Cahill, 2001) probably through an interaction with the PAL enzyme or its encoding gene (Ward *et al.*, 1989b; McDonald and Cahill, 1999). The action of negative regulation by ABA of defence components may also extend beyond the phenylpropanoid pathway, for example, the negative regulation by ABA of β -1,3-glucanase involved in callose accumulation (Rezzonico *et al.*, 1998). A major problem with trying to combine the results from previous studies to understand ABA regulation of plant defence components, is that the observations were obtained from research involving different pathogens interacting with a wide range of plants (eg. French bean (*Phaseolus vulgaris* (L.)), soybean, tobacco (*Nicotiana tabacum* (L.)) and tomato).

In this chapter the role of ABA in plant / pathogen interactions is analysed for the first time using the Arabidopsis / *P. parasitica* model system. An advantage in utilising this system is the already extensive understanding of the pathogen-specific resistant and susceptible interactions. For example, the RPP proteins that conferred resistance to the avirulent *P. parasitica* isolates utilised in this study have been characterised [Landsberg *erecta* (Ler) resistance to *P. parasitica* (Pp) Emoy2 (conferred by RPP5 and RPP8) and PpNoks1 (RPP5) and Columbia 0 (Col-0) resistance to PpEmoy2 (RPP4), PpHind4 (RPP19) and PpCala2 (RPP2) (Holub and Beynon, 1997; Van Der Biezen and Jones 1998; Martin *et al.*, 2003)]. Components or products of the phenylpropanoid pathway (eg. PAL, SA and lignin) and other defence responses (eg. HR and callose) are also known to be important in these interactions.

In this chapter, I also investigate a range of ABA manipulations in interactions with *P. parasitica* via both chemical treatments [exogenous ABA and ABA biosynthesis inhibitors (norflurazon and fluridone)] and by using Arabidopsis ABA deficient or ABA insensitive mutants. The previously characterised Arabidopsis ABA deficient mutants *aba1-1*, *aba1-3* and *aba1-4* [each impaired in functional zeaxanthin epoxidase (Rock and Zeevaart, 1991)], *aba2-1* [impaired in conversion of xanthoxin to ABA-aldehyde (Leon-Kloosterziel *et al.*, 1996)], *aba3-1* and *aao3* [impaired in conversion of ABA-aldehyde to ABA (Schwartz *et al.*, 1997; Seo *et al.*, 2000)] and the Arabidopsis ABA insensitive mutants *abi1-1* and *abi2-1* (impaired in similar 2C class protein serine/threonine phosphatases [Leung *et al.*, 1997]) were investigated. Together these approaches clearly demonstrate a regulatory role for ABA in Arabidopsis / *P. parasitica* interactions and also highlight

a number of defence responses that are regulated by changes in ABA concentrations within plant tissues.

2.2 Materials and methods

2.2.1 Source and background of Arabidopsis wild types and mutants

Seeds of Arabidopsis wild type (wt) Landsberg *erecta* (Ler) and Columbia-0 (Col-0) were obtained from Lehle Seeds (Texas, USA). Seeds of Arabidopsis ABA deficient mutants *aba1-1*, *aba1-3*, *aba1-4*, *aba2-1*, *aba3-1* and ABA insensitive mutants *abi1-1*, *abi2-1* were obtained from the Arabidopsis Biological Resource Center (Ohio, USA). Seeds of the Arabidopsis ABA deficient mutant *aao3* were obtained from Tomokazu Koshiba (Tokyo Metropolitan University, Tokyo, Japan). Seeds of the Arabidopsis enhanced disease susceptibility mutant *eds1.1* were obtained from Dr. Eric Holub (Horticulture Research International, Wellesbourne, UK). The ABA deficient mutants *aba1-1*, *aba1-3*, *aba1-4*, *aao3* and ABA insensitive mutants *abi1-1*, *abi2-1* were of the Ler (wt) background (Koornneef *et al.*, 1982; Koornneef *et al.*, 1984; Seo *et al.*, 2000). The ABA deficient mutants *aba2-1* and *aba3-1* were of the Col-0 (wt) background (Leon-Kloosterziel *et al.*, 1996) and the enhanced disease mutant *eds1.1* of the Wassilewskija-0 background.

2.2.2 Growth of Arabidopsis wild type and mutant plants

All Arabidopsis seeds were surface sterilised with 10% (v/v) sodium hypochlorite containing 0.1% (v/v) Triton X-100 for 2 min and rinsed four times with sterile distilled water (dH₂O) (all reagents cited in this thesis were of analytical grade and of the highest purity). Twenty-five seeds were placed on Murashige and Skoog (MS) medium (Appendix 1) within each 9 cm diameter Petri plate and vernalised for 4 d in the dark at 4°C. After vernalisation the plates were placed in a controlled environment cabinet (Convion Controlled Environments Ltd., Manitoba,

Canada) at 21°C under a 10 / 14 h light / dark cycle to promote germination and growth. Light was provided by eight 60 W fluorescent lights (Osram Australia Pty. Ltd., New South Wales, Australia) that were at a height of 0.25 m above the plants. After 2 wk, four plants were transferred from MS medium to soil (terracotta and tub mixture, Debec Pty. Ltd., Victoria, Australia) within each 5 cm diameter pot.

If the plants were to be inoculated with a *P. parasitica* conidial suspension their pots were kept within sealed transparent containers. The sealed containers prevented cross-contamination with other *P. parasitica* isolates and also prevented the wilting of ABA deficient and ABA insensitive mutants. If instead the plants were grown for maintenance of *P. parasitica* cultures and the production of conidial inoculum, the pots containing seedlings were covered with clear plastic. The covering helped the plants acclimatise for 1 d following their transplantation before its removal. Plants grown under the latter conditions produced much larger leaves, that assisted in the production of greater quantities of conidiophores. After transfer to soil all plants were grown in a controlled environment room at 21°C under a 12 / 12 h light / dark cycle. Light was provided by two 400 W high-pressure sodium lights (Osram Australia Pty. Ltd.) that were at a height of 1.5 m above the plants.

2.2.3 ABA and ABA biosynthesis inhibitor treatment of *Arabidopsis*

For treatment of plants with ABA, solutions of \pm cis-trans ABA in 1% (v/v) methanol were prepared. The final concentrations used were calculated for the active, + isomer. A solution of 1% (v/v) methanol therefore served as the control treatment. Norflurazon (Novartis Crop Protection Australia Ltd., New South Wales, Australia) solutions were prepared in dH₂O, and therefore dH₂O served as the control. Fluridone (Novartis Crop Protection Australia Ltd.) solutions were prepared in 0.4%

(v/v) dimethylsulfoxide (DMSO) and therefore 0.4% (v/v) DMSO served as the control.

For treatment with ABA, norflurazon and fluridone, solutions were applied to plants via root uptake. Root uptake was enabled by carefully removing plants from MS medium after 2 wk and placing the roots within Petri plate and then covering with filter paper (No.1, Whatman International Ltd., Maidstone, England). The filter paper was then moistened with 2 ml of the appropriate treatment solution. The plates were closed and placed within the controlled environment room. After 20 h the plants were removed from their treatments and transferred to soil as previously described in section 2.2.2.

2.2.4 ABA extraction and quantification

ABA was extracted from plant tissues based on the method previously described by Vermeer *et al.* (1987). The tops of 10 plants were excised from their roots, rinsed with dH₂O and the excess surface water absorbed by tissue paper. The plant tissue was immediately frozen in liquid nitrogen and ground to a fine powder with a mortar and pestle. Fifty micrograms fresh weight (f. wt.) of the powder was weighed into two 1.5 ml Eppendorf tubes. The powder in each tube was suspended in 0.5 ml 80% (v/v) methanol and placed on an orbital shaker (Ratek Instruments Pty. Ltd., Victoria, Australia) at 120 rpm overnight. The tubes were centrifuged at 14,000 g (Microcentrifuge, Denver Instruments, Colorado, USA) for 10 min and 0.4 ml of the supernatant collected from each tube and combined. A syringe filter (0.45 µm, Pall-Gelman Sciences, Michigan, USA) coupled to a C18 cartridge (Sep-pak, Waters Corporation, Massachusetts, USA) was rinsed with 3 ml 80% (v/v) methanol before the combined supernatants were applied. The ABA was then eluted from the C18 cartridge with 2 ml 80% (v/v) methanol. The filtrate was evaporated to dryness

(speedvac concentrator, SC200, Thermo Savant, New York, USA). The residue was resuspended in 0.4 ml ethyl acetate and an equal volume of 0.5 M potassium dihydrogen phosphate (pH 3.0). The solution was mixed with a vortex (Ratek Instruments Pty. Ltd.) and centrifuged at 14,000 g for 5 min. The ethyl acetate layer containing the ABA was removed and dried under a stream of nitrogen. The residue was resuspended in 200 µl 10% (v/v) methanol and stored at -20°C until analysis.

The extracted ABA was quantified by an indirect enzyme-linked immunosorbent assay (ELISA) (Cahill and Ward, 1989a; Mohr and Cahill, 2001). Dilutions of each extract were run in triplicate in the indirect ELISA utilising an (+)-ABA monoclonal antibody (Agdia Inc., Indiana, USA). The amount of ABA in each sample was calculated from logit transformation of standard curve data as previously described (Liao *et al.* 1995). The linear range of the indirect ELISA was 2.5-125 pg. ABA concentrations were expressed as ng g⁻¹ f. wt..

2.2.5 *P. parasitica* culture and maintenance

P. parasitica (*Pp*) isolates *PpEmoy2*, *PpHind4*, *PpCala2* and *PpNoks1* were obtained from Dr. Eric Holub as oospores within dried Arabidopsis leaf tissue. The dried leaf tissue was applied to the surface of pots containing moist soil and seeds of Arabidopsis mutant *eds1.1* (Dangl *et al.*, 1992). The mutant is hypersusceptible to *P. parasitica* (Parker *et al.*, 1996) and therefore aided more prolific *P. parasitica* infection. The pots were sprayed daily with dH₂O and incubated within sealed transparent containers in a growth cabinet (S.E.M. (SA) Pty. Ltd., South Australia, Australia) at 16°C under a 10 / 14 h light / dark cycle. Light was provided by four 8 W fluorescent lights (Osram Australia Pty. Ltd.) that were at a height of 0.3 m above the leaves.

After 1 wk the emerging cotyledons were checked daily under a dissecting microscope (Carl Zeiss Pty. Ltd., New South Wales, Australia) for the presence of conidiophores. As conidiophores appeared on cotyledons these plants were rubbed on the remaining cotyledons within the pot. By 3 wk conidiophores of each isolate were present in sufficient numbers to begin preparing inoculum. However, to preserve plants that profusely produced conidiophores, every 7-10 d leaves bearing conidiophores were rub inoculated on to fresh 3-4 wk old plants grown specifically for maintenance and production of conidial suspensions (Koch and Slusarenko 1990). The rub inoculated plants were kept within sealed transparent containers and sprayed daily with dH₂O. The isolate *PpEmoy2* was maintained on *eds1.1*, *PpHind4* and *PpCala2* on Ler (wt) and *PpNoks1* on Col-0 (wt) on which the isolates were virulent.

2.2.6 *P. parasitica* inoculum, inoculation procedure and interaction assessment

For inoculation a conidial suspension at a density of 10^5 spores ml⁻¹ in distilled H₂O was prepared from leaves infested with conidiophores (Dangl *et al.*, 1992). Plants were inoculated with the relevant conidial suspension 1 d after planting in soil, a period of time set aside to allow the plants to acclimatise to growth in soil. Plants treated with ABA or ABA biosynthesis inhibitors were inoculated immediately after they were planted in soil. Five rosette leaves per plant were each inoculated with a 2 µl drop by micropipette (Holub *et al.*, 1994). Eight plants were inoculated with an isolate per experiment. After inoculation the plants were then incubated within the growth cabinet and sprayed daily with a dH₂O mist, from a hand held sprayer. The interactions between *Arabidopsis* / *P. parasitica* were assessed using a dissecting microscope 7 d after inoculation by counting the number of conidiophores (up to a maximum of 20) and / or noting the presence of necrotic

lesions produced on each leaf (Warren *et al.*, 1998). Images of leaves bearing conidiophores or necrotic lesions were captured using a camera (Carl Zeiss Pty. Ltd.) mounted on the dissecting microscope. Images of whole leaves were also captured using a digital still camera (MVC-FD81, Sony Corp., Tokyo, Japan).

2.2.7 Histochemical staining and detection of H₂O₂ in *Arabidopsis* leaf tissue inoculated with *P. parasitica*

For each histochemical stain that was used and the detection of H₂O₂, the tops of four plants were excised from their roots, therefore, 20 inoculated leaves were analysed. The plant tops were cleared of photosynthetic pigments by immersion three times in 5 ml of absolute methanol over 3 d. The methanol was changed each day to ensure all photosynthetic pigments were removed from the tissue prior to being subjected to each histochemical staining procedure (a-f) detailed below. All stained tissue was viewed under white light illumination using a compound research microscope (Axioskop 20, Carl Zeiss Pty. Ltd.), and aniline blue staining for callose was viewed under ultraviolet (UV) light (using a UV [excitation wavelength 365nm, emission 420nm] filter set). Images of stained tissues were captured using a Spot RT digital camera (Spot Diagnostic Instruments Inc., Michigan, USA) mounted on the light microscope and stored in a computer.

a) The spread of *P. parasitica* and the necrosis of *Arabidopsis* cells was detected by lactophenol-trypan blue (LTB) stain (Koch and Slusarenko 1990). The cleared plant tops were boiled for 1 min in 1 ml LTB stain (Appendix 1). When cool, the leaves were removed from the LTB stain and placed in 1 ml chloral hydrate (1 g ml⁻¹) for 1 h on an orbital shaker at 120 rpm, to remove excess stain. The tissue was mounted in chloral hydrate on a glass slide for light microscopy. *P. parasitica* hyphae, oospores

and conidiophores as well as necrotic leaf cells stained dark blue. Healthy leaf cells stained light blue.

b) The presence of hydrogen peroxide (H_2O_2) was detected by a 3,3'-diaminobenzidine (DAB) polymerisation reaction (Thordal-Christensen *et al.*, 1997). Two week old plants were removed from MS medium and root uptake of DAB (1 mg ml^{-1}) (Appendix 1) was performed as previously described in section 2.2.3. After treatment for 4 h the plants were transferred to soil and inoculated as previously described in section 2.2.6. One day after inoculation the plant tops were excised from their roots and cleared of photosynthetic pigments, rinsed and mounted in dH_2O on glass slides for light microscopy. The presence of H_2O_2 was visualised as a reddish / brown precipitate within cells.

c) Lignin was visualised using the phloroglucinol / hydrochloric acid (Phl / HCl) stain (Mauch-Mani and Slusarenko, 1996). After clearing, the plant tops were incubated in 1 ml of 1% (w/v) phloroglucinol (Phl) in 70% (v/v) ethanol (Appendix 1) overnight at room temperature (RT) in the dark. The tissue was mounted on glass slides with a few drops of concentrated hydrochloric acid (HCl). After 5 min excess HCl was drained from the slides and replaced with dH_2O for light microscopy. The presence of lignin within leaf tissue was indicated by the red / purple stain of cells and cell walls.

d) Phenolic structures were visualised using toluidine blue 0 (TB0) staining (Cadena-Gomez and Nicholson, 1987). The cleared plant tops were incubated in 1 ml 0.1% (w/v) TB0 in absolute ethanol (Appendix 1) for 30 min. The tissues were rinsed once with 50% (v/v) ethanol and then twice with dH_2O , before mounting on glass slides in dH_2O for light microscopy. Using this method the presence of phenolic structures was indicated by a light blue / green staining in cells and cell walls.

- e) Suberin was detected by Sudan black B (SBB) staining (Southerton and Deverall, 1990). Cleared plant tops were rinsed with dH₂O before immersion in 1 ml 5 M potassium hydroxide (KOH) for 1 h. The KOH was removed and replaced with 1 ml SBB (0.3 g ml⁻¹) in 70% (v/v) ethanol (Appendix 1) for 4 h. The tissue was removed and rinsed twice in 50% (v/v) ethanol and once in dH₂O before it was mounted in dH₂O for light microscopy. Suberin within cells and tissues was stained blue / black.
- f) Callose within cells and tissues was detected by aniline blue (AB) stain (Southerton and Deverall, 1990; Tang *et al.*, 1999). Following clearing, the plant tops were suspended overnight in 1 ml 0.5% (w/v) AB in 0.15 M di potassium hydrogen orthophosphate. The tissues were rinsed twice with dH₂O before being mounted on glass slides. The presence of callose was visible (under UV light) as a bright yellow / green fluorescence produced within cells.

2.2.8 Thioglycolic acid derivatisation of wall bound phenolics

Wall bound phenolics of plant tissues were derivatised via thioglycolic acid (TGA) precipitation (Lee *et al.*, 2001; Mohr and Cahill, 2001). Seven days after inoculation the tops of 10 plants were excised from their roots. Pigmentation and soluble phenolics were removed over 3 d by three changes of 5 ml absolute methanol. The cleared tissue was dried in an oven at 30°C for 24 h and the dry weight (d. wt.) recorded. The dried tissue was suspended in 0.5 ml 10% (v/v) TGA in 2 M HCl (v/v), heated for 4 h at 100°C in a water bath (Thermoline L&M, New South Wales, Australia) and then allowed to cool for 10 min. The solution and all tissue was then transferred to a 1.5 ml Eppendorf tube and centrifuged at 14,000 g for 15 min. The supernatant was decanted and the pellet washed with 0.5 ml dH₂O before centrifugation at 14,000g for 10 min. The supernatant was decanted and 0.5 ml 1 M sodium hydroxide (NaOH) added and mixed with a vortex to solubilise the

TGA derivatives. The suspension was then incubated overnight at 4°C before centrifugation at 14,000 g for 10 min. The NaOH supernatant was collected and added to a fresh 1.5 ml Eppendorf tube and the thioglycolic acid derivatives were then precipitated by adding 0.2 ml concentrated HCl and incubating in an ice bath for 1 h. The reddish / brown precipitate was pelleted by centrifugation for 10 min at 14,000 g. The supernatant was decanted and the precipitate dissolved in 1 ml 0.5 M NaOH. The absorbance (A) of each resultant orange solution was determined at 335nm (Graham and Graham, 1991). Concentrations of wall bound TGA derivatives were expressed as $A_{335\text{nm}} \text{ mg}^{-1} \text{ d. wt.}$.

2.2.9 SA extraction and quantification

SA was extracted and quantified by reverse-phase high performance liquid chromatography (HPLC) (Raskin *et al.*, 1989). Five days after inoculation the roots were removed from the tops of 10 plants, ground in liquid nitrogen with a mortar and pestle and the f. wt. of the powder recorded. The powder was then suspended in 1 ml 90% (v/v) methanol and the subsequent suspension mixed on a vortex and then sonicated (Unisonics Pty. Ltd., New South Wales, Australia) for 15 min. The suspension was centrifuged at 14,000 g for 10 min. A 0.9 ml aliquot of supernatant was collected and 1 ml absolute methanol added to the remaining pellet. The pellet was resuspended by mixing with a vortex before a further centrifugation. A 1 ml aliquot of supernatant was combined with the first aliquot and dried (speed vac concentrator, SC200). The residue was resuspended in 0.5 ml 5% (v/v) trichloroacetic acid (TCA) by mixing on a vortex and 10 min sonication. The TCA was removed and centrifuged at 14,000 g for 5 min. The supernatant was then partitioned two times (10 min each) against 0.75 ml of 1:1 (v/v) ethyl acetate/ cyclohexane. The top organic phase containing the free SA was dried under nitrogen

and the aqueous phase containing the conjugated SA was acidified with 0.5 ml concentrated HCl. The mixture was heated at 80°C for 1 h and the released SA extracted by partitioning twice against 1:1 ethyl acetate / cyclohexane and dried as previously described. Both extracts were resuspended in 0.2 ml 55% acetonitrile (ACN) 45% dH₂O with 4% (v/v) acetic acid and mixed on a vortex before centrifugation at 14,000 g for 5 min.

An aliquot of each extract (0.1 ml) was added to a 0.25 ml glass insert within a 2 ml glass vial with a screw top and rubber septum (Agilent Technologies, California, USA). Extracts were analysed automatically by reversed-phase HPLC (Agilent Technologies). The chromatography column used was a C18 analytical column (Alltima 250 mm x 4.6 mm, Alltech Associates Inc., Illinois, USA) fitted with a guard column (Alltech Associates Inc.). The HPLC was pre-programmed for gradient elution (55% (v/v) ACN: 45% dH₂O with 4% (v/v) acetic acid at the time of injection to 80% ACN: 20% dH₂O with 4% (v/v) acetic acid over 10 min) at a flow rate of 1.0 ml min⁻¹. SA in the eluate was detected by passage through a fluorescence detector (excitation 305 nm and emission 405 nm, 1100 Series, Agilent Technologies). The C18 column was washed for 7 min with 55% (v/v) ACN: 45% dH₂O with 4% (v/v) acetic acid prior to each sample application. The lower detection limit was 10 pg and the SA concentration was expressed as µg g⁻¹ f. wt..

2.2.10 Total RNA isolation from plant tissues

Total RNA was isolated from plant tissue using a TRIzol method (Arabidopsis Functional Genomics Consortium, http://www.arabidopsis.org/info/2010_projects/comp_proj/AFGC). For each sample, the tops of 10 plants were excised from their roots and rinsed in dH₂O. Surface moisture was removed with tissue paper before the plants were ground in liquid nitrogen with a mortar and

pestle. The ground tissue was added to a 1.5 ml Eppendorf tube and suspended in 1.5 ml of TriReagent (Molecular Research Center, Ohio, USA). Each tube was stored in liquid nitrogen until all samples for a particular experiment were prepared. The tubes were then incubated at 60°C for 15 min prior to mixing with a vortex. The tubes were then centrifuged at 14,000 g for 10 min at 4°C. The supernatant was transferred to a new tube and 0.3 ml chloroform added. The solution was again mixed and then incubated at RT for 5 min. The solution was centrifuged at 14,000 g for 15 min at 4°C. The top aqueous phase was transferred to a new tube with 0.7 ml isopropanol. The tube was mixed by gentle inversion before incubation at RT for 15 min. The mixture was centrifuged at 14,000 g for 10 min at 4°C and the supernatant discarded. The remaining pellet was washed with 0.5 ml of 70% (v/v) ethanol (ice cold) and centrifuged for 10 min at 4°C and the supernatant again discarded. The pellet was air dried for 10 min before being resuspended in 50 µl of diethyl pyrocarbonate (DEPC) treated dH₂O.

The isolated total RNA was treated with DNase I (DNA-free, Ambion Inc., Texas, USA) to eliminate any contaminating DNA. Initially 5 µl of 10X DNase I buffer and 1 µl of DNase I was added to the total RNA before gentle mixing and incubation at 37°C for 30 min. Five microliters of DNase inactivation reagent was added to the sample and mixed by pipetting. The mixture was incubated for 2 min at RT. The tube was centrifuged at 10,000 g for 1 min to pellet the DNase inactivation reagent. The total RNA (DNA free) was removed and quantified according to its A_{260nm} (RNeasy Mini Handbook, Qiagen, California, USA).

2.2.11 Abundance of *Arabidopsis* *PAL1* and *PR-1* mRNA transcripts

The abundance of mRNA transcripts of *Arabidopsis* *PAL1* (*AtPAL1*) and *PR-1* (*AtPR-1*) from total RNA was quantified by reverse transcription-polymerase chain

reaction (RT-PCR). Firstly the nucleotide sequence of both genes was obtained from the National Centre for Biotechnology Information (NCBI, <http://www.ncbi.nlm.nih.gov/>). Primers for *AtPAL1* 5'-CTATGTTATGCGGCGGAGAC-3' and 5'-TCCGATGAGAAGTAGCACCA-3' and primers for *AtPR1* 5'-TTCTTCCCTCGAAAGCTCAA-3' and 5'-TCCTGCATATGATGCTCCTT-3' were designed using primer design software (Primer3, Whitehead Institute for Biomedical Research, Massachusetts, USA) to produce a 342 base pair (bp) and a 512 bp product respectively. The *AtPAL1* and *AtPR-1* primers were constructed by Geneworks (South Australia, Australia). Universal internal standard primers for 18S (QuantumRNA™ 18S, Ambion Inc.) produced a 315 bp product.

RT-PCR was performed using OneStep RT-PCR (Qiagen Pty. Ltd.). A master mix was prepared with OneStep RT-PCR buffer (1X), dNTP mix (400 µM of each dNTP), primers (both to 0.6 µM each), OneStep RT-PCR enzyme mix and RNase-free water. Aliquots of the master mix were dispensed in appropriate volumes into 200 µl Ultra Flux™ dome cap PCR tubes (Astral Scientific, New South Wales, Australia). Total RNA (500 ng) was added to each PCR tube. Neither the combination of *AtPAL1* or *AtPR-1* primers with 18S primers provided a reliable multiplex RT-PCR. Therefore identical tubes for *AtPAL1* or *AtPR-1* and 18S were prepared for each sample and run simultaneously. The thermal cycler (PTC-100, MJ Research Inc., Massachusetts, USA) was pre-heated to 50°C before the reaction tubes were added. The conditions for RT-PCR were as follows; 1) 30 min at 50 °C, 2) 15 min at 95 °C, 3) a three-step cycle for the desired number of cycles, 30 sec at 94 °C, 30 sec at 62 °C, and 45 sec at 72 °C and 4) 10 min at 70 °C.

Equal volumes of each reaction were assessed via separation on a 1% (w/v) agarose gel in 0.5x tris-borate-EDTA (TBE). A negative control for each set of reactions was run on the gel as well as a 100 bp molecular ladder to confirm the approximate fragment size of each PCR product. The gel was stained with 5 μ M ethidium bromide (EtBr) in 0.5x TBE and the products visualised by their fluorescence under UV. Images were captured by an Eagle Eye™ II (Stratagene, California, USA) and the density of each product determined by EagleSight (Stratagene). The abundance of *AtPAL1* or *AtPR-1* transcripts were equalised based on the differences between the abundance of 18S transcript densities (the internal standard indicated the discrepancies in the amount of total RNA between RT-PCR samples). The differences between equalised *AtPAL1* or *AtPR-1* transcripts of the various samples being compared were expressed as a percentage relative to the sample with the largest *AtPAL1* or *AtPR-1* transcript density (eg. 100%).

2.2.12 Statistical analysis

The mean and standard error of the mean (s.e.m.) were calculated and the significance of differences between means of two independent values was analysed by an unpaired parametric t-test (GraphPad Prism version 3.00, GraphPad Software, California, USA). The significance of differences between percentages were calculated by an unpaired, non-parametric t-test (Mann-Whitney test, GraphPad Prism version 3.00).

2.3 Results

2.3.1 Establishment of *P. parasitica* cultures and characterisation of *Arabidopsis* / *P. parasitica* resistant and susceptible interaction phenotypes

One to two weeks after *eds1.1* germination in soil containing previously diseased leaf tissue, plants infected by *P. parasitica* were identified by conidiophore

production on cotyledons (Figure 2.1a). A week after rub inoculation with the initial conidiophore bearing *eds1.1* plants, conidiophores proliferated on the remaining uninfected plants within the pot (Figure 2.1b). Seven to 10 days after rub inoculation of 4-5 wk old susceptible plants sufficient conidiophores were produced for generation of conidial inoculum (Figure 2.1c). In contrast, a week after seedling rub inoculation of 4-5 wk old resistant plants there was no sporulation and dark minute HR flecks were visible (Figure 2.1d).

Seven days after inoculation with conidia from a virulent isolate, conidiophores emerged from susceptible leaves of 3 wk old plants (Figure 2.1e). In contrast, inoculations with conidia from an avirulent isolate produced no conidiophores on resistant leaves (Figure 2.1f). LTB staining of susceptible leaves revealed spreading hyphae with haustoria, oospores and conidiophores (Figure 2.1g-i). LTB staining of resistant leaves revealed only small clusters of HR cells at the site of inoculation (Figure 2.1j). Based on LTB staining of leaves 7 d after inoculation, Ler (wt) was resistant to avirulent isolates *PpEmoy2* and *PpNoks1* and susceptible to virulent isolates *PpHind4* and *PpCala2* and Col-0 (wt) resistant to avirulent isolates *PpEmoy2*, *PpHind4* and *PpCala2* and susceptible to the virulent isolate *PpNoks1* (Figure 2.2a-h and Table 2.1).

2.3.2 Treatment with ABA of *Arabidopsis* / *P. parasitica* resistant interactions

In a preliminary experiment, 1, 10 and 100 μ M ABA treatment of a resistant interaction did not alter the occurrence of minute HR flecks or the number of conidiophores on leaves (Figure 2.3a-d and Table 2.2). Further 100 μ M ABA treatment of resistant interactions, did not alter the development of HR within cells (Figure 2.4a-h). Treatment of plants with 100 μ M ABA caused a significant ($p < 0.05$)

Figure 2.1 Establishment of *P. parasitica* cultures, inoculation procedure and visualisation of interactions with *Arabidopsis*.

(a) Conidiophores (*PpEmoy2*) (white arrow) on cotyledons (*eds1.1*) 1-2 wk following germination in soil containing dried, diseased leaf tissue.

(b) Conidiophores (*PpEmoy2*) (white arrow) proliferated on many plants (*eds1.1*) 1 wk after rub inoculation, using the conidiophore bearing cotyledons from **(a)**.

(c) Conidiophores (*PpEmoy2*) (white arrow) covered the surface of rosette leaves on a 4-5 wk old susceptible plants (*eds1.1*, grown for *P. parasitica* maintenance), 7-10 d after rub inoculation with conidiophore bearing plants from **(b)**.

(d) Dark, minute HR flecks (white arrow) amongst trichomes (black arrow) on a rosette leaf of a 4-5 wk old resistant plant (Ler (wt)), 7-10 d after rub inoculation with conidiophore (*PpEmoy2*) bearing plants from **(b)**.

(e) Conidiophores (white arrow) on rosette leaves of 3 wk old susceptible plants (*eds1.1*), 7 d after inoculation with a conidial suspension from a virulent (*PpEmoy2*) isolate.

(f) No conidiophores on rosette leaves of 3 wk old resistant plants (Ler (wt)), 7 d after inoculation with a conidial suspension from an avirulent (*PpEmoy2*) isolate.

(g) to (i) LTB stained susceptible leaf tissue from **(e)**. **(g)** Spreading hyphae (white arrow) with haustoria (black arrow). **(h)** Oospores (white arrow). **(i)** A conidiophore on the leaf surface (white arrow). Note: vascular tissue (white arrowhead).

(j) Small clusters of HR cells (white arrow) at sites of penetration within LTB stained resistant leaf tissue from **(f)**. Note: vascular tissue (white arrowhead).

Bar is equivalent to **(a)** 0.75 mm, **(b)** 2 mm, **(c)** 7.5 mm, **(d)** 0.5 mm, **(e, f)** 15 mm and **(g-j)** 100 μ m.

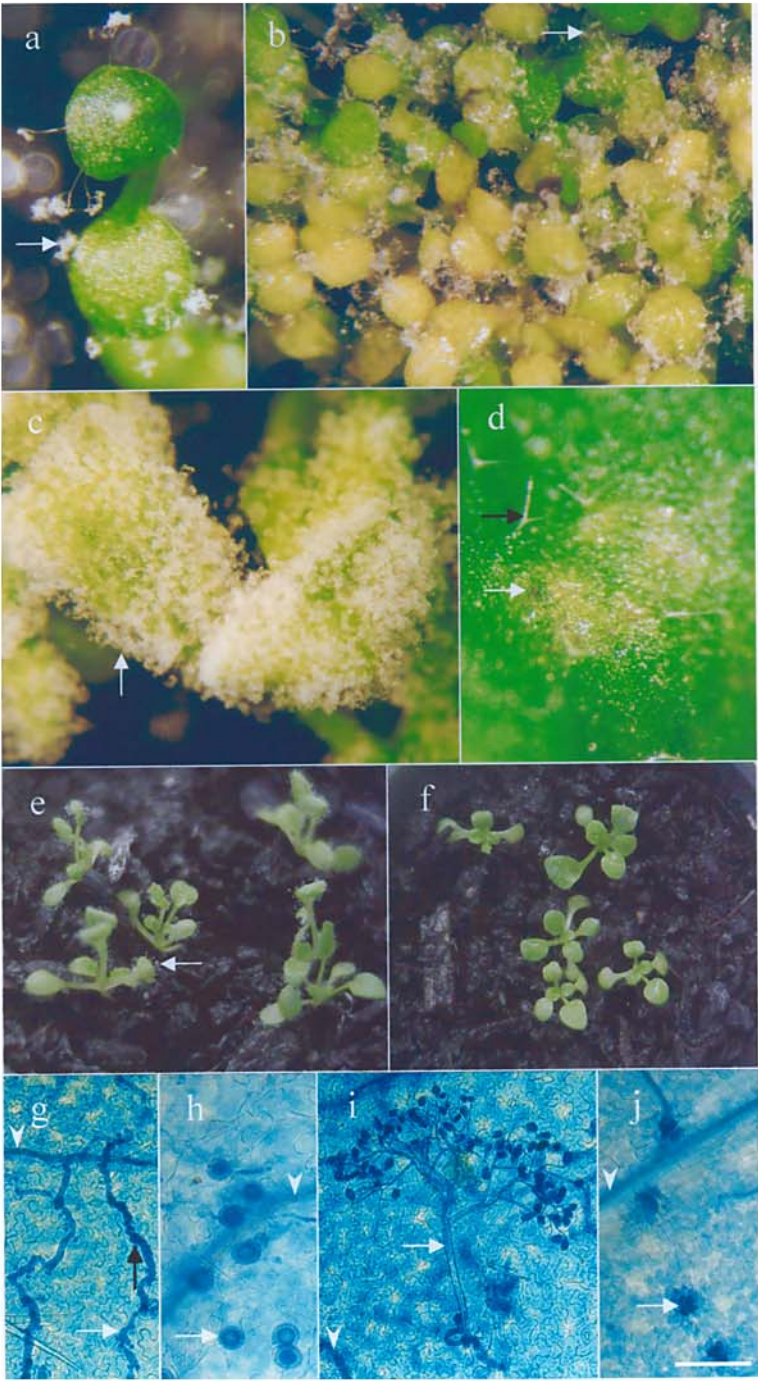


Figure 2.2 Visualisation of interactions between *Arabidopsis* and *P. parasitica*.

Leaves stained with LTB 7 d after inoculation.

(a) and **(d)** Resistant interactions between Ler (wt) leaf tissue and avirulent *PpEmoy2* and *PpNoks1* isolates respectively, showing HR cells (white arrow) at sites of penetration. Note: vascular tissue (white arrowhead).

(b) and **(c)** Susceptible interactions between Ler (wt) leaf tissue and virulent *PpHind4* and *PpCala2* isolates respectively, showing spreading hyphae (white arrow) and **(b, c insets)** oospores (black arrow). Note: vascular tissue (white arrowhead).

(e), **(f)** and **(g)** Resistant interactions between Col-0 (wt) and avirulent *PpEmoy2*, *PpHind4* and *PpCala2* isolates respectively, showing HR cells (white arrow) at sites of penetration. Note: vascular tissue (white arrowhead).

(h) A susceptible interaction between Col-0 (wt) and a virulent *PpNoks1* isolate showing spreading hyphae (white arrow) and **(h inset)** oospores (black arrow). Note: vascular tissue (white arrowhead).

Bar is equivalent to **(a-h)** 350 μm and **(b, c, h insets)** 500 μm . Representative images from two independent experiments.

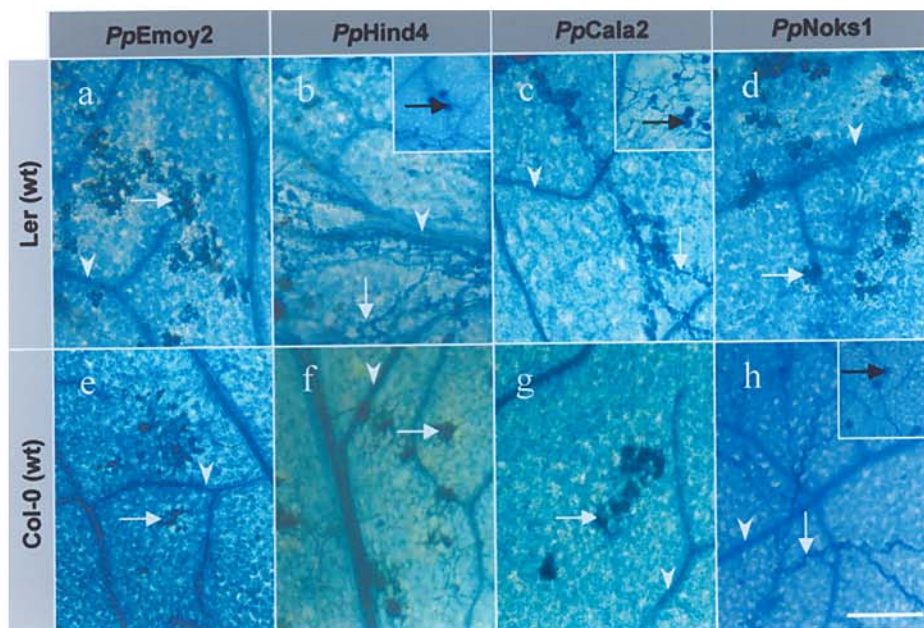


Table 2.1 Summary of resistant (R) and susceptible (S) Arabidopsis / *P. parasitica* interactions

Arabidopsis (ecotype)	<i>P. parasitica</i> (isolate)			
	<i>PpEmoy2</i>	<i>PpHind4</i>	<i>PpCala2</i>	<i>PpNoks1</i>
Ler (wt)	R	S	S	R
Col-0 (wt)	R	R	R	S

Figure 2.3 Preliminary observations on the effect of ABA treatment on resistant interactions between *Arabidopsis* and *P. parasitica*.

(a) to (d) Minute HR flecks on Ler (wt) leaves, 7 d after inoculation with an avirulent (*PpEmoy2*) isolate. **(a)** Plants treated with 1% (v/v) methanol (control), **(b)** 1, **(c)** 10 and **(d)** 100 μ M ABA. White arrow: HR cells. Black arrow: leaf trichome. Bar is equivalent to 1 mm. Representative images from a single experiment.

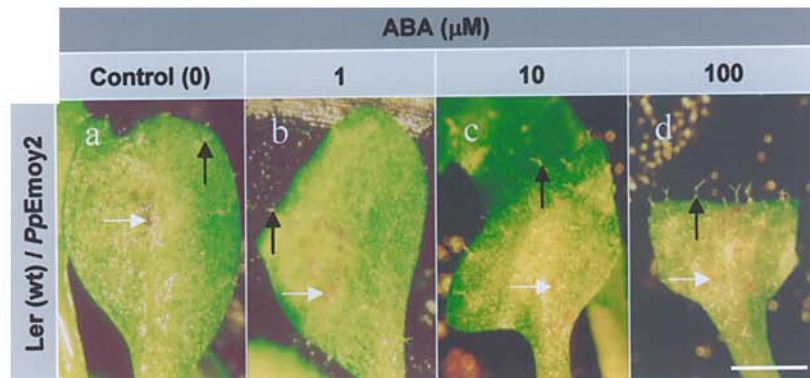


Table 2.2 Number of *P. parasitica* conidiophores on Arabidopsis leaves treated with ABA

Arabidopsis (ecotype)	<i>P. parasitica</i> (isolate)	ABA (μ M)	Conidiophores (number leaf ⁻¹)*
Ler (wt)	<i>PpEmoy2</i>	Control (0)	0
		1	0
		10	0
		100	0

* Conidiophores on 40 leaves of eight plants were analysed for each treatment.

Figure 2.4 Visualisation of resistant interactions between *Arabidopsis* and *P. parasitica* following treatment of plants with ABA.

Leaves stained with LTB 7 d after inoculation.

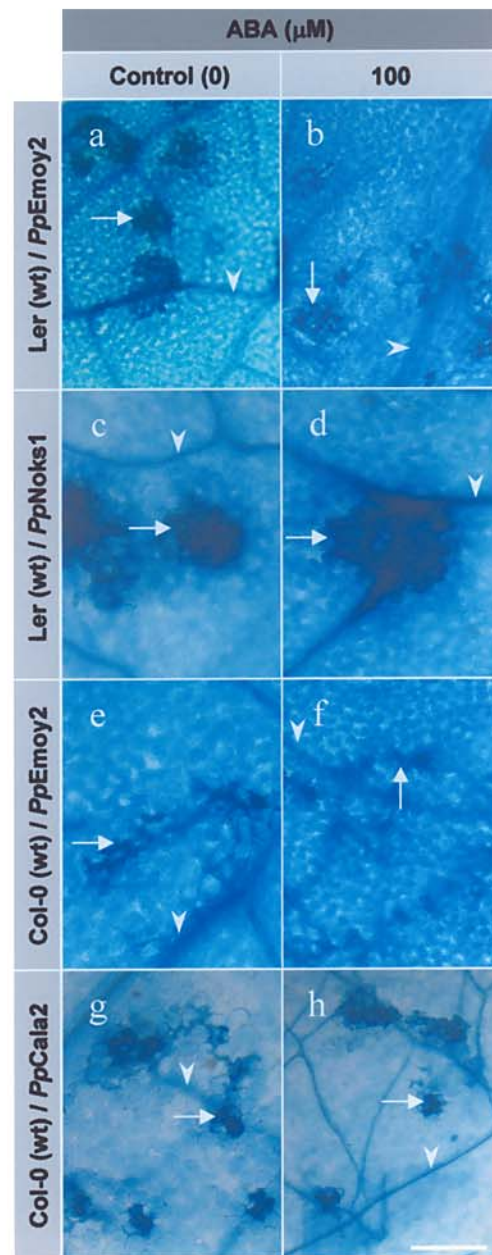
(a) and **(b)** Ler (wt) leaves inoculated with an avirulent (*PpEmoy2*) isolate, showing HR cells (white arrow). Note: vascular tissue (white arrowhead). **(a)** Plants treated with 1% (v/v) methanol (control) or **(b)** 100 μ M ABA prior to inoculation.

(c) and **(d)** Ler (wt) leaves inoculated with an avirulent (*PpNoks1*) isolate, showing HR cells (white arrow). Note: vascular tissue (white arrowhead). **(c)** Plants treated with 1% (v/v) methanol or **(d)** 100 μ M ABA prior to inoculation.

(e) and **(f)** Col-0 (wt) leaves inoculated with an avirulent (*PpEmoy2*) isolate, showing HR cells (white arrow). Note: vascular tissue (white arrowhead). **(e)** Plants treated with 1% (v/v) methanol or **(f)** 100 μ M ABA prior to inoculation.

(g) and **(h)** Col-0 (wt) leaves inoculated with an avirulent (*PpCala2*) isolate, showing HR cells (white arrow). Note: vascular tissue (white arrowhead). **(e)** Plants treated with 1% (v/v) methanol or **(f)** 100 μ M ABA prior to inoculation.

Bar is equivalent to 100 μ m. Representative images from two independent experiments.



55.6 fold increase in endogenous ABA concentration prior to inoculation, but did not affect the development or phenotype of newly formed leaves (Figure 2.5a-c).

2.3.3 Treatment with ABA biosynthesis inhibitors of *Arabidopsis* / *P. parasitica* susceptible interactions

Preliminary 1, 10 and 100 μM norflurazon (a pyridazinone herbicide and an ABA biosynthesis inhibitor) treatments of a susceptible interaction reduced the production of conidiophores per leaf as the inhibitor concentration increased (Figure 2.6a-d and Table 2.3). Further 100 μM norflurazon treatments of susceptible interactions caused a significantly ($p < 0.05$) 1.8 fold reduction in the number of conidiophores per leaf (Figure 2.7a). Treatments with 100 μM of a pyridinone herbicide (also an ABA biosynthesis inhibitor) fluridone, also significantly ($p < 0.05$) reduced conidiophores per leaf by at least 1.7 fold. Both treatments did not significantly ($p > 0.05$) alter the number of leaves without a conidiophore but significantly ($p < 0.05$) reduced the number of leaves bearing ≥ 20 conidiophores by at least 3.3 fold (Figure 2.7b and c). Despite conidiophore reductions, there was no change in hyphal spread or oospore production within leaves (Figure 2.8a-h). Treatment with 100 μM norflurazon or 100 μM fluridone had no significant ($p > 0.05$) effect on concentrations of endogenous ABA but resulted in dramatic photobleaching (yellow-white) of newly formed leaves (Figure 2.9a-d).

2.3.4 Characterisation of *Arabidopsis* ABA deficient mutant and ABA insensitive mutant interactions with avirulent and virulent isolates of *P. parasitica*

When seeds of Ler background were germinated and the seedlings maintained on MS media for 2 wk, the wild type, ABA deficient mutants *aba1-1*, *aba1-3*, *aba1-4*, *aao3* and ABA insensitive mutants *abi1-1* and *abi2-1* were

Figure 2.5 Effect of ABA uptake via the roots on endogenous ABA concentrations in the tops of plants and the health of plants.

(a) Endogenous ABA concentrations of 1% (v/v) methanol (control) and 100 μ M ABA treated Ler (wt) tops of plants immediately prior to leaf inoculation. Each column represents the mean \pm s.e.m of two independent experiments.

(b) and **(c)** Healthy newly formed Ler (wt) leaves (white arrow) 7 d after 1% (v/v) methanol and 100 μ M ABA treatment respectively. Bar is equivalent to 1 mm. Representative images from two independent experiments.

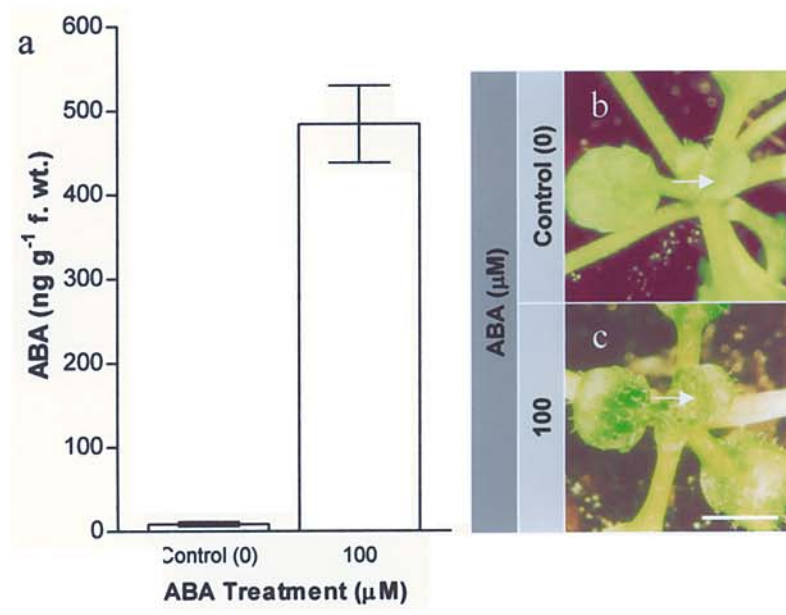


Figure 2.6 Preliminary observations on the effect of ABA biosynthesis inhibitor (norflurazon) treatment on susceptible interactions between Arabidopsis and *P. parasitica*.

(a) to (d) Conidiophores on Ler (wt) leaves, 7 d after inoculation with a virulent (*PpHind4*) isolate. (a) Plants treated with dH₂O (control), (b) 1, (c) 10, and (d) 100 μ M norflurazon. White arrow: *P. parasitica* conidiophore. Black arrow: leaf trichome. Bar is equivalent to 1 mm. Representative images from a single experiment.

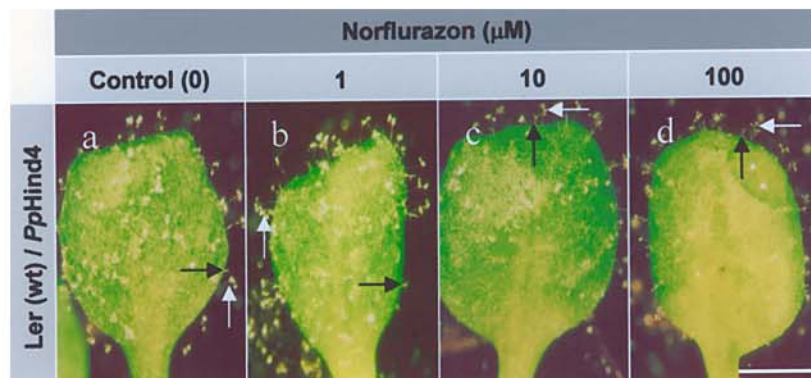


Table 2.3 Number of *P. parasitica* conidiophores on Arabidopsis leaves treated with an ABA biosynthesis inhibitor

Arabidopsis (ecotype)	<i>P. parasitica</i> (isolate)	Norflurazon (μM)	Conidiophores (number leaf ⁻¹)*
Ler (wt)	<i>PpHind4</i>	Control (0)	20.0 ± 0.0
		1	17.4 ± 1.4
		10	16.6 ± 1.8
		100	9.8 ± 1.6

* The mean ± s.e.m. of 40 leaves from eight plants are presented for each treatment.

Figure 2.7 Production of *P. parasitica* conidiophores 7 d after inoculation of *Arabidopsis* leaves that had been treated with an ABA biosynthesis inhibitor.

(a) Number of conidiophores per leaf, **(b)** number of leaves bearing no conidiophores and **(c)** number of leaves bearing ≥ 20 conidiophores. (□) Ler (wt) / *PpHind4* and (▨) Col-0 (wt) / *PpNoks1* susceptible interactions with 0.4% (v/v) DMSO (control), 100 μ M norflurazon or 100 μ M fluridone treatment prior to inoculation. Each column represents the mean \pm s.e.m. from four independent experiments.

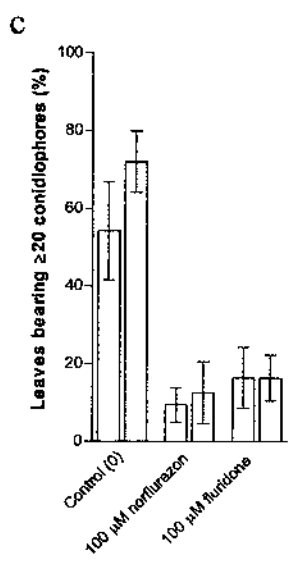
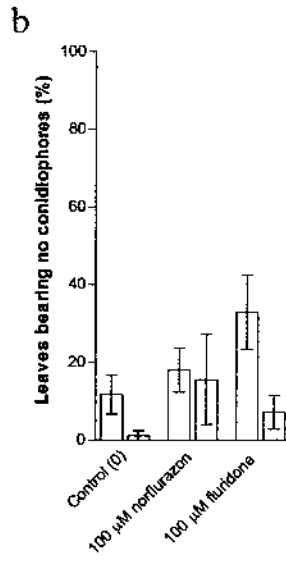
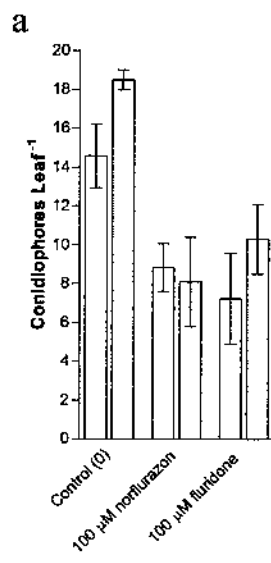


Figure 2.8 Visualisation of susceptible interactions between Arabidopsis and *P. parasitica* following treatment of plants with ABA biosynthesis inhibitors.

Leaves stained with LTB 7 d after inoculation.

(a) to (d) Ler (wt) leaves inoculated with a virulent (*PpHind4*) isolate, showing hyphal spread (white arrow) and oospores (black arrow). Note: vascular tissue (white arrowhead). (a) Plants treated with dH₂O (control) or (b) 100 µM norflurazon prior to inoculation. (c) Plants treated with 0.4% (v/v) DMSO (control) or (d) 100 µM fluridone prior to inoculation.

(e) to (h) Col-0 (wt) leaves inoculated with a virulent (*PpNoks1*) isolate, showing hyphal spread (white arrow) and oospores (black arrow). Note: vascular tissue (white arrowhead). (e) Plants treated with dH₂O or (f) 100 µM norflurazon prior to inoculation. (g) Plants treated with 0.4% (v/v) DMSO or (h) 100 µM fluridone prior to inoculation.

Bar is equivalent to (a-f) 200 µm and (g, h) 100 µm. Representative images from four independent experiments.

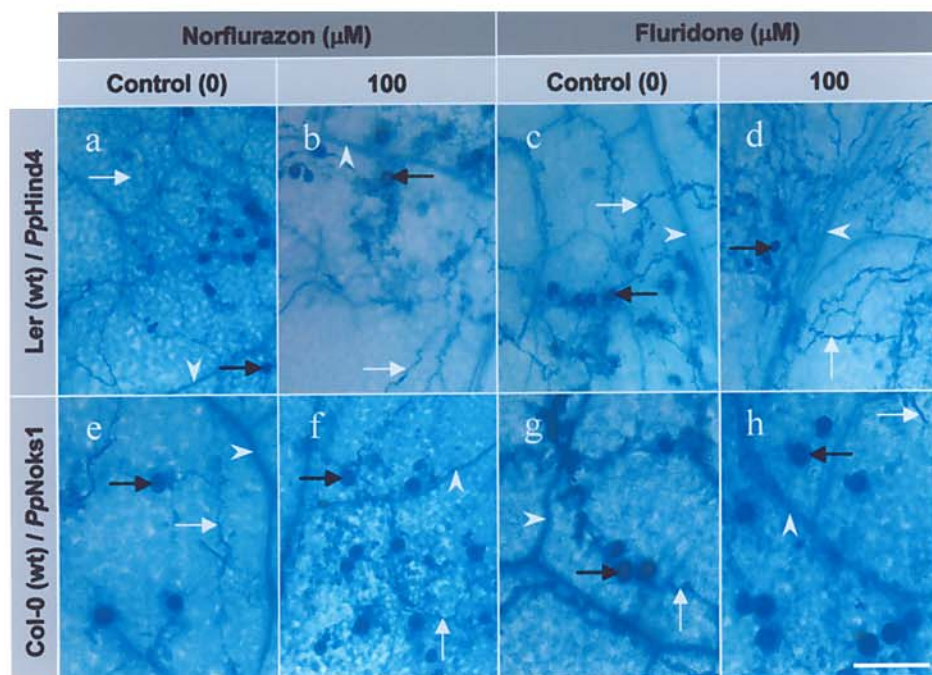
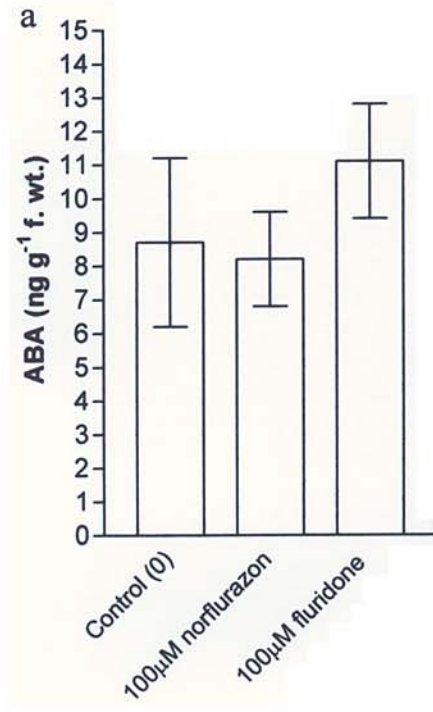


Figure 2.9 Effect of ABA biosynthesis inhibitor uptake via the roots on endogenous ABA concentrations in the tops of plants and the health of plants.

(a) Endogenous ABA concentrations of 0.4% (v/v) DMSO (control) and 100 μ M norflurazon and 100 μ M fluridone treated Ler (wt) tops of plants immediately prior to leaf inoculation. Each column represents the mean \pm s.e.m. from two independent experiments.

(b) Healthy, newly formed Ler (wt) leaves (white arrow) 7 d after 0.4% (v/v) DMSO treatment.

(c) and **(d)** Yellow / white (photobleached) newly formed Ler (wt) leaves (white arrow) 7 d after 100 μ M norflurazon or 100 μ M fluridone treatments respectively. Bar equivalent to 3 mm. Representative images from four independent experiments.



phenotypically similar (Figure 2.10a-g). However, the concentration of endogenous ABA within the ABA deficient mutants prior to inoculation was significantly ($p < 0.05$) at least 3.3 fold less than that of Ler (wt) plants (Figure 2.10k). The insensitivity of *abi1-1* and *abi2-1* seed stocks to ABA was confirmed by the ability of the seeds to germinate on MS medium containing 10 μ M ABA (that inhibited germination of wild type seeds) (data not shown). When seed of Col-0 background were germinated and the seedlings maintained on MS media the wild type and ABA deficient mutants *aba2-1* and *aba3-1* of Col-0 (wt) background were also phenotypically similar (Figure 2.10h-j). The concentration of ABA within *aba2-1* and *aba3-1* was significantly ($p < 0.05$) less (1.8 fold) than that for Col-0 (wt) (Figure 2.10l).

Inoculation of Ler (wt), *abal-3*, *abal-4*, *aao3*, *abi1-1* and *abi2-1* leaves with avirulent isolates resulted in dark minute HR flecks at the site of inoculation that were typical of resistant interactions (Figure 2.11a-d, i-s). Inoculation of Col-0 (wt), *aba2-1* and *aba3-1* leaves with an avirulent isolate also resulted in typical resistant interactions (Figure 2.11t-v). In contrast, inoculation of *abal-1* leaves with avirulent isolates resulted in large, dark, HR pits spread across most of the inoculated resistant leaf (Figure 2.11e-h).

Inoculation of Ler (wt), *abal-3* and *abi1-1* leaves with virulent isolates resulted in hyphal spread, oospore and conidiophore production consistent with susceptible interactions (Figure 2.12a-d, q-x). Inoculation of *aao3*, *abi2-1*, Col-0 (wt), *aba2-1* and *aba3-1* leaves with a virulent isolate also resulted in hyphal spread and oospore production (Figure 2.12z-d'). In contrast, inoculation of *abal-1* leaves with virulent isolates resulted in large HR-like pits with varying hyphal spread into healthy tissue and varying numbers of conidiophores, from none or one to many in

Figure 2.10 Comparison of growth form at different endogenous ABA concentrations for Arabidopsis ABA deficient and ABA insensitive mutants compared with wild type plants.

(a) to (j) Plants 2 wk of age, grown on MS medium within Petri plates.

(a) to (g) Plants of Ler (wt) background. **(a)** Ler (wt), **(b)** ABA deficient mutant *aba1-1*, **(c)** *aba1-3*, **(d)** *aba1-4* and **(e)** *aao3* and **(f)** ABA insensitive mutant *abi1-1* and **(g)** *abi2-1*.

(h) to (j) Plants of Col-0 (wt) background **(h)** Col-0 (wt), **(i)** ABA deficient mutant *aba2-1* and **(j)** *aba3-1*. Bar is equivalent to 4 mm. Representative images from two independent experiments.

(k) and (l) Endogenous ABA concentrations in the tops of plants immediately prior to leaf inoculation. **(k)** Ler (wt) and Arabidopsis ABA deficient and ABA insensitive mutants from **(a)** to **(g)**. **(l)** Col-0 (wt) and Arabidopsis ABA deficient mutants from **(h)** to **(j)**. Each column represents the mean \pm s.e.m. from two independent experiments (except *aba1-4* which is from a single experiment).

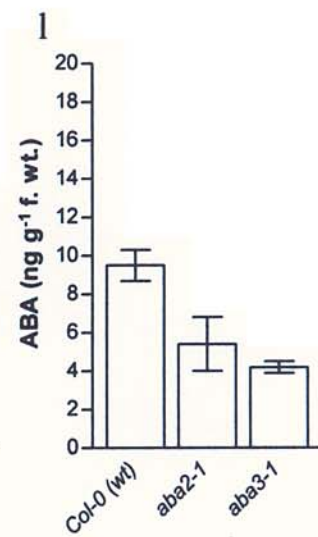
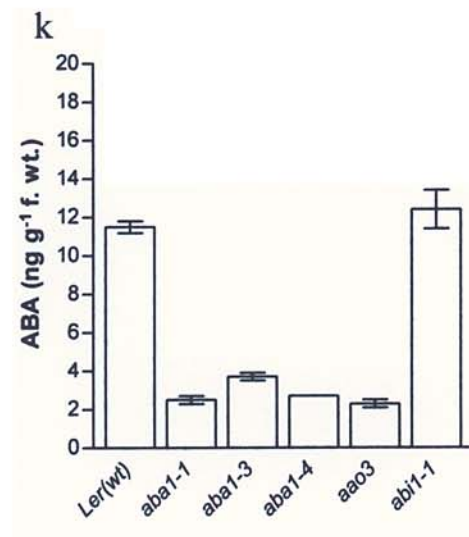
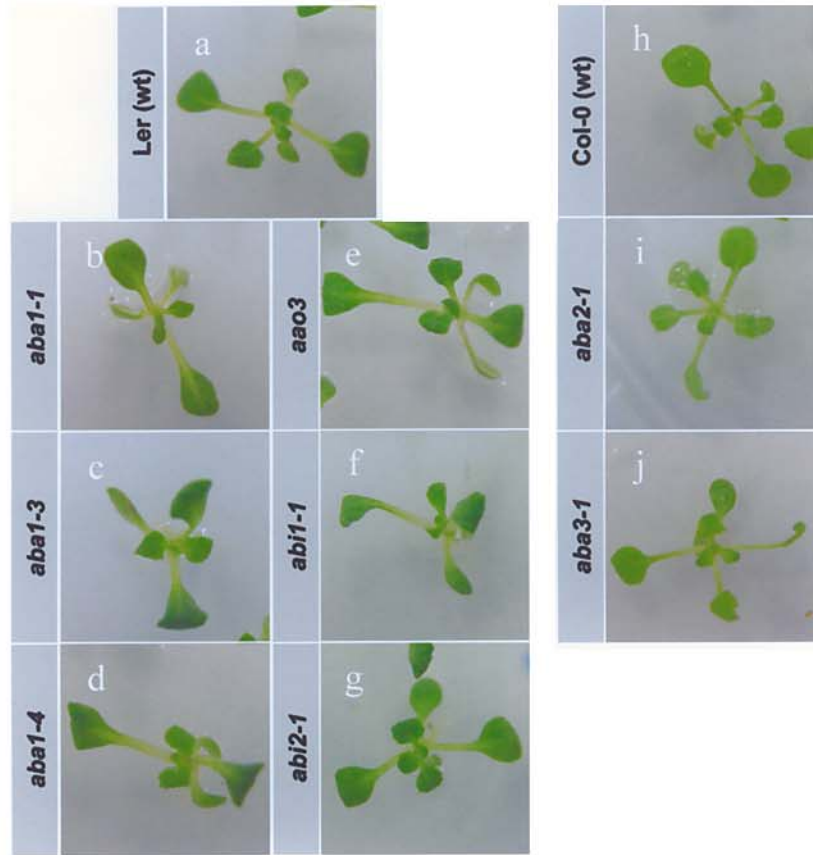


Figure 2.11 Resistant interactions of Arabidopsis ABA deficient and ABA insensitive mutant leaves following inoculation with avirulent isolates of *P. parasitica*.

All images taken 7 d after inoculation. **(b, d, f, h, j, l, n, p-v)** Leaves stained with LTB 7 d after inoculation.

(a, b) and **(c, d)** Ler (wt) leaves inoculated with the avirulent *PpEmoy2* and *PpNoks1* isolates respectively, showing minute HR flecks (white arrow). Note: vascular tissue (white arrowhead)

(e, f) and **(g, h)** ABA deficient mutant *aba1-1* leaves inoculated with the avirulent *PpEmoy2* and *PpNoks1* isolates respectively, showing extensive HR pits (black arrow). Note: vascular tissue (white arrowhead)

(i, j) and **(k, l)** ABA deficient mutant *aba1-3* leaves inoculated with the avirulent *PpEmoy2* and *PpNoks1* isolates respectively, showing minute HR flecks (white arrow). Note: vascular tissue (white arrowhead)

(m, n) and **(o, p)** ABA insensitive mutant *abi1-1* leaves inoculated with the avirulent *PpEmoy2* and *PpNoks1* isolates respectively showing minute HR flecks (white arrow). Note: vascular tissue (white arrowhead)

(q) to **(v)** Inoculations of leaf tissue with the avirulent *PpEmoy2* isolate, showing small clusters of HR cells (white arrow). Note: vascular tissue (white arrowhead) **(q)** ABA deficient mutant *aba1-4* and **(r)** *aoa3*, **(s)** ABA insensitive mutant *abi2-1*, **(t)** Col-0 (wt), **(u)** ABA deficient mutant *aba2-1* and **(v)** *aba3-1*. Bar is equivalent to **(a, c, e, g, i, k, m, o)** 0.75 mm, **(b, d, f, h, j, l, n, p)** 200 μ m and **(q-v)** 100 μ m.

Representative images from three independent experiments.

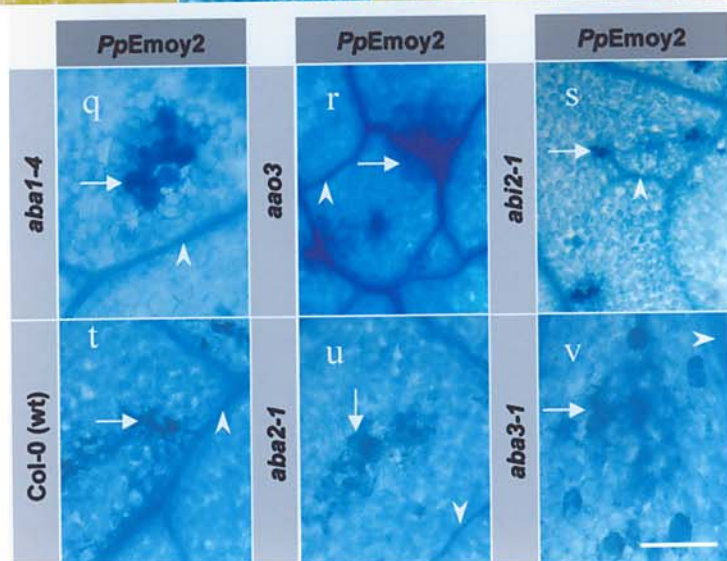
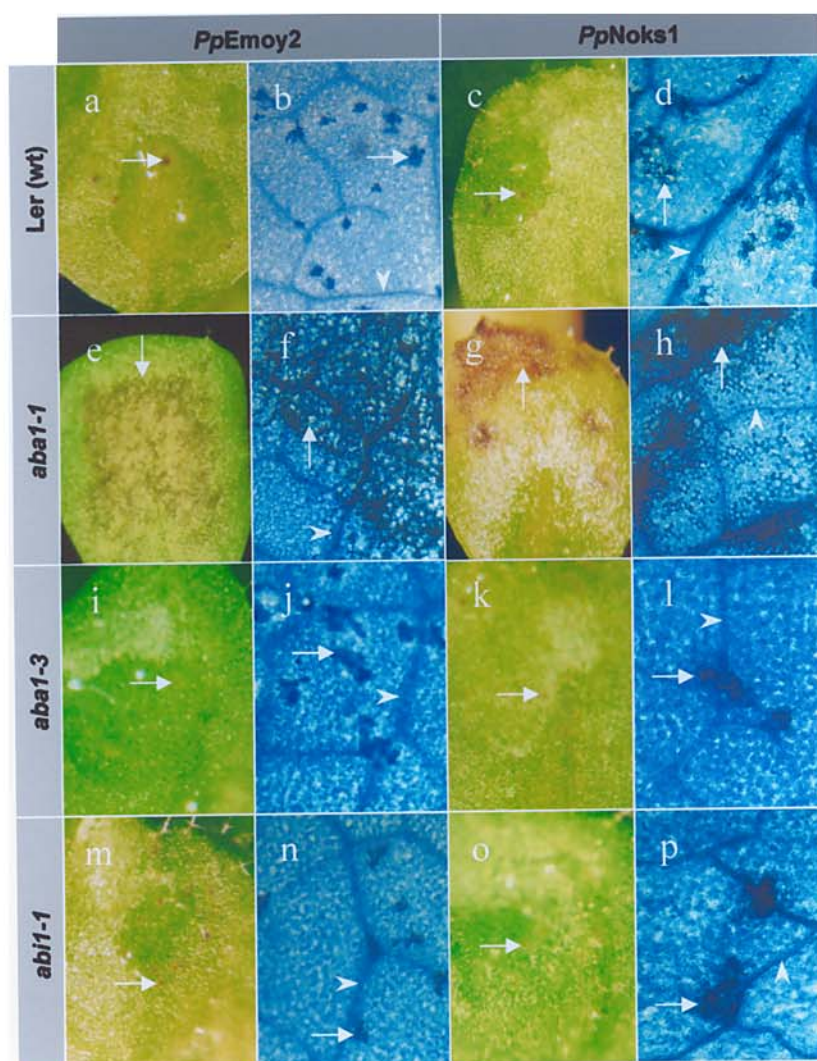
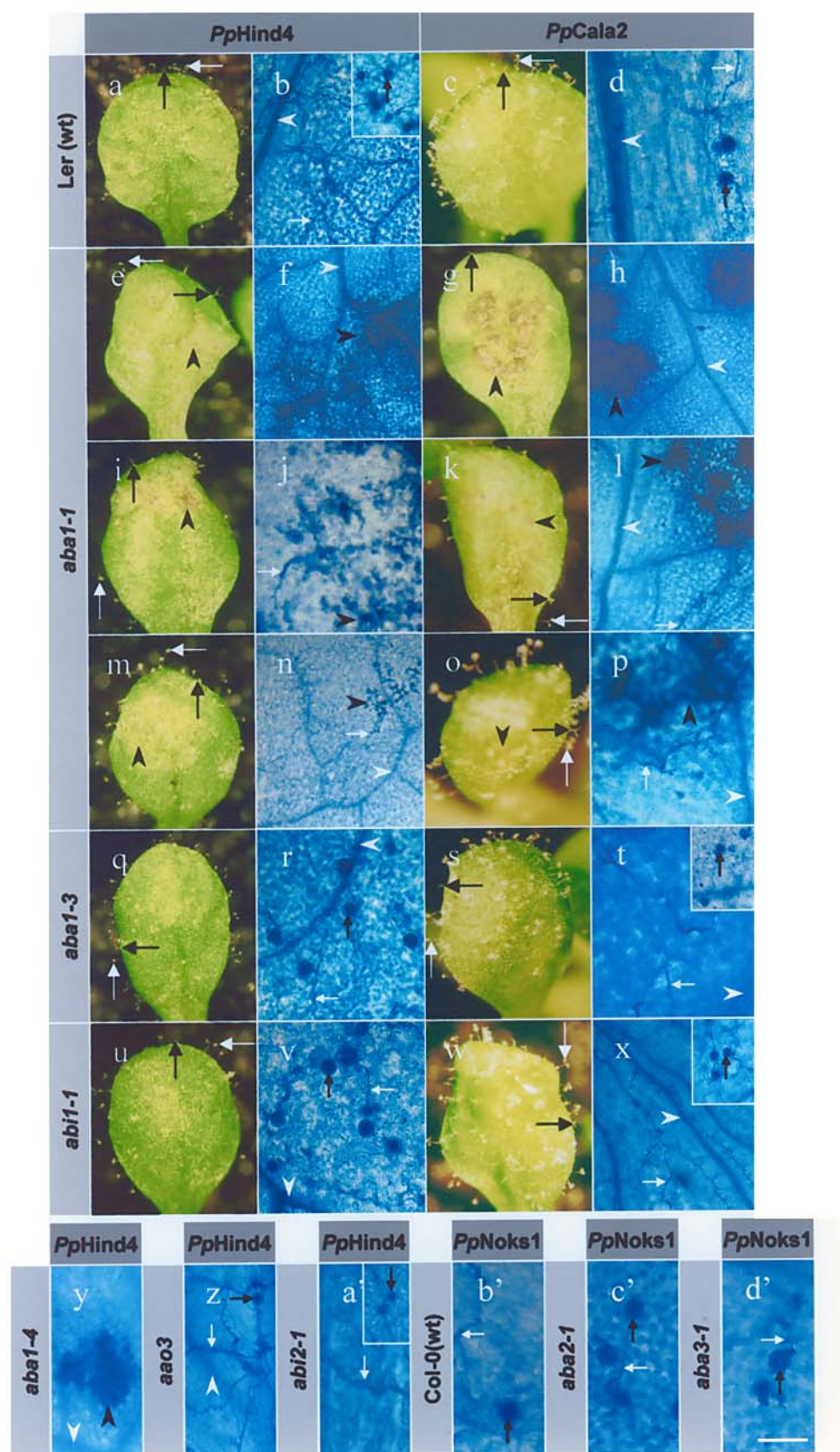


Figure 2.12 Interactions of Arabidopsis ABA deficient and ABA insensitive mutant leaves and following inoculation with virulent isolates of *P. parasitica*.

All images taken 7 d after inoculation. Note: vascular tissue (white arrowhead), leaf trichome (black arrow). (b, d, f, h, j, l, n, p, r, t, v, x-d') Leaves stained with LTB. (a, b, b inset) and (c, d) Susceptible interactions between Ler (wt) leaves and virulent *PpHind4* and *PpCala2* isolates respectively, showing conidiophores (white arrow), hyphal spread (small white arrow) and oospores (small black arrow). (e, f, i, j, m, n) and (g, h, k, l, o, p) Intermediate interactions between ABA deficient mutant *aba1-1* leaves and virulent *PpHind4* and *PpCala2* isolates respectively, showing HR-like pits (black arrowhead) with limited conidiophores (white arrow) or hyphal spread (small white arrow). (q, r) and (s, t, t inset) Susceptible interactions between ABA deficient mutant *aba1-3* leaves and virulent *PpHind4* and *PpCala2* isolates respectively, showing conidiophores (white arrow), hyphal spread (small white arrow) and oospores (small black arrow). (u, v) and (w, x, x inset) Susceptible interactions between ABA insensitive mutant *abi1-1* leaves and virulent *PpHind4* and *PpCala2* isolates respectively, showing conidiophores (white arrow), hyphal spread (small white arrow) and oospores (small black arrow). (y) Resistant interaction between ABA deficient mutant *aba1-4* leaves and the virulent *PpHind4* isolate, showing a small cluster of HR-like cells (black arrowhead). (z, a') and (b', c', d') Susceptible interactions between leaf tissue inoculated with virulent *PpHind4* and *PpNoks1* isolates respectively, showing conidiophores (white arrow), hyphal spread (small white arrow) and oospores (small black arrow). (z) ABA deficient mutant *aao3*, (a') ABA insensitive mutant *abi2-1*, (b') Col-0 (wt), (c') ABA deficient mutant *aba2-1* and (d') *aba3-1*. Bar is equivalent to (a, c, e, g, i, k, m, o, q, s, u, w) 0.75 mm, (b, d, f, h, j, l, n, p, r, t, v, x-d') 200 μ m (b, t, x, a' insets) 400 μ m and (y-d') 100 μ m. Representative images from three independent experiments.



interactions that were intermediate between resistance and susceptibility (Figure 2.12e-p). Inoculation of *aba1-4* leaves with a virulent isolate resulted in a small area of HR-like cell death at the site of penetration, in a phenotypically resistant interaction (Figure 2.12y).

Inoculation of Ler (wt), *abi1-1*, *abi2-1*, Col-0 (wt), *aba2-1* or *aba3-1* leaves with virulent isolates did not significantly ($p>0.05$) alter the production of conidiophores on leaves (Figure 2.13a-f). However, inoculation of *aba1-3* leaves with virulent isolates significantly ($p<0.05$) reduced the number of conidiophores per leaf by at least 1.2 fold and leaves bearing ≥ 20 conidiophores by at least 1.5 fold when compared to Ler (wt) leaves (Figure 2.13a and c). Inoculation of *aba1-1* leaves with virulent isolates significantly also ($p<0.05$) reduced the number of conidiophores per leaf and leaves bearing ≥ 20 conidiophores but to a greater extent than *aba1-3* leaves, with at least 2.3 and 3.0 fold reductions respectively, when compared to Ler (wt) leaves (Figure 2.13a and c). The number of *aba1-1* leaves without a conidiophore was significantly ($p<0.05$) greater (at least 1.6 fold) than Ler (wt) leaves (Figure 2.13b). No conidiophores were produced on *aba1-4* leaves after inoculation with a virulent isolate (data not shown). The *aba1-4* mutant plants did not produce fertile seeds and therefore no more plants were available for further experimental analysis (data not shown).

2.3.5 Number of conidiophores on ABA deficient mutants inoculated with a virulent isolate of *P. parasitica* following treatment with ABA

The 100 μ M ABA treatment of *aba1-1* plants induced at least a 152.4 fold increase in the concentration of endogenous ABA prior to inoculation, similar to the concentration in 100 μ M ABA treated Ler (wt) plants (Figure 2.14a). The number of conidiophores per leaf and leaves bearing ≥ 20 conidiophores on ABA treated *aba1-1*

Figure 2.13 Production of *P. parasitica* conidiophores 7 d after inoculation of *Arabidopsis* ABA deficient and ABA insensitive mutant leaves.

(a) Number of conidiophores per leaf, (b) number of leaves bearing no conidiophores and (c) number of leaves bearing ≥ 20 conidiophores. Ler (wt), ABA deficient mutant *aba1-1* and *aba1-3* and ABA insensitive mutant *abi1-1* and *abi2-1* inoculated with virulent (□) *PpHind4* or (▨) *PpCala2* isolates. Each column represents the mean \pm s.e.m. from three independent experiments (except *abi2-1* which is from a single *PpHind4* inoculation and not inoculated with *PpCala2*).

(d) Number of conidiophores per leaf, (e) number of leaves bearing no conidiophores and (f) number of leaves bearing ≥ 20 conidiophores. Col-0 (wt) and ABA deficient mutant *aba2-1* and *aba3-1* inoculated with the (■) virulent *PpNoks1* isolate. Each column represents the mean \pm s.e.m. from four independent experiments.

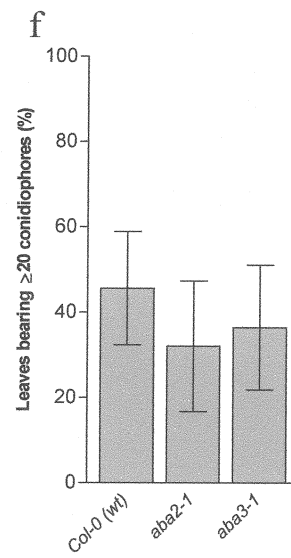
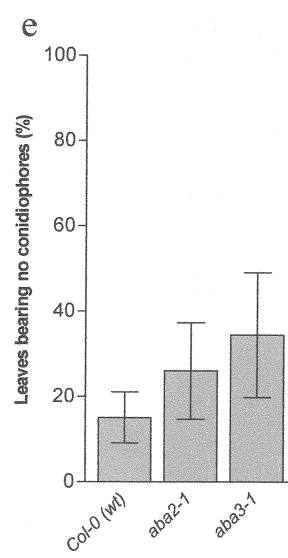
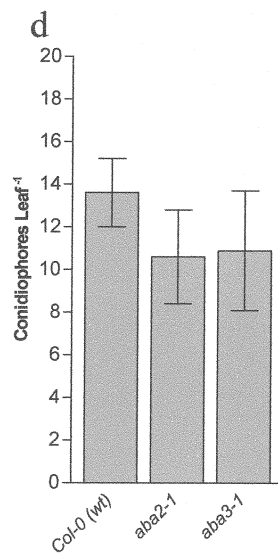
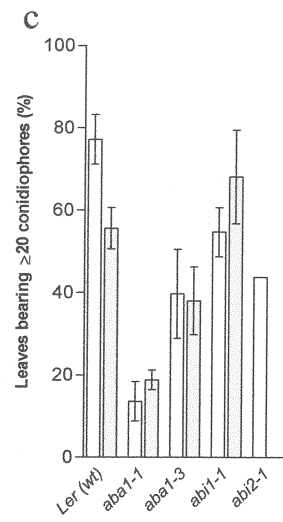
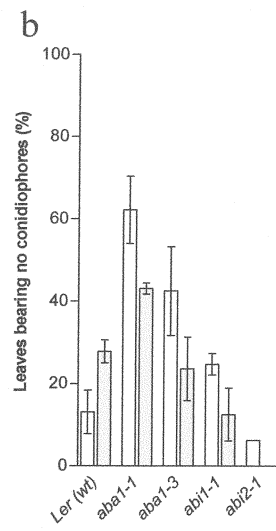
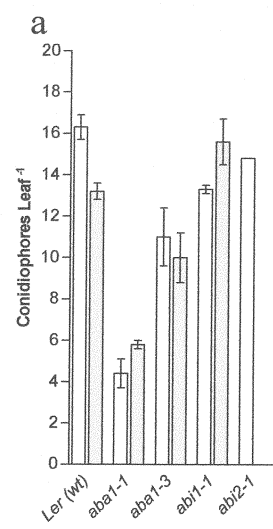
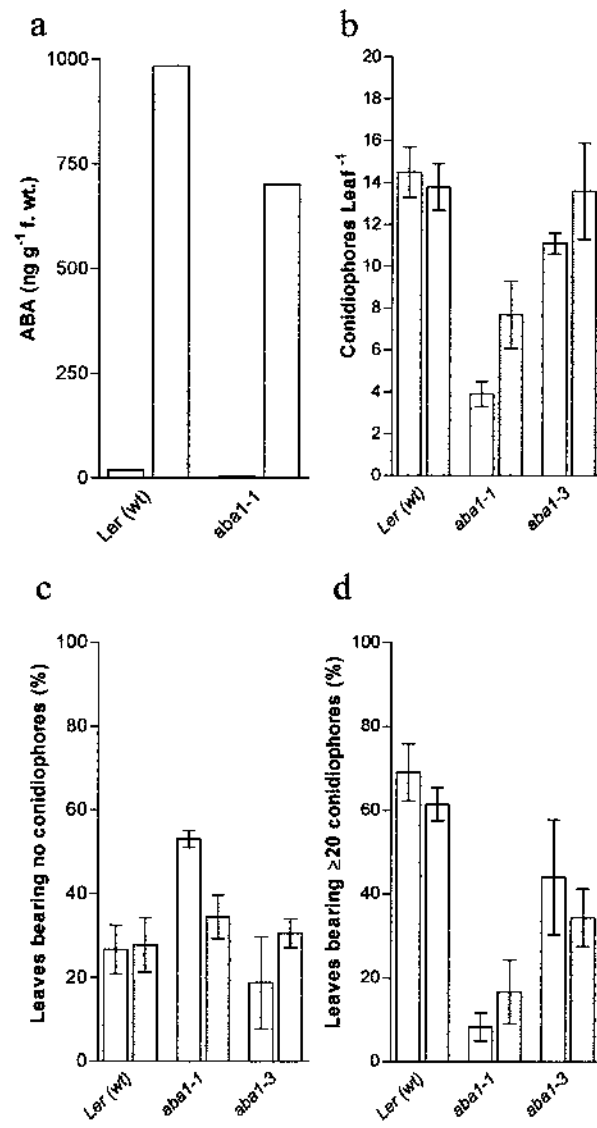


Figure 2.14 Production of *P. parasitica* conidiophores 7 d after inoculation of *Arabidopsis* ABA deficient mutant leaves that had been treated with ABA.

(a) Endogenous ABA concentrations of (□) 1% (v/v) methanol (control) and (▨) 100 μ M ABA treated Ler (wt) and ABA deficient mutant *aba1-1* tops of plants immediately prior to leaf inoculation (treatment of *aba1-3* was not assessed). Each column represents the mean of a single experiment, with the tops of ten plants for each treatment.

(b) Number of conidiophores per leaf, (c) number of leaves bearing no conidiophores and (d) number of leaves bearing ≥ 20 conidiophores 7 d after inoculation with a virulent (*PpHind4*) isolate. Ler (wt) and ABA deficient mutant *aba1-1* and *aba1-3* treated with (□) 1% (v/v) methanol and (▨) 100 μ M ABA prior to inoculation. Each column represents the mean \pm s.e.m. from four independent experiments.



plants following inoculation with a virulent isolate were still significantly ($p < 0.05$) less than Ler (wt), by at least 1.8 and 3.7 fold respectively (Figure 2.14b and d). However, ABA treatment of *aba1-1* drastically reduced the number of leaves without a conidiophore by 1.5 fold to 34.5%, not significantly ($p > 0.05$) different from ABA treated or untreated Ler (wt) leaves (Figure 2.14c).

2.3.6 Comparison of morphological, anatomical and biochemical components in interactions between ABA deficient and ABA insensitive mutants of Arabidopsis and *P. parasitica*

2.3.6.1 Early detection of necrosis in avirulent and virulent inoculations of ABA deficient and ABA insensitive mutants

Four days after inoculation of Ler (wt), *aba1-3* and *abil-1* leaves with an avirulent isolate, small areas of HR cells were visible for the first time at the sites of penetration (Figure 2.15a, c and d). Conversely, at the same time after inoculation with a virulent isolate, only spreading hyphae were visible (Figure 2.15e, g and h). In contrast, both avirulent and virulent inoculation of *aba1-1* leaves developed extensive necrosis with no visible hyphae (Figure 2.15b and f).

2.3.6.2 H₂O₂ production in avirulent and virulent inoculations of ABA deficient and ABA insensitive mutants

After DAB treatment and prior to inoculation, H₂O₂ was only detected in the vascular tissue of Arabidopsis leaves (data not shown). One day after control treatment, avirulent or virulent inoculation of Ler (wt), *aba1-1*, *aba1-3* or *abil-1* leaves and the removal of photosynthetic pigments, no necrosis was visible (data not shown). Therefore, 1 d after DAB treatment and an avirulent isolate inoculation of Ler (wt), *aba1-1*, *aba1-3* and *abil-1* leaves the intense brown colouration at sites of penetration was attributed to H₂O₂ production (Figure 2.16a-d). In contrast,

Figure 2.15 Early stages of *P. parasitica* hyphal spread or necrosis development in Arabidopsis ABA deficient and ABA insensitive mutant leaves.

Leaves stained with LTB 4 d after inoculation.

(a) to (d) Resistant interactions between Arabidopsis leaves and an avirulent (*PpEmoy2*) isolate. **(a)** Development of small clusters of HR cells (white arrow) at the site of penetration in Ler (wt) leaf tissue. **(b)** Development of a large area of HR cells (white arrow) at and away from the site of penetration in ABA deficient mutant *aba1-1* leaf tissue. **(c)** and **(d)** Development of small clusters of HR cells (white arrow) at the site of penetration in ABA deficient mutant *aba1-3* and ABA insensitive mutant *abil-1* leaf tissue respectively. Note: vascular tissue (white arrowhead).

(e) to (h) Interactions between Arabidopsis leaves and a virulent (*PpHind4*) isolate. **(e)** Hyphal spread (white arrow) at the site of penetration in Ler (wt) leaf tissue, in a developing susceptible interaction. **(f)** Development of a large area of HR-like cells (white arrow) at and away from the site of penetration in *aba1-1* leaf tissue, in a developing intermediate interaction. **(g)** and **(h)** Hyphal spread (white arrow) at the site of penetration in *aba1-3* and *abil-1* leaf tissue respectively, in developing susceptible interactions. Note: vascular tissue (white arrowhead). Bar is equivalent to 150 μ m. Representative images from two independent experiments.

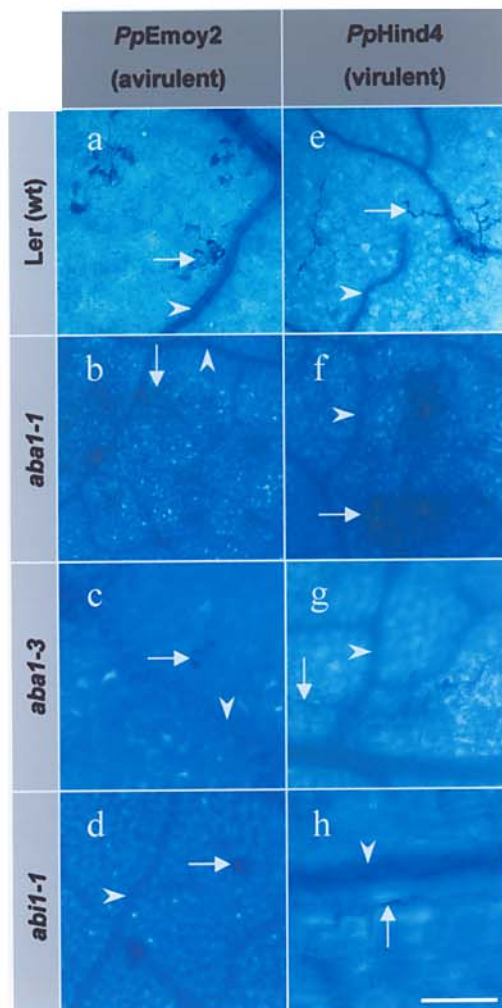


Figure 2.16 DAB detection of H₂O₂ production in Arabidopsis ABA deficient and ABA insensitive mutant leaves inoculated with *P. parasitica*.

Leaves cleared of photosynthetic pigments 1 d after DAB treatment and inoculation.

(a) to (d) DAB detection of H₂O₂ production (white arrow) in cells at the site of inoculation in developing resistant interactions between Arabidopsis leaves and an avirulent (*PpEmoy2*) isolate. (a) Ler (wt), (b) ABA deficient mutant *aba1-1* and (c) *aba1-3* and (d) ABA insensitive mutant *abil-1*. Note: vascular tissue (white arrowhead).

(e) to (h) DAB detection of H₂O₂ production in interactions between Arabidopsis leaves and a virulent (*PpHind4*) isolate. (e) No H₂O₂ production at the site of inoculation in Ler (wt) leaf tissue, in a developing susceptible interaction (f) H₂O₂ production (white arrow) at the site of inoculation in *aba1-1* leaf tissue, in a developing intermediate interaction. (g) and (h) No H₂O₂ production at the site of inoculation in *aba1-3* and *abil-1* leaf tissue respectively, in a developing susceptible interaction. Note: vascular tissue (white arrowhead). Bar is equivalent to 200 μ m.

Representative images from two independent experiments.



inoculation with a virulent isolate only produced H₂O₂ at the site of penetration in *aba1-1* leaf tissue (Figure 2.16e-h).

2.3.6.3 Lignin accumulation in avirulent and virulent inoculations of ABA deficient and ABA insensitive mutants

The PhI / HCl stain of *Arabidopsis* leaves prior to inoculation detected lignin within vascular tissue (data not shown). Seven days after inoculation of Ler (wt), *aba1-3* and *abi1-1* leaves with an avirulent isolate, lignin was detected within a small number of leaf cells at the site of penetration (Figure 2.17a, c and d). When the same plants were inoculated with a virulent isolate, lignin was only faintly detected in occasion cells associated with hyphal spread (Figure 2.17e, g, and h). In contrast, the inoculation of *aba1-1* with either an avirulent or virulent isolate resulted in lignin being detected in large areas of leaf cells (Figure 2.17b, and c). The detection of phenolics was similar in both avirulent and virulent inoculations with TB0 stain (data not shown).

Suberin was not detected within the vascular tissue or in association with sites of penetration in either avirulent or virulent inoculations of Ler (wt) or *aba1-1* (data not shown). Therefore, the wall bound TGA derivatives extracted from Ler (wt), *aba1-1*, *aba1-3* and *abi1-1* following avirulent or virulent inoculation were attributed to lignin accumulation (Figure 2.18). Seven days after avirulent or virulent inoculation of *aba1-1* leaves the accumulation of wall bound TGA derivatives (lignin) was significantly ($p < 0.05$) and at least 2.1 fold greater, than Ler (wt), *aba1-3* or *abi1-1* leaves (Figure 2.18).

Figure 2.17 Detection of lignin deposition in Arabidopsis ABA deficient and ABA insensitive mutant leaves inoculated with *P. parasitica*.

Leaves stained with PhI / HCl, 7 d after inoculation.

(a) to (d) Detection of lignin in resistant interactions between Arabidopsis leaves and an avirulent (*PpEmoy2*) isolate. **(a)** Lignin (white arrow) in cells at the site of penetration in Ler (wt) leaf tissue. **(b)** A large accumulation of lignin (white arrow) at and away from the site of penetration in ABA deficient mutant *aba1-1* leaf tissue. **(c)** and **(d)** Lignin (white arrow) in cells at the site of penetration in ABA deficient mutant *aba1-3* and ABA insensitive mutant *abil-1* leaf tissue respectively. Note: vascular tissue (white arrowhead).

(e) to (h) Detection of lignin in interactions between Arabidopsis leaves and a virulent (*PpHind4*) isolate. **(e)** Small, scattered accumulations of lignin (white arrow), associated with hyphal spread in Ler (wt) leaf tissue, in a susceptible interaction **(f)** A large accumulation of lignin (white arrow) at and away from the site of penetration in *aba1-1* leaf tissue, in an intermediate interaction. **(g)** and **(h)** Small, scattered accumulations of lignin (white arrow), associated with hyphal spread in *aba1-3* and *abil-1* leaf tissue respectively, in susceptible interactions. Note: vascular tissue (white arrowhead). Bar is equivalent to 200 μ m. Representative images from two independent experiments.

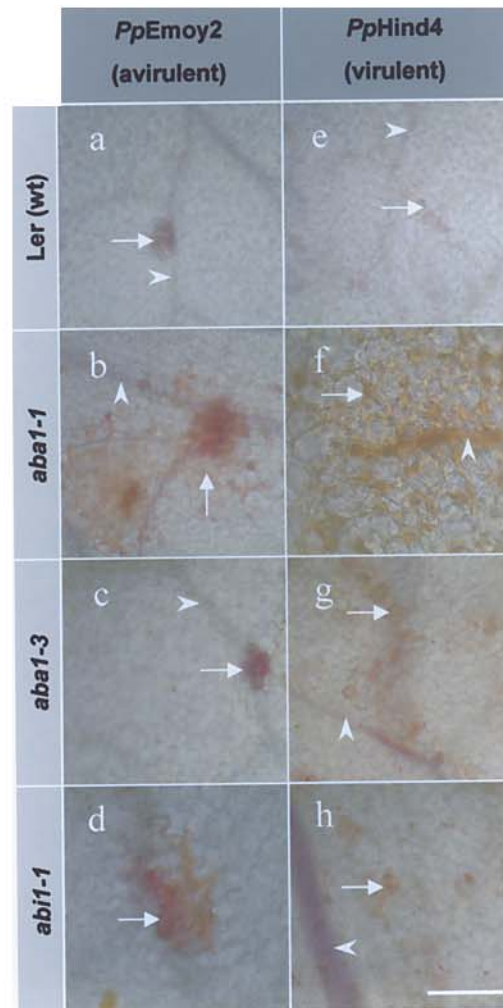
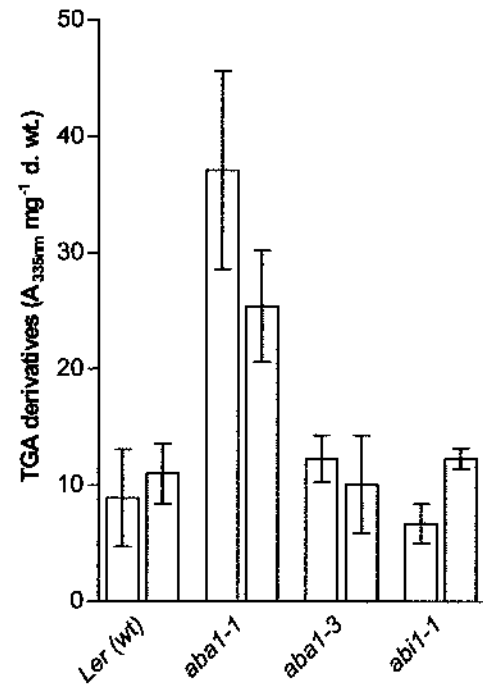


Figure 2.18 Wall bound TGA derivatives 7 d after inoculation of Arabidopsis ABA deficient and ABA insensitive mutant leaves.

Wall bound TGA derivatives of Ler (wt), ABA deficient mutant *aba1-1* and *aba1-3* and ABA insensitive mutant *abi1-1* plants, 7 d after (□) avirulent (*PpEmoy2*) or (■) virulent (*PpHind4*) isolate inoculation. Each column represents the mean \pm s.e.m, from three independent experiments.



2.3.6.4 Callose accumulation in avirulent and virulent inoculations of ABA deficient and ABA insensitive mutants

Prior to inoculation of *Arabidopsis* leaves, callose was detected by AB stain within vascular tissue and the base of leaf trichomes (data not shown). Seven days after inoculation of Ler (wt), *aba1-3* and *abi1-1* with an avirulent isolate, callose was visible within a small number of leaf cells at sites of penetration (Figure 2.19a, c and d). Following inoculation of the same plants with a virulent isolate, callose was restricted to intense collars at the base of haustoria and faintly in hyphae (Figure 2.19e, g and h). However, inoculation of *aba1-1* leaves with an avirulent or virulent isolate produced callose deposition in a large number of cells with punctate distribution (Figure 2.19b and f). In virulent inoculations of *aba1-1* leaves, callose was also associated with cells adjacent to hyphal spread away from the site of inoculation (Figure 2.19f).

2.3.6.5 *AtPAL1* mRNA transcript accumulations in avirulent and virulent inoculations of ABA deficient mutants

Prior to inoculation or 1 d after inoculation of Ler (wt), *aba1-1* and *aba1-3* leaves with either an avirulent or virulent isolate, the abundance of *AtPAL1* mRNA transcripts were similar (Figure 2.20a-c). However, 3 d after inoculation of *aba1-1* leaves with an avirulent isolate, the abundance of *AtPAL1* transcripts was 1.4 fold greater than Ler (wt) leaves (Figure 2.20d). Inoculation of *aba1-1* leaves with a virulent isolate also had a 1.1 fold greater abundance of *AtPAL1* transcripts than Ler (wt) leaves (Figure 2.20e).

Figure 2.19 Callose deposition in Arabidopsis ABA deficient and ABA insensitive mutant leaves inoculated with *P. parasitica*.

Leaves stained with AB, 7 d after inoculation.

(a) to (d) Detection of callose in resistant interactions between Arabidopsis leaves and an avirulent (*PpEmoy2*) isolate. **(a, a inset)** Callose (white arrow) in cells surrounding the site of penetration in Ler (wt) leaf tissue. **(b, b inset)** Punctate distribution of callose (white arrow) in a large area of cells surrounding the site of penetration in ABA deficient mutant *abal-1* leaf tissue, in an intermediate interaction. **(c, c inset)** and **(d, d inset)** Callose (white arrow) in cells surrounding the site of penetration in ABA deficient mutant *abal-3* and ABA insensitive mutant *abil-1* leaf tissue respectively. Note: vascular tissue (white arrowhead).

(e) to (h) Detection of callose in interactions between Arabidopsis leaves and a virulent (*PpHind4*) isolate. **(e, e inset)** Callose collars (small white arrow) at the base of haustoria on spreading hyphae (white arrow) within Ler (wt) leaf tissue, in a susceptible interaction. **(f, f inset)** Punctate distribution of callose (small white arrowhead) in cells surrounding the site of penetration, cells following spreading hyphae (white arrow) and collars (small white arrow) at the base of haustoria within *abal-1* leaf tissue, in an intermediate interaction. **(g, g inset)** and **(h, h inset)** Callose collars (small white arrow) at the base of haustoria on spreading hyphae (white arrow) within *abal-3* and *abil-1* leaf tissue respectively, in susceptible interactions. Bar is equivalent to **(a-h)** 400 μ m and **(a-h insets)** 70 μ m. Representative images from two independent experiments.

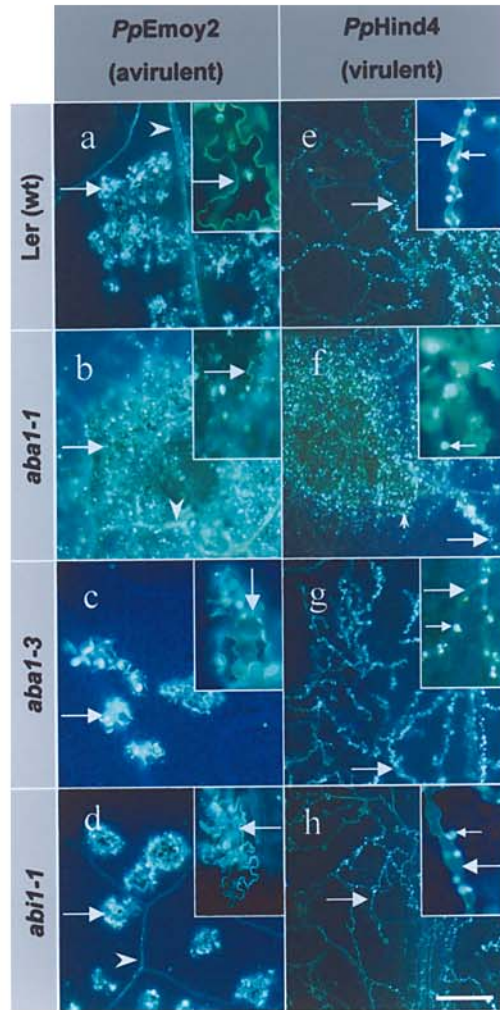


Figure 2.20 Abundance of *AtPAL1* mRNA transcripts in Arabidopsis ABA deficient mutant leaves inoculated with *P. parasitica*.

(a) to (e) Negative images of EtBr stained 1% (w/v) agarose gels containing the products from simultaneous *AtPAL1* (24 cycles) and 18S (22 cycles) RT-PCR reactions. Accompanied by a figure that shows the equalised, relative abundance of *AtPAL1* from each gel. Each RT-PCR was conducted on total RNA extracted from Ler (wt), ABA deficient mutant *aba1-1* and *aba1-3* leaves.

(a) Prior to inoculation.

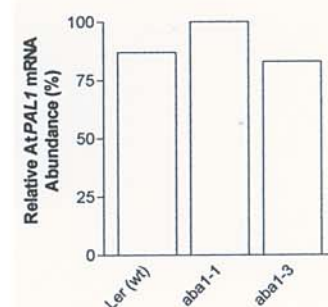
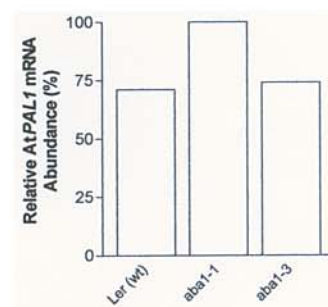
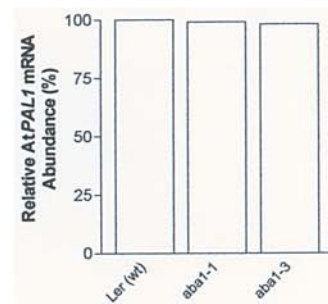
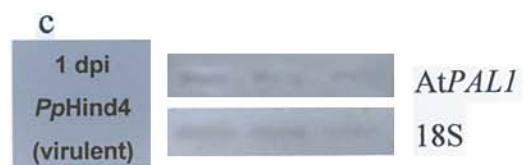
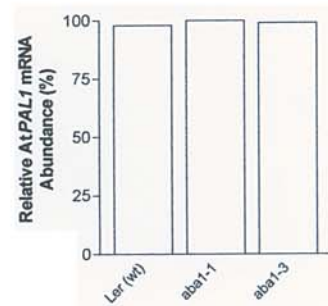
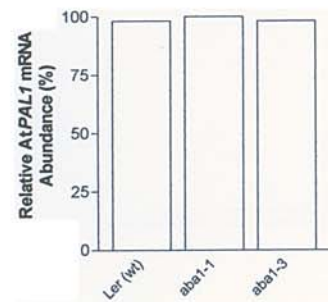
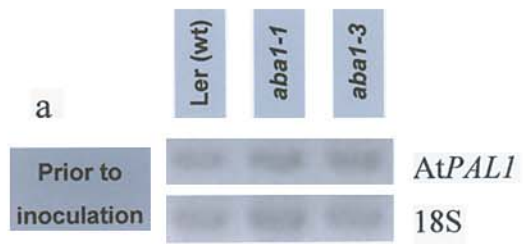
(b) One day post inoculation (dpi) with an avirulent (*PpEmoy2*) isolate.

(c) One dpi with a virulent (*PpHind4*) isolate.

(d) Three dpi with an avirulent (*PpEmoy2*) isolate.

(e) Three dpi with a virulent (*PpHind4*) isolate.

(a-c) Image from a single experiment. (d, e) Representative image from two independent experiments.



2.3.6.6 SA accumulations in avirulent and virulent inoculations of ABA deficient and ABA insensitive mutants

Five days after inoculation of Ler (wt), *abal-1*, *abal-3* or *abil-1* leaves with an avirulent isolate, the concentrations of free and conjugated SA were at least 1.2 fold higher than when inoculated with a virulent isolate (Figure 2.21a and b). The concentration of free and conjugated SA was at least 1.1 fold lower in ABA deficient and ABA insensitive mutant leaves when inoculated by either avirulent or virulent isolates, compared with wild type leaves (Figure 2.21a and b).

2.3.6.7 *AtPR-1* transcript accumulations in avirulent and virulent inoculations of ABA deficient mutants

The abundance of *AtPR-1* transcripts was at least 1.04 fold greater 3 d after avirulent and virulent isolate inoculations of Ler (wt) and *abal-1* than immediately prior to inoculation (Figure 2.22a and b). However, the abundance of *AtPR-1* transcripts was at least 1.1 fold lower in *abal-3* leaves 3 d after avirulent and virulent isolate inoculation compared to Ler (wt), *abal-1* (Figure 2.22c and d).

2.4 Discussion

In this chapter, the regulatory role of ABA in plant / pathogen interactions was investigated for the first time with an *Arabidopsis* / pathogen system. An *Arabidopsis* based pathogen system was chosen because of the unparalleled understanding of disease resistance signalling pathways discovered in this plant (Shapiro 2000; Thomma *et al.*, 2001a). In particular, the interactions between *Arabidopsis* and *P. parasitica* were studied because of the already extensive knowledge of molecular and biochemical mechanisms behind pathogen-specific resistance in this system (Slusarenko and Schlaich, 2003). A further advantage of an *Arabidopsis* based approach was the wide array of characterised *Arabidopsis* mutants

Figure 2.21 SA accumulation in Arabidopsis ABA deficient and ABA insensitive mutant leaves inoculated with *P. parasitica*.

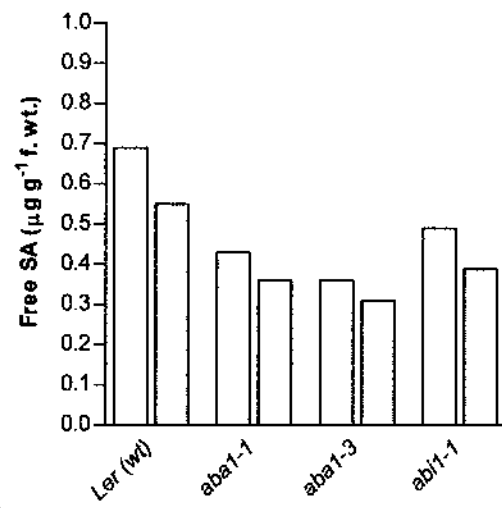
(a) to **(b)** SA concentrations of Ler (wt), ABA deficient mutant *abal-1* and *abal-3* and ABA insensitive mutant *abi1-1* 5 d after (□) avirulent (*PpEmoy2*) or (■) virulent (*PpHind4*) isolate inoculation.

(a) Free SA.

(b) Conjugated SA.

This experiment was repeated with similar results and the results from one experiment are shown.

a



b

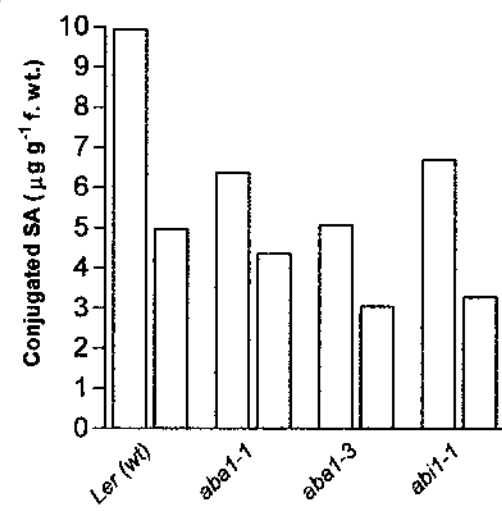


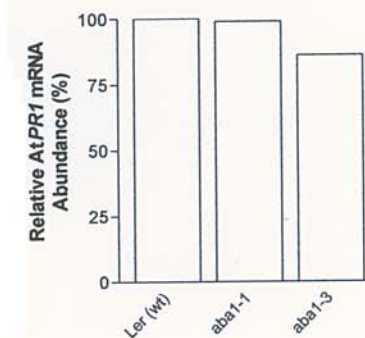
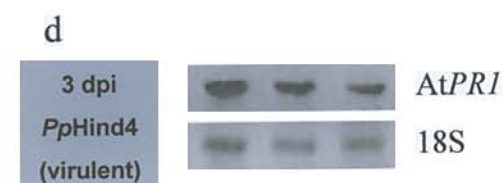
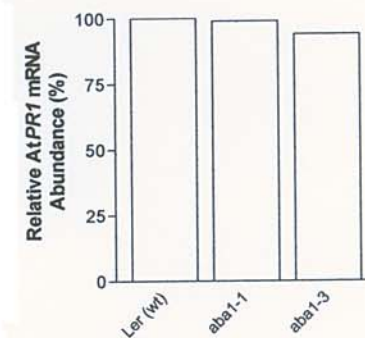
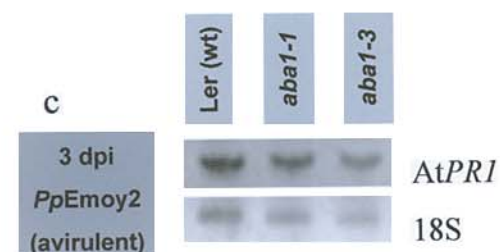
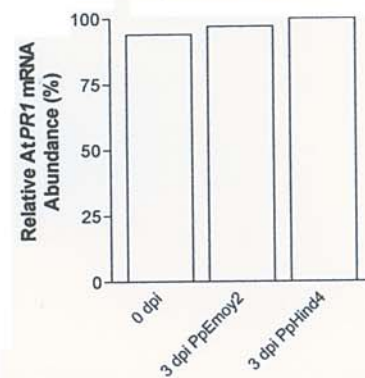
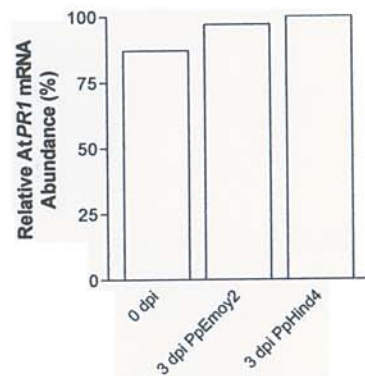
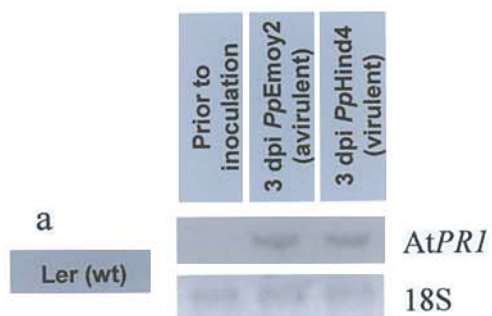
Figure 2.22 Abundance of *AtPR-1* mRNA transcripts in Arabidopsis ABA deficient mutants leaves inoculated with *P. parasitica*.

(a) to (d) Negative images of EtBr stained 1% (w/v) agarose gels containing the products from simultaneous *AtPR-1* (20 cycles) and 18S (22 cycles) RT-PCR reactions. Accompanied by a figure that shows the equalised, relative abundance of *AtPR-1* from each gel. Each RT-PCR was conducted on total RNA extracted from inoculated Arabidopsis leaves.

(a) and (b) Ler (wt) and ABA deficient mutant *abal-1* leaves respectively, prior to inoculation and 3 d post inoculation (dpi) with an avirulent (*PpEmoy2*) or virulent (*PpHind4*) isolate respectively.

(c) and (d) Three dpi of Ler (wt), ABA deficient mutant *abal-1* and *abal-3* leaves, with an avirulent (*PpEmoy2*) or virulent (*PpHind4*) isolate respectively.

(a-d) Images from single experiments.



with altered ability to sense or synthesise ABA (Finkelstein and Rock, 2002). Inoculation of many of these mutants with avirulent and virulent isolates of *P. parasitica* rapidly provided insight into ABA regulation of defence responses (Table 2.4 and Table 2.5).

The mutants of *Arabidopsis* with a reduced ability to synthesise ABA (ABA deficient mutants) *aba1-1*, *aba1-3* and *aba1-4*, were phenotypically identical to wild type plants but contained relatively low concentrations of ABA when compared with wild type plants. When inoculated with virulent isolates of *P. parasitica*, the residual ABA within these ABA deficient mutants influenced the outcome of the interaction. The mutant with the lowest ABA concentration, *aba1-4* (Rock and Zeevaart, 1991), developed a reaction that phenotypically resembled resistance, which was in complete contrast to the susceptible interaction of wild type plants. The less severely affected *aba1-1* mutant (Rock and Zeevaart, 1991), developed an intermediate interaction with necrosis, restricted pathogen growth and limited conidiophore production. The least severely affected *aba1-3* mutant (Rock and Zeevaart, 1991), developed what appeared to be a normal susceptible interaction but with fewer conidiophores. The *Arabidopsis* ABA deficient mutants *aba2-1*, *aba3-1* and *aao3*, are less severely affected in the amount of ABA accumulated within their tissues than *aba1-1* and *aba1-4* (Koornneef *et al.*, 1982; Leon-Kloosterziel *et al.*, 1996; Schwartz *et al.*, 1997; Seo *et al.*, 2000). When inoculated with a virulent isolate of *P. parasitica*, these mutants developed susceptible interactions that were phenotypically similar to wild type plants. Clearly then ABA is an important molecule in determining the response of *Arabidopsis* to a virulent pathogen.

The tomato mutants *sitiens* and *flacca* are deficient in ABA [impaired in the conversion of ABA-aldehyde to ABA (Marin and Marion-Poll, 1997)] and are to

Table 2.4 The effect of deficiency of ABA or insensitivity to ABA in mutants of *Arabidopsis* on interactions with avirulent and virulent isolates of *P. parasitica*.

Arabidopsis ^a	ABA concentration ^b	<i>P. parasitica</i> ^c	HR ^d	Hyphae ^e	Oospores ^f	Conidiophores ^g	Interaction phenotype ^h
Ler (wt)	B	<i>PpEmoy2</i>	P	A	A	A	R
		<i>PpNoks1</i>	P	A	A	A	R
		<i>PpHind4</i>	A	P	P	P - H	S
		<i>PpCala2</i>	A	P	P	P - H	S
<i>aba1-1</i>	L	<i>PpEmoy2</i>	P*	A	A	A	R
		<i>PpNoks1</i>	P*	A	A	A	R
		<i>PpHind4</i>	P*	P	A	P - L ⁺	I
		<i>PpCala2</i>	P*	P	A	P - L ⁺	I
<i>aba1-3</i>	L	<i>PpEmoy2</i>	P	A	A	A	R
		<i>PpNoks1</i>	P	A	A	A	R
		<i>PpHind4</i>	A	P	P	P - M ⁺	S
		<i>PpCala2</i>	A	P	P	P - M ⁺	S
<i>aba1-4</i>	L	<i>PpEmoy2</i>	P	A	A	A	R
		<i>PpHind4</i>	P*	A	A	A	R
<i>aaos3</i>	L	<i>PpEmoy2</i>	P	A	A	A	R
		<i>PpHind4</i>	A	P	P	P - NA	S
<i>abi1-1</i>	S	<i>PpEmoy2</i>	P	A	A	A	R
		<i>PpNoks1</i>	P	A	A	A	R
		<i>PpHind4</i>	A	P	P	P - H	S
		<i>PpCala2</i>	A	P	P	P - H	S
<i>abi2-1</i>	NA	<i>PpEmoy2</i>	P	A	A	A	R
		<i>PpHind4</i>	A	P	P	P - H	S
Col-0 (wt)	B	<i>PpEmoy2</i>	P	A	A	A	R
		<i>PpNoks1</i>	A	P	P	P - H	S
<i>aba2-1</i>	L	<i>PpEmoy2</i>	P	A	A	A	R
		<i>PpNoks1</i>	A	P	P	P - M	S
<i>aba3-1</i>	L	<i>PpEmoy2</i>	P	A	A	A	R
		<i>PpNoks1</i>	A	P	P	P - M	S

^a Arabidopsis genotype. ^b ABA concentrations (prior to inoculation): higher (H), lower (L) or similar (S) to basal (B) concentrations of wild type plants. ^c *P. parasitica* isolate. ^d HR, ^e Hyphae, ^f Oospores and ^g Conidiophores (7 dpi): presence (P) or absence (A). ^g Conidiophores leaf⁻¹ (7 dpi): <8 low (L), >8 and <12 medium (M) and >12 high (H). ^h Interaction phenotype: resistant (R), intermediate (I) or susceptible (S). Red text denotes a change compared to wild type plants. * denotes a HR that differed from that of wild type plants. + denotes a significant change in conidiophores leaf⁻¹ compared to wild type plants. NA, not assessed.

Table 2.5 The effect of deficiency of ABA or insensitivity to ABA in mutants of Arabidopsis on components of defence when inoculated with avirulent or virulent isolates of *P. parasitica*.

Arabidopsis ^a	<i>P. parasitica</i> ^b	Interaction ^c	HR ^d	H ₂ O ₂ ^e	Lignin ^f	Callose ^g	AtPAL1 ^h	SA ⁱ	AtPR-1 ^j
Ler (wt)	<i>PpEmoy2</i>	R	M	P	L - clustered	cluster	B	B	B
	<i>PpHind4</i>	S	A	A	L - scattered	collars	B	B	B
<i>abal-1</i>	<i>PpEmoy2</i>	R	E	P	H - expanded	punctate	I	D	U
	<i>PpHind4</i>	I	E	P	H - expanded	punctate	I	D	U
<i>abal-3</i>	<i>PpEmoy2</i>	R	M	P	L - clustered	cluster	U	D	D
	<i>PpHind4</i>	S	A	A	L - scattered	collars	U	D	D
<i>abil-1</i>	<i>PpEmoy2</i>	R	M	P	L - clustered	cluster	NA	D	NA
	<i>PpHind4</i>	S	A	A	L - scattered	collars	NA	D	NA

^a Arabidopsis genotype. ^b *P. parasitica* isolate. ^c Interaction phenotype (7 dpi): resistant (R), intermediate (I) or susceptible (S). ^d Development of a HR (4 dpi): minute (M) necrotic flecks, expansive (E) necrotic pits or absent (A). ^e H₂O₂ (1 dpi): presence (P) or absence (A). ^f Lignin accumulation (7 dpi): TGA derivatives (A_{335nm} mg⁻¹ d. wt.) <15 low (L) or >15 (H) and Phl / HCl stained as a small cluster at the site of inoculation, expanded at and away from the site of inoculation or scattered amongst cells associated with hyphal spread. ^g Callose (7 dpi): clustered at the site of inoculation, punctate distribution at and away from the site of inoculation and collars at the base of haustoria. ^h AtPAL1, ⁱ SA (5 dpi) and ^j AtPR-1 (3 dpi): increased (I), decreased (D) or unchanged (U) compared to basal (B) levels present in wild type plants. Red text denotes a change compared to wild type plants. NA, not assessed.

date the only other ABA deficient mutants to be examined in interactions with a pathogen (Kettner and Dorffling, 1995; Audenaert *et al.*, 2002). Both tomato ABA deficient mutants were more resistant to the necrotrophic fungus *B. cinerea* than wild type plants (Audenaert *et al.*, 2002). These observations were in agreement with increased resistance of Arabidopsis ABA deficient mutants to the biotrophic Oomycete, *P. parasitica*, in the present study. The norflurazon (ABA biosynthesis inhibitor) treatment of soybeans, reduced the concentration of ABA and resulted in a more resistant interaction with a virulent race of the hemibiotrophic Oomycete, *P. sojae* (McDonald and Cahill, 1999; Mohr and Cahill, 2001), also in agreement with the present study. A lower than usually encountered concentration of ABA in a range of plants has therefore increased resistance to virulent pathogens from varied evolutionary backgrounds and pathogenic lifestyles.

In contrast to many of the previous studies, a detailed investigation then followed to determine the components of defence that had made *aba1-1* mutants more resistant to a virulent isolate of *P. parasitica*. The components of defence that ABA has previously been shown to regulate, include members of the phenylpropanoid pathway, and the key entry enzyme into the pathway, PAL that has altered gene transcription or activity (Ward *et al.*, 1989a; McDonald and Cahill, 1999; Audenaert *et al.*, 2002). The necessity for a functional phenylpropanoid pathway lead by PAL in Arabidopsis resistance to *P. parasitica* was previously shown by specific AIP (2-aminoindan-2-phosphonic acid) inhibition of PAL activity (Mauch-Mani and Slusarenko, 1996). In their study, Mauch-Mani and Slusarenko (1996) showed that AIP treatment of Arabidopsis resulted in a completely susceptible interaction when inoculated with an avirulent isolate of *P. parasitica*. In the current study, the abundance of *AtPAL1* transcripts was greater in both avirulent

and virulent *P. parasitica* inoculations of *aba1-1* mutants than wild type plants. This observation was therefore consistent with the concentration of ABA negatively regulating PAL, and the activation of the phenylpropanoid pathway being important for Arabidopsis resistance to *P. parasitica*.

Accumulation of the cell wall strengthening phenylpropanoid-derived compound, lignin (Dixon and Paiva, 1995), has previously been shown to be critical for effective resistance of wheat (*Triticum aestivum* (L.) Em. Thell.) to a stem rust fungus (*Puccinia graminis* Pers. f.sp. *tritici* Erics. and E. Henn.), by specific inhibition of lignin biosynthesis by cinnamyl-alcohol dehydrogenase (CAD) inhibitors, OH-PAS [*N*(*O*-hydroxyphenyl)sulfinamoyl-tertiobutyl acetate] and NH₂-PAS [*N*(*O*-aminophenyl)sulfinamoyl-tertiobutyl acetate] (Moershbacher *et al.*, 1990). In Arabidopsis, specific inhibition of lignin by OH-PAS also caused a shift towards susceptibility when inoculated with an avirulent isolate of *P. parasitica* (Mauch-Mani and Slusarenko, 1996). In the current study, large accumulations of lignin within *aba1-1* mutants when inoculated with a virulent isolate of *P. parasitica* was in contrast to the reaction of wild type plants where little lignin accumulated, and was therefore likely to be a factor that had caused a reduction in the susceptibility of *aba1-1* plants. Increased accumulations of lignin in *aba1-1* mutants compared with wild type plants following inoculation with either avirulent or virulent isolates of *P. parasitica*, was likely to be a direct result of increased *PAL* gene transcription.

In tomato *sitiens* mutants inoculated with *B. cinerea*, increased PAL activity was linked to increased SA-dependent signalling when *sitiens* plants required less BTH [benzo(1,2,3)thiadiazole-7-carbothioic acid, an SA analog] to accumulate *PR1a* (an indicator of SA-dependent signalling) gene transcripts than wild type plants

(Audenaert *et al.*, 2002). Increased resistance in *sitiens* mutants was therefore suggested by Audenaert *et al.* (2002) to be a result of ABA regulation of SA-dependent defence in tomato. The susceptibility of transgenic *Arabidopsis* plants expressing the bacterial *nahG* gene (encodes the enzyme, salicylate hydroxylase that inactivates SA) to many avirulent isolates of *P. parasitica*, has previously highlighted the importance of SA accumulation in *Arabidopsis* / *P. parasitica* resistant interactions (Delaney *et al.*, 1994; McDowell *et al.*, 2000; Rairdan and Delaney, 2002). In the current study, the increased resistance of *Arabidopsis abal-1* mutants to virulent isolates of *P. parasitica* compared to wild type plants was not associated with increased SA or *PR-1* accumulation. However, it has been shown in *Arabidopsis sid* (SA induction-deficient) mutants, that the SA required for *Arabidopsis* resistance to *P. parasitica* is synthesised via isochorismate synthase (ICS), independent of PAL and the phenylpropanoid pathway (Nawrath and Metraux, 1999; Wildermuth *et al.*, 2001). It would therefore be of interest to determine if increased SA accumulations occurred in *sitiens* mutants inoculated with *Botrytis cinerea*, and if so were they PAL or ICS dependent.

Development of an extensive and rapid HR-like lesion in *abal-1* mutants following inoculation with virulent isolates of *P. parasitica*, was in complete contrast to the lack of necrosis in wild type plants. The HR-like lesions in *abal-1* mutants were similar in appearance to the HR necrotic pits previously described during resistant interactions between certain *Arabidopsis* ecotypes and avirulent isolates of *P. parasitica* (Holub *et al.*, 1994). However, no hyphal spread or conidiophore production was associated with the necrotic pits described by Holub *et al.* (1994). The development of HR-like cells, not stimulated by gene-for-gene recognition but by treatment with the synthetic immunomodulator 2,6-dichloroisonicotinic acid

(INA) has previously been shown to limit hyphal spread and conidiophore production of virulent isolates of *P. parasitica* (Uknes *et al.*, 1992). The HR-like necrosis in *aba1-1* mutants was therefore likely to also be a contributing factor to the reduced hyphal spread and limited conidiophore production following inoculation with virulent isolates of *P. parasitica*, but not necessarily as a result of gene-for-gene recognition.

Extensive necrosis that was accompanied with reduced hyphal spread and limited conidiophore production has also previously been described in Arabidopsis *lsd1* (lesions stimulating disease response) mutants following inoculation with a virulent isolate of *P. parasitica* (Dietrich *et al.*, 1994; Aviv *et al.*, 2002). *LSD1* encodes a zinc-finger protein and has been proposed to function as a negative regulator of a pro-death signal (Dietrich *et al.*, 1997). Superoxide (O_2^-) was identified as a possible candidate for the pro-death signal in *lsd1* mutants because a dependency for O_2^- was required for necrosis development (Jabs *et al.*, 1996). The rapid accumulation of ROS, in particular O_2^- and H_2O_2 , is a characteristic early feature of the HR in many plants following perception of avirulent pathogens (Lamb and Dixon, 1997). In the presence of reducing compounds in plants of sufficient affinity for oxygen (O_2) such as NADPH, O_2^- is formed from O_2 and dismutates spontaneously to form H_2O_2 (Hippeli *et al.*, 1999; Mahalingam and Fedoroff, 2003). In the current study, H_2O_2 was detected in *aba1-1* leaves inoculated with virulent isolates of *P. parasitica* but not in wild type plants, and also indicated that O_2^- had also been produced. A possible mechanism for the development of extensive necrosis in *aba1-1* mutants could therefore be that low ABA concentrations reduced the effectiveness of LSD1. The O_2^- produced following avirulent or virulent *P. parasitica* isolate inoculation of *aba1-1* may therefore have been enough to stimulate

a HR-like necrosis that spread away from the site of inoculation. The unusual stimulation of the HR-like necrosis could also account for the punctate distribution of callose that varied in appearance from the callose deposited in wild type plants following inoculation with avirulent isolates of *P. parasitica*.

The *Arabidopsis* mutant *coi1* (coronatine insensitive) that is affected in the JA-responsive pathway and *ein3* (ethylene insensitive) have previously been shown to have enhanced susceptibility to *B. cinerea* (Thomma *et al.*, 1998; Thomma *et al.*, 1999a). The use of JA and Et insensitive mutants of *Arabidopsis* therefore identified the importance of both these hormones in *Arabidopsis* resistance to *B. cinerea*. In the present study, the insensitivity of *abi1-1* and *abi2-1* to ABA did not affect *Arabidopsis* interactions with avirulent or virulent *P. parasitica* when compared with reactions in wild type plants. The ABA signal transduction pathways that involve ABI1-1 and ABI2-1 proteins [2C class protein serine / threonine phosphatases (Leung *et al.*, 1997)] are therefore unlikely to be involved in the determination of *Arabidopsis* resistance or susceptibility to *P. parasitica*.

The addition of norflurazon to soybeans prior to inoculation with a virulent race of *P. sojae*, resulted in pathogen restriction in a manner similar to that which occurs during resistance (McDonald and Cahill, 1999). In the current study, application of norflurazon or a structurally different phytoene desaturase inhibitor, fluridone (Bartels and Watson, 1978) at a concentration of 100 μ M to *Arabidopsis* prior to inoculation with a virulent isolate of *P. parasitica*, caused a reduction in the number of conidiophores produced in susceptible interactions. However, hyphal spread and the production of oospores was similar to that found in normal susceptible interactions. Treatment of *Arabidopsis* with norflurazon and fluridone did not reduce endogenous ABA concentrations but was sufficient to cause photobleaching of

newly formed leaves, indicating that the chemicals had been taken up by the plants. Photobleaching occurs due to a reduction in chlorophyll synthesis and has been shown to be accompanied by reduced growth and altered leaf morphology (Abrous *et al.*, 1998; Popova 1998). The reduction in conidiophore numbers found following norflurazon or fluridone treatment were therefore unlikely to have been an indicator of an interaction influenced by ABA, but an affect of reduced plant vigour that influenced the lifecycle of the biotrophic pathogen.

Previously, the addition of 100 μ M ABA to soybeans prior to inoculation with an avirulent race of *P. sojae*, resulted in pathogen spread in a manner similar to that during susceptibility (McDonald and Cahill, 1999). In the present study, treatment of *Arabidopsis* with a range of ABA concentrations up to and including 100 μ M, prior to inoculation with avirulent isolates of *P. parasitica*, did not alter the interaction phenotype. This was unexpected, but is in accordance with previously work on tomato, where application of 100 μ M ABA did not induce susceptibility of leaves to non-virulent *B. cinerea* strains (Kettner and Dorffling, 1995). Therefore, ABA application may have suppressed a component or components of defence that were critical in the resistance of soybean to avirulent races of *P. sojae*. However, the same component or components if suppressed in *Arabidopsis* or tomato may not be critical in the containment of avirulent isolates of *P. parasitica* or non-virulent strains of *B. cinerea* respectively. Further investigation and a greater understanding of ABA regulation of defence components in these plant / pathogen interactions would be required before this issue could be resolved.

In the present study, the use of ABA deficient mutants of *Arabidopsis* identified that ABA is a regulator of the outcome of the interactions of *Arabidopsis* with *P. parasitica*. The molecular and biochemical basis of interactions between

Arabidopsis and the biotrophic, bacterium, *Pseudomonas syringae* pv. *tomato* are as well defined as those of Arabidopsis / *P. parasitica*. In chapter 3, the same approaches that were used in this chapter will be utilised to investigate the regulatory role of ABA in Arabidopsis / *P. syringae* pv. *tomato* resistant and susceptible interactions. In particular, chapter 3 is focussed on the identification of similarities and differences in ABA regulation of components of Arabidopsis defence induced by a pathogen from a different kingdom and pathogenic habit to *P. parasitica*.

Chapter 3: The influence of abscisic acid on interactions of Arabidopsis with the biotrophic, bacterial pathogen, *Pseudomonas syringae* pathovar *tomato*

Chapter summary

In the previous chapter a regulatory role for abscisic acid (ABA) in Arabidopsis resistance to a biotrophic Oomycete, *Peronospora parasitica*, was identified for the first time. Another commonly studied pathogen of Arabidopsis is the biotrophic bacteria, *Pseudomonas syringae* pathovar (pv.) *tomato*. The two pathogens have very different pathogenic lifestyles and are from different kingdoms. In the current study, ABA also played a regulatory role in Arabidopsis defence against *P. syringae* pv. *tomato*. When ABA concentrations were raised by exogenous ABA or stimulated by drought stress, Arabidopsis became susceptible to an avirulent strain of the pathogen. Susceptibility was characterised by an increase in the development of leaf chlorosis and bacterial numbers. Increased concentrations of ABA had reduced the accumulation of lignin by 41%, mRNA transcripts for phenylalanine ammonia-lyase and a pathogenesis-related gene (*PR-1*) by 17% and 6% respectively and salicylic acid by 61%. The results indicate that increased ABA negatively regulates the phenylpropanoid pathway during resistance of Arabidopsis to an avirulent strain of *P. syringae* pv. *tomato*.

Part of the research detailed in this chapter has been published. The primary author contributed 100% of the research:

Mohr PG, Cahill DM (2003) Abscisic acid influences the susceptibility of *Arabidopsis thaliana* to *Pseudomonas syringae* pv. *tomato* and *Peronospora parasitica*. *Functional Plant Biology* **30**, 461-469.

3.1 Introduction

Pseudomonas syringae pathovar (pv.) *tomato* Cuppels, the casual agent of 'bacterial speck' in tomato, also causes disease when artificially infiltrated into Arabidopsis leaves (Dong *et al.*, 1991). The *avrRpt2* gene has been identified in an avirulent strain of *P. syringae* pv. *tomato* denoted '1065' (hereafter *Pst*1065) and following transformation into a virulent strain of *P. syringae* pv. *tomato* denoted 'DC3000' (hereafter *Pst*DC3000) converted this strain into an avirulent strain (Whalen *et al.*, 1991). The corresponding disease resistance (R) gene *RPS2* that recognises the *avrRpt2* gene product has been identified in Arabidopsis (Kunkel *et al.*, 1993; Yu *et al.*, 1993). Identification of gene-for-gene interactions in the Arabidopsis / *P. syringae* pv. *tomato* system, has meant that it is now a widely used model plant / pathogen system.

RPS2 is an R protein with a region of leucine-rich repeats (LRR), a nucleotide binding site (NBS) and a leucine-zipper (LZ) (Katagiri *et al.*, 2002). *AvrRpt2* is recognised by *RPS2* and is a hydrophilic protein that during pathogenesis is most likely secreted via the type III secretion system (Mudgett and Staskawicz, 1999; Casper-Lindley *et al.*, 2002). It has been suggested that *AvrRpt2* might be indirectly perceived by *RPS2* after binding of a third component 'p75' (of plant origin), that has been found in association with *RPS2* and *AvrRpt2* in a single complex (Leister and Katagiri, 2000). The search for resistance signalling components downstream of *RPS2* has resulted in the identification of proteins such as *NDR1* (Martin *et al.*, 2003). *NDR1*, the best characterised of these proteins, is a membrane bound protein required for LZ-NBS-LRR R protein specified resistance (Century *et al.*, 1995; Aarts *et al.*, 1998). Currently our knowledge of the specific

defence pathways and their components that are important for resistance to *P. syringae* pv. *tomato* is very limited.

Gene-for-gene mediated resistance via *RPS2* is typically associated with a rapid hypersensitive response (HR) upon delivery of AvrRpt2 protein into Arabidopsis cells (Wu *et al.*, 2003). HR is likely to be an important factor in limiting multiplication of a biotrophic pathogen such as *P. syringae* pv. *tomato* that require healthy cells to survive (Heath 2000). In contrast, the delayed necrosis found in susceptible interactions results from unrestricted pathogen multiplication (Whalen *et al.*, 1991). Hydrogen peroxide (H₂O₂) accumulation is a potential trigger of HR (Lamb and Dixon, 1997), and precedes HR development in Arabidopsis *RPS2* mediated resistance (Wolfe *et al.*, 2000). Accumulation of salicylic acid (SA) also plays an important role in pathogen-specific and systemic acquired resistance (SAR) mediated by *RPS2* (Delaney *et al.*, 1994; Rairdan and Delaney, 2002). The expression of pathogenesis-related gene 1 (*PR-1*) (an indicator of SA-dependent defence) has also been correlated with *RPS2* mediated pathogen-specific resistance and SAR (Cameron *et al.*, 1999; Thomma *et al.*, 2001b).

Defence components derived from the phenylpropanoid pathway (other than SA) may also influence the resistance of Arabidopsis to *P. syringae* pv. *tomato*. For example, expression of phenylalanine ammonia-lyase (*PAL*), that encodes the phenylpropanoid pathway entry enzyme, occurred in the early hours following *Pst*1065 infiltration (Davis *et al.*, 1991). Identical timing in expression of 4-coumarate:CoA ligase (*4CL*), that encodes a key phenylpropanoid enzyme leading to the synthesis of flavonoids and lignin, also occurred after inoculation with an avirulent strain of *P. syringae* (Lee *et al.*, 1995). However, expression of chalcone synthase (*CHS*) was not induced suggesting that phenylpropanoid flavonoids (eg.

flavonoid phytoalexins) may not be important in resistance of Arabidopsis to *P. syringae* pv. *tomato* (Dong *et al.*, 1991). In contrast, lignin accumulated in Arabidopsis leaves following inoculation with an avirulent strain of *P. syringae* that harboured *avrRpt2* (Lee *et al.*, 2001).

The phytoalexin, camalexin that is derived from the tryptophan pathway accumulated in Arabidopsis following inoculation with *P. syringae* pv. *tomato*, but a correlation with resistance has not been found (Glazebrook and Ausubel, 1994). Arabidopsis *ein2* (ethylene insensitive) and *jar1* (jasmonate insensitive) mutations do not alter in their resistance to *P. syringae* (Nandi *et al.*, 2003). Transcripts of *PDF1.2* (an indicator of jasmonic acid (JA) / ethylene (Et) dependent defences) were only weakly detected in resistant interactions to *P. syringae* pv. *tomato* (Thomma *et al.*, 2001b). Therefore it is likely that the JA / Et pathway and camalexin do not make major contributions to resistance against *P. syringae*.

Studies that have involved the interactions between various plant species and fungal, Oomycete and viral pathogens have highlighted the possibility of abscisic acid (ABA) influencing the susceptibility or resistance of these interactions (for example: Fraser 1982; Mohr and Cahill, 2001; Audenaert *et al.*, 2002). In the previous chapter, it was also clearly demonstrated that ABA influenced the resistance or susceptibility of Arabidopsis / *P. parasitica* (an Oomycete pathogen) interactions. The influence of ABA on Arabidopsis / *P. syringae* pv. *tomato* interactions examined in this chapter, therefore forms an extension of the previous chapter. In this chapter, a completely different pathogen, from a different kingdom that has a different mode of pathogenicity and life cycle was utilised to determine if ABA is involved in regulating the outcome of Arabidopsis / *P. syringae* pv. *tomato* interactions. In

particular, the effect of ABA on *Arabidopsis* defence components was investigated and compared to results obtained in the previous chapter.

3.2 Materials and methods

3.2.1 Source and growth of *Arabidopsis* plants

The source and background of *Arabidopsis Landsberg erecta* (Ler) and Columbia-0 (Col-0) wild type (wt), ABA deficient mutant (*aba1-1*, *aba1-3*, *aba2-1* and *aba3-1*) and ABA insensitive mutant (*abi1-1*) seeds was described in section 2.2.1 of chapter 2. The method for sterilisation, vernalisation, germination of seeds on Murashige and Skoog (MS) plates and planting seedlings after 2 wk into soil was as described in section 2.2.2 of chapter 2, except that only three seedlings were planted in each 5 cm diameter pot. Plants that were to be subjected to vacuum infiltration were planted through 8 mm holes punched in plastic mesh that covered the soil on the top of the pots. For experiments involving Ler (wt) plants only, the seedling pots were covered with clear plastic to maintain humidity for the first day following transplantation. For experiments involving wild type plants and ABA deficient or ABA insensitive mutants, the seedling pots were kept within sealed transparent containers after transplantation to maintain high humidity and thus prevent wilting of the ABA mutants. After transplantation all plants were grown in a controlled environment room at 21°C under a 12/12 h light / dark cycle. Light was provided by two 400W high-pressure sodium lights (Osram Australia Pty. Ltd., New South Wales, Australia) at a height of 1.5 m above the plants. Experiments were conducted on 5-6 wk old plants.

3.2.2 Treatment of plants with ABA and ABA biosynthesis inhibitors

ABA, norflurazon and fluridone were prepared as described in section 2.2.3 of chapter 2, except the root uptake treatments varied. Prior to treatment, soil was

removed from the roots of plants by a gentle rinse with distilled water (dH₂O). Root uptake was then enabled by immersing the roots in 35 ml of the treatment solution within a Petri plate. The plate was placed in a sealed transparent container to maintain high humidity, and returned to the controlled environment room. After 20 h plants were removed from the treatment solution and the roots were covered with filter paper (No.1, Whatman International Ltd., Maidstone, England) moistened with dH₂O, within another sealed transparent container.

3.2.3 Imposition of simulated drought stress

For drought stress treatments Ler (wt) plants were removed from pots and the soil was carefully rinsed from the roots with dH₂O. Remaining surface water on the roots was removed with absorbent paper that was left in contact with the roots for 5 min. The roots of the plants were then placed on fresh absorbent paper and returned to the controlled environment room for 2 h. At the time of inoculation with *P. syringae* pv. *tomato* the roots were rehydrated by covering with filter paper moistened with dH₂O, within sealed transparent plastic containers.

3.2.4 ABA extraction from leaves and quantification

ABA was extracted from 10 rosette leaves (excised from five plants) and quantified by an indirect enzyme-linked immunosorbent assay as described in section 2.2.4 of chapter 2. The concentration of ABA was expressed as ng g⁻¹ fresh weight (f. wt.).

3.2.5 *Pseudomonas syringae* pv. *tomato* cultures

Pseudomonas syringae pv. *tomato* (*Pst*) strains *Pst*DC3000 and *Pst*1065 (Whalen *et al.*, 1991) were obtained from Prof. Roger Innes (Indiana University, Indiana, USA). The two strains were cultured on King's B (KB) medium (King *et al.*,

1954) (Appendix 1). *Pst*DC3000 was grown in KB containing 50 $\mu\text{g ml}^{-1}$ rifampicin and kanamycin and *Pst*1065 in KB containing only 50 $\mu\text{g ml}^{-1}$ rifampicin.

3.2.6 Procedure for inoculation of *Arabidopsis* leaves with *P. syringae* pv. *tomato*

*Pst*DC3000 and *Pst*1065 inoculum was prepared based on the method of Davis *et al.* (1991). The bacteria were cultured at 30°C and 200 rpm on an incubated orbital shaker (Ratek Instruments Pty. Ltd., Victoria, Australia) until $A_{600\text{nm}} = 1.5\text{-}2.0$ in liquid KB medium. The bacteria were then pelleted by centrifugation (Beckman Coulter Inc., California, USA) at 10,000 g and resuspended in an equal volume of sterile 10 mM MgCl_2 . The bacterial suspensions were then diluted to approximately 10^8 colony forming units (cfu) ml^{-1} ($A_{600\text{nm}} = 1.0$) with sterile 10 mM MgCl_2 for inoculum that generated visible leaf disease symptoms as previously described (Dong *et al.*, 1991). A solution of sterile 10 mM MgCl_2 therefore served as the control inoculum.

For experiments that used only Ler (wt) inoculation, fully expanded rosette leaves were gently syringe infiltrated (needleless 1 ml syringe) with bacterial suspension to the abaxial surface as previously described (Katagiri *et al.*, 2002). Syringe infiltrated leaves were marked with a permanent marker at the base of the midrib for later identification. The growth of ABA deficient and ABA insensitive mutants and wild type plants in sealed transparent containers (required for ABA mutant survival) produced narrow rosette leaves that were unable to be syringe infiltrated. Therefore, in experiments that used wild type plants and ABA deficient or ABA insensitive mutants, all leaves of the plants were vacuum infiltrated with bacterial suspension for 2 min as previously described (Katagiri *et al.*, 2002). The bacterial suspension used for vacuum infiltration had a surfactant, 0.01% (v/v) vac-in-stuff (Lehle Seeds, Texas, USA) added, to aid infiltration (Whalen *et al.*, 1991).

Following inoculation all plants were placed in sealed transparent containers and incubated in a controlled environment growth cabinet (Thermoline L and M, New South Wales, Australia) at 25°C under a 12/12 h light / dark cycle. Light was provided by 12 36W fluorescent lights (GE Lighting Australia, New South Wales, Australia) at a distance of 0.5 m above the plants. Images of infiltrated leaves and plants were captured using a digital still camera (MVC-FD81, Sony Corp., Tokyo, Japan).

3.2.7 Determination of bacterial numbers within leaves

Bacterial numbers within leaves were determined following the infiltration of a bacterial suspension diluted to a density of 10^5 cfu ml⁻¹ in sterile 10 mM MgCl₂ as previously described (Whalen *et al.* 1991). At appropriate times after syringe infiltration *P. syringae* pv. *tomato* was isolated from three leaf discs (excised from three individual plants) made using a 6 mm diameter cork borer. Leaf discs were unable to be excised from the narrow leaves of ABA deficient and ABA insensitive mutants and wild type plants, grown in sealed transparent containers. Therefore the f. wt. of six vacuum infiltrated leaves (excised from three individual plants) was determined before bacterial isolation.

Leaf tissue (leaf discs or vacuum infiltrated leaves) was ground with a plastic pestle in a 1.5 ml Eppendorf tube, with 0.3 ml sterile 10 mM MgCl₂. Dilutions of the extract were then prepared in sterile 10 mM MgCl₂ and spread onto KB medium plates containing the appropriate antibiotics. Bacterial numbers were determined by counting the number of colonies formed following incubation of the plates for 2 d at 30°C (Memmert, Schwabach, Germany). Bacterial numbers within syringe infiltrated leaves were then expressed as log (cfu/cm²) and vacuum infiltrated leaves as log (cfu mg⁻¹ f. wt.).

3.2.8 Effect of ABA or ABA biosynthesis inhibitors on growth of *P. syringae* pv. *tomato* in culture

The effect of ABA, norflurazon and fluridone on the growth of *P. syringae* pv. *tomato* was determined by growing the relevant bacterial strain on media supplemented with one of the compounds. ABA, norflurazon and fluridone were prepared as described in section 2.2.3 in chapter 2, but were used at a concentration of 100 μM . *P. syringae* pv. *tomato* at a density of 10^8 cfu ml⁻¹ was spread on each plate and incubated for 2 d at 30°C. The number of bacteria was expressed as log (cfu ml⁻¹).

3.2.9 Histochemical staining and detection of H₂O₂ in *Arabidopsis* leaf tissue infiltrated with *P. syringae* pv. *tomato*

For each histochemical stain used and the detection of H₂O₂, five leaves were excised at the base of the petiole. The leaves were cleared of photosynthetic pigments as described in section 2.2.7 of chapter 2, in preparation for each of the histochemical staining and the detection of H₂O₂ procedures (a-f) below. All stained leaf tissue was viewed under white light illumination using a compound research microscope (Axioskop 20, Carl Zeiss Pty. Ltd., New South Wales, Australia). Aniline blue staining for callose was viewed under ultraviolet (UV) light (UV [excitation wavelength 365nm, emission 420nm] filter set). Images of stained tissues were captured and stored as described in section 2.2.7 of chapter 2.

- a) Following infiltration the necrosis of *Arabidopsis* leaf cells was detected by lactophenol-trypan blue (LTB) stain as described in section 2.2.7a of chapter 2. Necrotic leaf cells stained a dark blue, healthy cells stained light blue.
- b) The presence of H₂O₂ within inoculated leaves was detected by a 3,3'-diaminobenzidine (DAB) polymerisation reaction (Thordal-Christensen *et al.*, 1997).

To facilitate DAB uptake at appropriate times after infiltration, leaves were excised from plants and the leaf tip also excised (1-2 mm from the apex). The leaves were floated on 5 ml of DAB (Appendix 1) within the wells of a 6 well Costar microplate (Corning Cable Systems Pty. Ltd., Victoria, Australia). The tray was then incubated under the same conditions as the infiltrated plants for 2 h. After the leaves were cleared of photosynthetic pigments, the presence of H₂O₂ within leaf cells was visualised as a reddish / brown precipitate.

c) Lignin was visualised using phloroglucinol / hydrochloric acid (Phl / HCl) stain as described in section 2.2.7c of chapter 2. The presence of lignin within leaf tissue was indicated by the red / purple stain of cells and cell walls.

d) Phenolic structures were visualised using toluidine blue 0 (TB0) staining as described in section 2.2.7d of chapter 3. The presence of phenolic structures was indicated by a light blue / green staining of cells and cell walls.

e) Suberin was detected by Sudan black B (SBB) staining as described in 2.2.7e of chapter 2. The presence of suberin with leaf tissue was indicated by blue / black staining.

f) Callose was detected by aniline blue (AB) staining as described in section 2.2.7f of chapter 2. Callose was visible under UV light as bright yellow / green fluorescence produced within cells.

3.2.10 Extraction and quantification of wall bound phenolics, salicylic acid and total RNA from leaves infiltrated with *P. syringae* pv. *tomato*

Following infiltration 10 leaves per sample were excised from five plants, in preparation for extraction and quantification in the procedures (a-c) below.

- a) Wall bound phenolics of leaf tissues were derivatised via thioglycolic acid precipitation as described in section 2.2.8 of chapter 2. Concentrations of wall bound TGA derivatives were expressed as $A_{335\text{nm}} \text{ mg}^{-1}$ dry weight (d. wt.).
- b) Free and conjugated SA was extracted and quantified by reverse-phase high performance liquid chromatography (HPLC) as described in section 2.2.9 of chapter 2. Concentrations of SA were expressed as $\mu\text{g g}^{-1}$ f. wt..
- c) Total RNA was isolated using a TRIzol method, DNA removed and quantified as described in section 2.2.10 of chapter 2 but with greater volumes, due to more leaf tissue. At the time after infiltration excised leaves were ground in liquid nitrogen with a mortar and pestle. The ground tissue was suspended in 5 ml of TriReagent (Molecular Research Centre Inc., Ohio, USA) and added to a 15 ml centrifuge tube (Edwards Instrument Co., New South Wales, Australia). Each tube was stored in liquid nitrogen until all samples for a particular experiment were prepared. The tubes were incubated at 60°C for 15 min prior to mixing with a vortex (Ratek Instruments Pty. Ltd.). The tubes were then centrifuged (Beckman Coulter Inc.) at 8,000 g for 10 min at 4°C. The supernatant was transferred to a new tube and 1 ml chloroform added. The solution was again mixed and then incubated at room temperature (RT) for 5 min, followed by centrifugation at 8,000 g for 15 min at 4°C. The aqueous (top) phase was transferred to a new tube containing 2.5 ml isopropanol. The tube was mixed by gentle inversion before incubation at RT for 15 min. The mixture was centrifuged at 8,000 g for 10 min at 4°C and the supernatant discarded. The remaining pellet was washed with 5 ml of 70% (v/v) ethanol (ice cold) and centrifuged for 10 min at 4°C and the supernatant again discarded. The resulting pellet was air dried for 10 min before being resuspended in 100 μl of diethyl pyrocarbonate (DEPC) treated dH_2O .

The isolated total RNA was treated with DNase I (DNA-free, Ambion Inc., Texas, USA) to eliminate contaminating DNA. Ten microlitres of 10X DNase I buffer and 2 μ l of DNase I were added to the total RNA before gentle mixing and incubation at 37°C for 30 min. Ten microliters of DNase inactivation reagent was then added to the sample and mixed by pipette agitation, followed by incubation for 2 min at RT. The RNA solution was then subjected to centrifugation (Denver instruments, Colorado, USA) at 10,000 g for 1 min to pellet the DNase inactivation reagent. The total RNA (DNA free) was removed and the concentration determined according to its $A_{260\text{nm}}$ (RNeasy Mini Handbook, Qiagen, California, USA).

3.2.11 Abundance of Arabidopsis *PAL1* and *PR-1* mRNA transcripts

The abundance of mRNA transcripts of Arabidopsis *PAL1* (*AtPAL1*) and *PR-1* (*AtPR-1*) mRNA in total RNA was determined by the fluorescence density of reverse transcription-polymerase chain reaction (RT-PCR) products separated on a 1% (w/v) agarose gel [in 0.5x tris-borate-EDTA (TBE)] and stained with ethidium bromide (EtBr), as described in section 2.2.11 of chapter 2. The abundance of *AtPAL1* and *AtPR-1* transcripts were equalised based on differences between the abundance of 18S transcript densities (the internal standard that indicated discrepancies in the amount of total RNA between RT-PCR samples). The differences between equalised *AtPAL1* and *AtPR-1* transcripts of the various samples being compared were then expressed as a percentage relative to the sample with the highest level of *AtPAL1* or *AtPR-1* which was taken as 100% expression.

3.2.12 Statistical analysis

The mean and standard error of the mean (s.e.m.) were calculated and the significance of differences between means of two independent values analysed by an

unpaired parametric t-test (GraphPad Prism version 3.00, GraphPad Software, California, USA).

3.3 Results

3.3.1 Characterisation of Arabidopsis / *P. syringae* pv. *tomato* resistant and susceptible interaction phenotypes

Disease symptoms were not visible on Ler (wt) leaves 1 d after syringe infiltration with the virulent (*Pst*DC3000) or avirulent (*Pst*1065) strain of *P. syringae* pv. *tomato* (Figure 3.1a and d). Three days after infiltration with the virulent strain of *P. syringae* pv. *tomato*, susceptibility was associated with necrosis spreading from the site of syringe infiltration surrounded by chlorosis, that developed further 5 d after infiltration (Figure 3.1b and c). In contrast, 3 and 5 d after infiltration with the avirulent strain of *P. syringae* pv. *tomato*, resistance was expressed as either no disease symptoms (data not shown) or necrosis confined to the point of syringe infiltration (Figure 3.1e and f). Disease symptoms did not develop on leaves following syringe infiltration of 10 mM MgCl₂ (control) (Figure 3.1g-i). The bacterial numbers of the virulent strain of *P. syringae* pv. *tomato* within leaves peaked at 1.9×10^8 cfu/cm² 3 d after infiltration, significantly ($p < 0.05$) greater (311 fold) bacterial numbers of the avirulent strain (Figure 3.1j).

3.3.2 Effect of addition of ABA or simulated drought stress on Arabidopsis syringe infiltrated with *P. syringae* pv. *tomato*

Treatment of Ler (wt) plants with 1, 10 and 100 μ M ABA prior to syringe infiltration of an avirulent strain of *P. syringae* pv. *tomato*, caused a concentration

Figure 3.1 Disease symptoms and leaf bacterial numbers following syringe infiltration of *P. syringae* pv. *tomato* into Arabidopsis leaves.

Leaves were syringe infiltrated on the left side of the midrib.

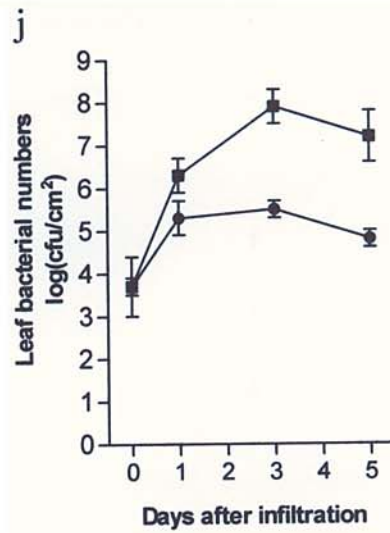
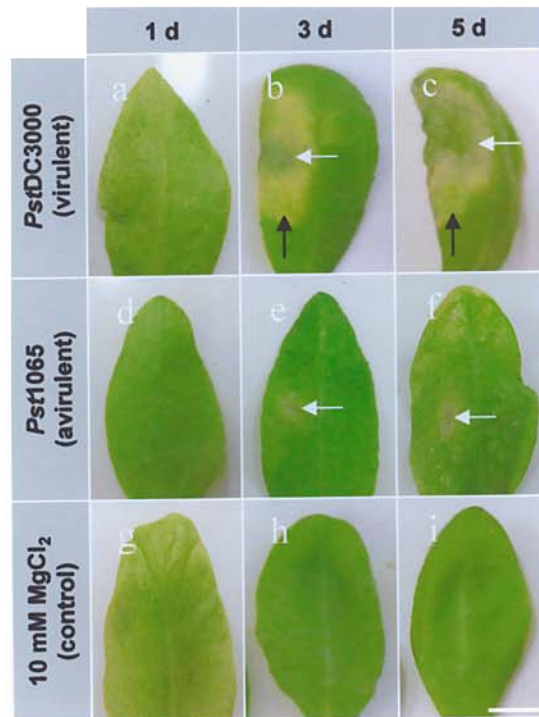
(a) to (c) Susceptible interactions between Ler (wt) leaves and the virulent strain of *P. syringae* pv. *tomato* (*Pst*DC3000). **(a)** Lack of disease symptoms 1 d after infiltration. **(b)** Necrosis spreading from the site of syringe infiltration (white arrow) surrounded by chlorosis (black arrow), 3 and **(c)** 5 d after infiltration.

(d) to (f) Resistant interactions between Ler (wt) leaves and the avirulent strain of *P. syringae* pv. *tomato* (*Pst*1065). **(d)** Lack of disease symptoms 1 d after infiltration. **(e)** Necrosis restricted to the site of syringe infiltration (white arrow) 3 and **(f)** 5 d after infiltration.

(g) to (i) Ler (wt) leaves following 10 mM MgCl₂ (control) infiltration. **(g)** Lack of disease symptoms 1, **(h)** 3 and **(i)** 5 d after infiltration.

Representative images from three independent experiments. Bar is equivalent to 5 mm.

(j) Bacterial numbers of the (■) virulent (*Pst*DC3000) and an (●) avirulent (*Pst*1065) strain of *P. syringae* pv. *tomato* within syringe infiltrated leaves. Each data point represents the mean \pm s.e.m. from four independent experiments.



dependent increase in both leaf chlorosis and bacterial numbers 3 d after infiltration (Figure 3.2a-d and g). The development of chlorosis in 100 μ M ABA treated leaves 3 d after infiltration with the avirulent strain of *P. syringae* pv. *tomato* and the significantly ($p < 0.05$) (108 fold) greater bacterial numbers than in 1% (v/v) methanol (control) treated leaves, was similar to the susceptible interaction of 1% (v/v) methanol treated leaves infiltrated with the virulent strain of *P. syringae* pv. *tomato* (Figure 3.2d and e). However, this interaction lacked the necrotic spread of a completely susceptible interaction. Treatment with 100 μ M ABA did not change the appearance of susceptible interactions, 3 d after infiltration with the virulent strain of *P. syringae* pv. *tomato* (Figure 3.2e and f). The endogenous ABA concentration in leaves following 100 μ M ABA treatment (prior to infiltration) was a significant ($p < 0.05$) greater (60 fold) than 1% (v/v) methanol treated leaves (Figure 3.2h), but did not affect the development or phenotype of leaves 3 d after treatment (Figure 3.3a and b). The addition of 100 μ M ABA to culture medium also had no effect on the growth of an avirulent strain of *P. syringae* pv. *tomato* (Figure 3.3c).

Drought stress of Ler (wt) plants prior to infiltration of the avirulent strain of *P. syringae* pv. *tomato* induced chlorosis on leaves 3 d after infiltration (Figure 3.4a and b). Drought stress also significantly ($p < 0.05$) increased (12 fold) the bacterial numbers of the avirulent strain of *P. syringae* pv. *tomato* within leaves, compared with unstressed (control) leaves (Figure 3.4c). The endogenous ABA concentration in leaves following drought stress (prior to infiltration) was significantly ($p < 0.05$) (eight fold) greater than those of unstressed leaves (Figure 3.4d).

Figure 3.2 Disease symptoms, leaf bacterial numbers and endogenous ABA concentrations of ABA treated Arabidopsis leaves following syringe infiltration with *P. syringae* pv. *tomato*.

Leaves were syringe infiltrated on the left side of the midrib.

(a) to (d) Disease symptoms on Ler (wt) leaves, 3 d after infiltration with the avirulent strain of *P. syringae* pv. *tomato* (*Pst*1065). (a) Necrosis localised at the site of infiltration (white arrow) on 1% (v/v) methanol (control) treated leaves. (b) Necrosis at the site of infiltration (white arrow) with some chlorosis (black arrow) on 1 μ M ABA treated leaves. (c) Necrosis at the site of infiltration (white arrow) surrounded by chlorosis (black arrow) on 10 and (d) 100 μ M ABA treated leaves.

(e) and (f) Necrosis spreading from the site of infiltration (white arrow) surrounded by chlorosis (black arrow) on Ler (wt) leaves, 3 d after infiltration with the virulent strain of *P. syringae* pv. *tomato* (*Pst*DC3000). (e) Plants treated with 1% (v/v) methanol or (f) 100 μ M ABA. Bar is equivalent to 5 mm. Representative images from three independent experiments.

(g) Bacterial numbers of the (■) virulent strain of *P. syringae* pv. *tomato* within 1% (v/v) methanol treated Ler (wt) leaves, and the (●) avirulent strain of *P. syringae* pv. *tomato* within 1% (v/v) methanol, (Δ) 1, (\square) 10 and (\circ) 100 μ M ABA treated Ler (wt) leaves. Each data point represents the mean \pm s.e.m. from three independent experiments. If error bars are not shown they were smaller than the data symbol.

(h) Endogenous ABA concentrations of 1% (v/v) methanol, 1, 10 and 100 μ M ABA treated Ler (wt) leaves immediately prior to infiltration. Each data point represents the mean \pm s.e.m. from three independent experiments.

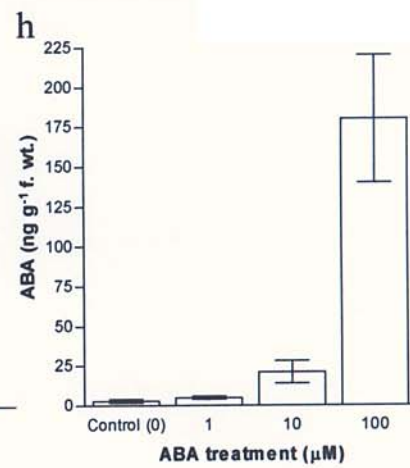
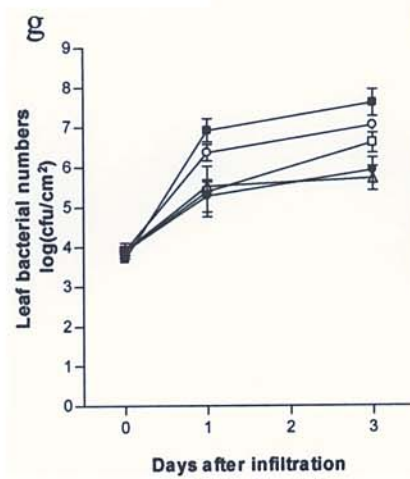
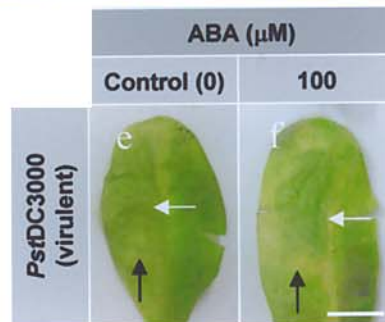
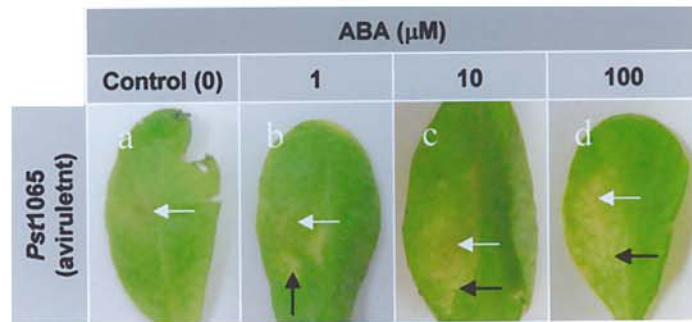


Figure 3.3 Effect of treatment with ABA on Arabidopsis leaf morphology and on growth in numbers of the avirulent strain of *P. syringae* pv. *tomato*.

(a) Healthy Ler (wt) leaves 3 d after 1% (v/v) methanol (control) and (b) 100 μ M ABA treatments. Note: the similarity in appearance of control and ABA treated leaves. Bar is equivalent to 20 mm. Representative images from two independent experiments.

(c) Growth of the avirulent strain of *P. syringae* pv. *tomato* (*Pst1065*) on culture medium containing 1% (v/v) methanol or 100 μ M ABA. Each column represents the mean \pm s.e.m. from two independent experiments.

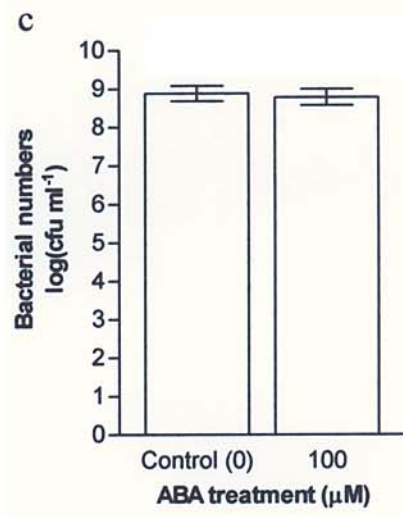
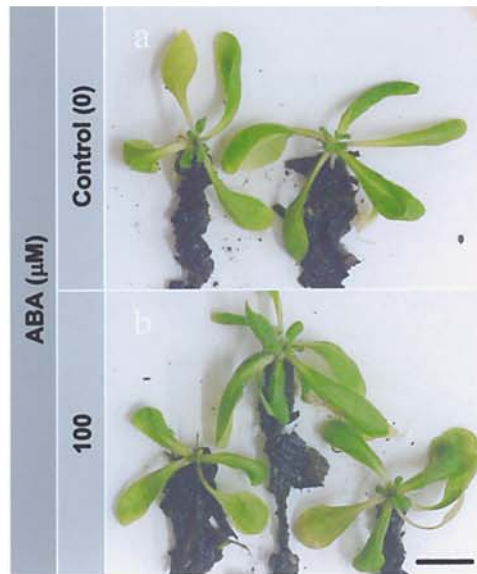


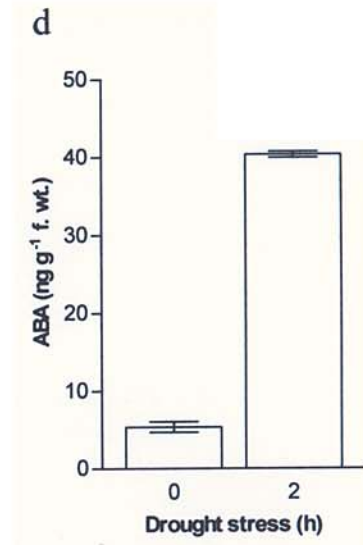
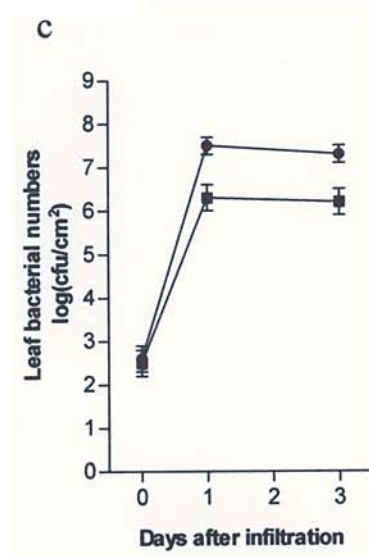
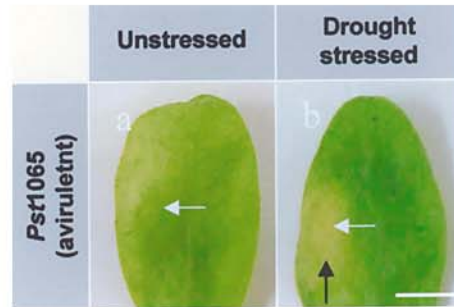
Figure 3.4 Disease symptoms, leaf bacterial numbers and endogenous ABA concentrations in leaves of drought stressed *Arabidopsis* following syringe infiltration with the avirulent strain of *P. syringae* pv. *tomato*.

(a) and (b) Leaves were syringe infiltrated on the left side of the midrib.

(a) and (b) Disease symptoms on Ler (wt) leaves, 3 d after infiltration with the avirulent strain of *P. syringae* pv. *tomato* (*Pst1065*). **(a)** Necrosis restricted to the site of infiltration (white arrow) on unstressed (control) leaves **(b)** Necrosis at the site of infiltration (white arrow) surrounded by chlorosis (black arrow) on drought stressed leaves. Bar is equivalent to 4 mm. Representative images from three independent experiments.

(c) Bacterial numbers within (■) unstressed and (●) drought stressed Ler (wt) leaves after syringe infiltration with the avirulent strain of *P. syringae* pv. *tomato* (*Pst1065*). Each data point represents the mean \pm s.e.m. of five independent experiments.

(d) Endogenous ABA concentrations with Ler (wt) leaves prior to (0 h) and after drought stress (2 h). Each column represents the mean \pm s.e.m. from two independent experiments.



3.3.3 Effect of ABA biosynthesis inhibitor treatment on leaves syringe infiltrated with *P. syringae* pv. *tomato*

Following treatment with norflurazon or fluridone the susceptibility of plants infiltrated with the virulent strain of *P. syringae* pv. *tomato* was phenotypically similar to that produced following dH₂O or 0.4% (v/v) dimethylsulfoxide (DMSO) (control) treatments 3 d after infiltration (Figure 3.5a-d). Bacterial numbers were also not significantly ($p>0.05$) different from controls (Figure 3.5g). Treatment of plants with norflurazon also did not alter the appearance of resistant interactions 3 d after infiltration with the avirulent strain of *P. syringae* pv. *tomato* (Figure 3.5e and f). The concentration of ABA within leaves following treatment with norflurazon or fluridone (prior to infiltration) were not significantly ($p>0.05$) different from controls (Figure 3.5h), but both treatments caused photobleaching of inflorescence stalks (Figure 3.6a-d). The addition of norflurazon or fluridone to the culture medium had no affect on the growth of the virulent strain of *P. syringae* pv. *tomato* (Figure 3.6e and f).

3.3.4 Development of disease symptoms in *Arabidopsis* ABA deficient and ABA insensitive mutants following vacuum infiltration with *P. syringae* pv. *tomato*

Three days after vacuum infiltration of both Ler (wt) and Col-0 (wt) plants, susceptibility to the virulent strain of *P. syringae* pv. *tomato* was associated with necrotic and water soaked leaves (Figure 3.7a and d). Following vacuum infiltration with the avirulent strain of *P. syringae* pv. *tomato* resistance was associated with only slight chlorosis of leaves (Figure 3.7b and e). No disease symptoms developed on leaves 3 d after vacuum infiltration with 10 mM MgCl₂ (control) (Figure 3.7c and f). The bacterial numbers within both Ler (wt) and Col-0 (wt) leaves 3 d after vacuum infiltration with a virulent strain of *P. syringae* pv. *tomato* were significantly

Figure 3.5 Disease symptoms, leaf bacterial numbers and endogenous ABA concentrations in *Arabidopsis* leaves treated with ABA biosynthesis inhibitors followed by syringe infiltration with *P. syringae* pv. *tomato*.

(a) to (f) Leaves were syringe infiltrated on the right side of the midrib.

(a) to (d) Susceptible disease symptoms on Ler (wt) leaves, 3 d after infiltration with the virulent strain of *P. syringae* pv. *tomato* (*Pst*DC3000). **(a)** Spreading necrosis (white arrow) and chlorosis (black arrow) from the site of infiltration on dH₂O (control) and **(b)** 100 μ M norflurazon treated leaves. **(c)** Spreading necrosis (white arrow) and chlorosis (black arrow) from the site of infiltration on 0.4% (v/v) DMSO (control) and **(d)** 100 μ M fluridone treated leaves.

(e) and (f) Resistant reactions on Ler (wt) leaves, 3 d after infiltration with the avirulent strain of *P. syringae* pv. *tomato* (*Pst*1065). **(e)** Necrosis restricted to the site of infiltration (white arrow) on dH₂O and **(f)** 100 μ M norflurazon treated leaves. Bar is equivalent to 5 mm. Representative images from two independent experiments.

(g) Bacterial numbers within (■) dH₂O, (□) 100 μ M norflurazon, (●) 0.4% (v/v) DMSO and (○) 100 μ M fluridone treated leaves infiltrated with an avirulent strain of *P. syringae* pv. *tomato*. Each data point represents the mean \pm s.e.m. from four independent experiments (except 0.4% (v/v) DMSO and 100 μ M fluridone that are from two independent experiments).

(h) Endogenous ABA concentrations within dH₂O, 100 μ M norflurazon, 0.4% (v/v) DMSO and 100 μ M fluridone treated leaves. Each column represents the mean \pm s.e.m. from four independent experiments (except 0.4% (v/v) DMSO and 100 μ M fluridone that are from two independent experiments).

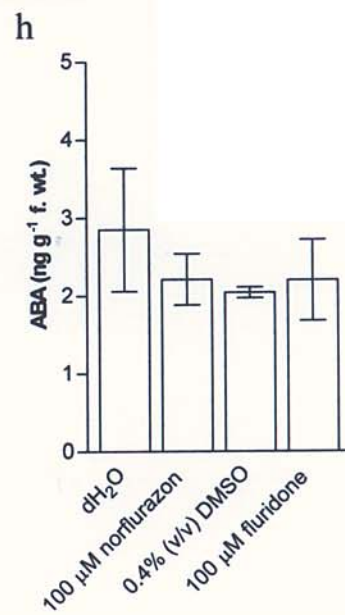
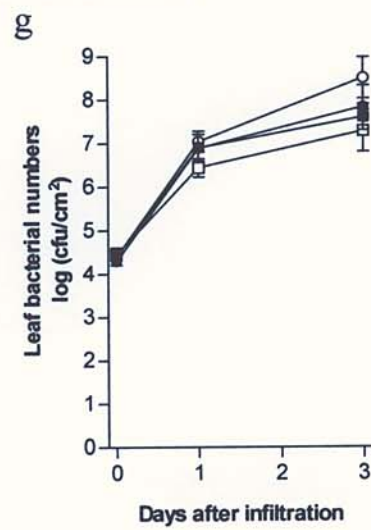
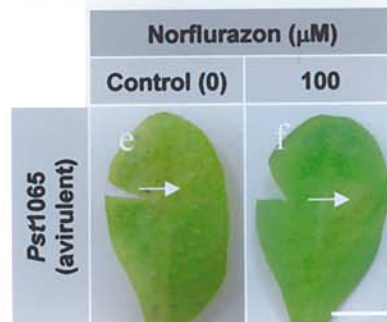
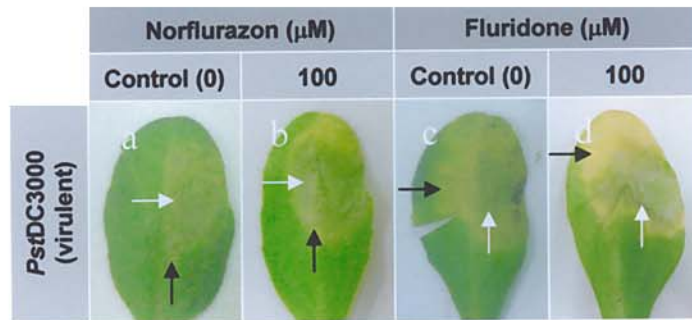


Figure 3.6 Effect of treatment with ABA biosynthesis inhibitors on Arabidopsis inflorescence stalks and the virulent strain of *P. syringae* pv. *tomato*.

(a) Healthy Ler (wt) inflorescence stalks 3 d after dH₂O (control) and (b) 0.4% (v/v) DMSO (control) treatments. (c) Photobleached Ler (wt) inflorescence stalks 3 d after 100 μ M norflurazon and (d) 100 μ M fluridone treatments. Bar is equivalent to 30 mm. Representative images from two independent experiments.

(e) Growth of the virulent strain of *P. syringae* pv. *tomato* (*Pst*DC3000) on culture medium containing dH₂O or 100 μ M norflurazon, (f) 0.4% (v/v) DMSO or 100 μ M fluridone. Each column represents the mean \pm s.e.m from two independent experiments.

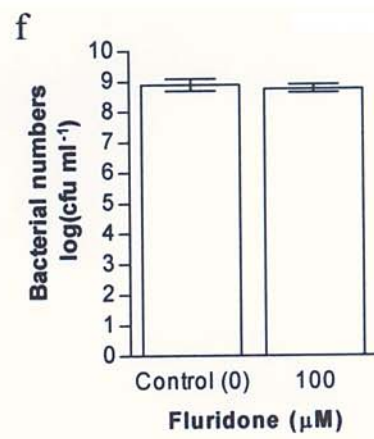
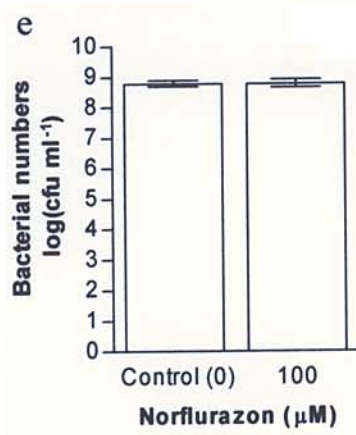
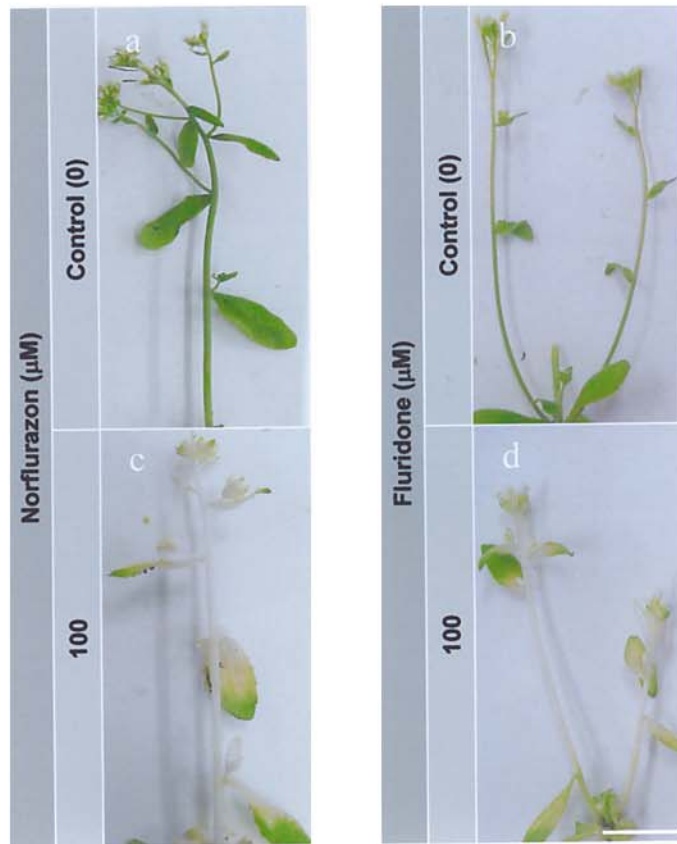
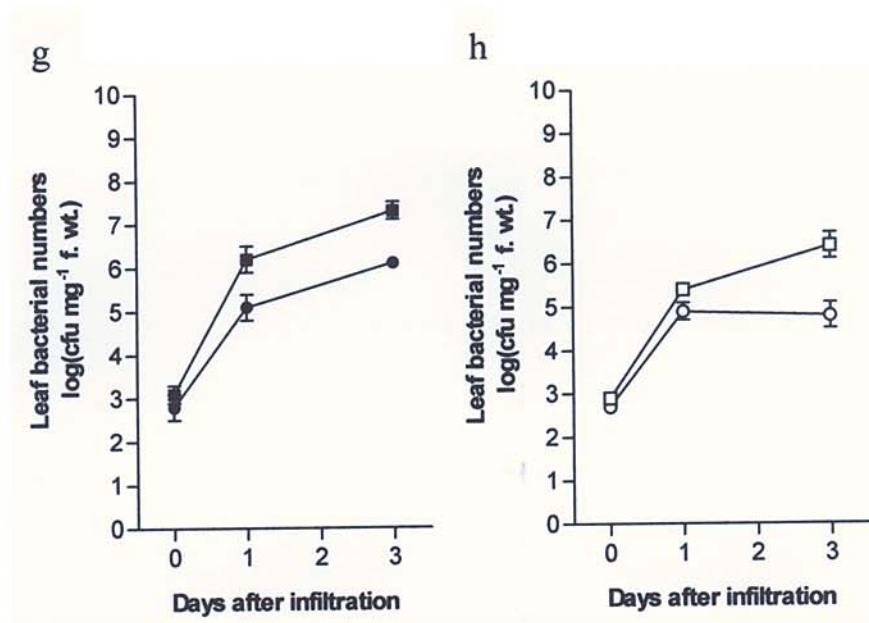
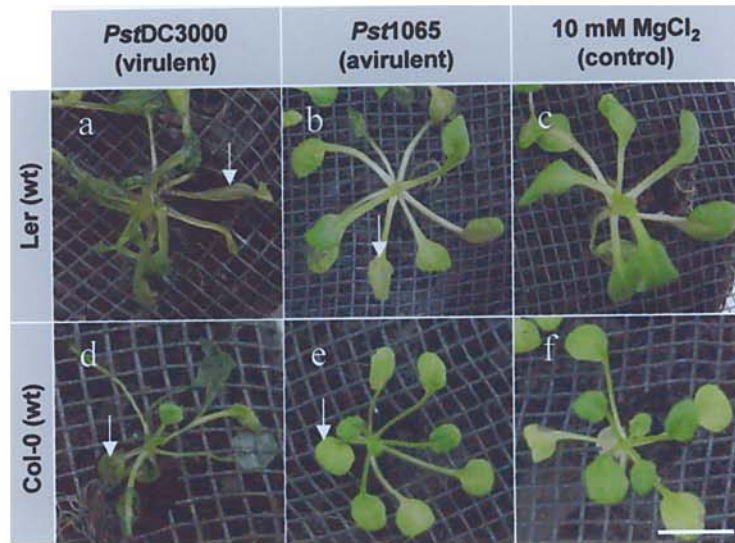


Figure 3.7 Disease symptoms and leaf bacterial populations following *P. syringae* pv. *tomato* vacuum infiltration of Arabidopsis plants.

(a) to (c) Disease symptoms on Ler (wt) leaves, 3 d after vacuum infiltration. **(a)** Necrotic and water soaked leaves (white arrow) after infiltration with the virulent strain of *P. syringae* pv. *tomato* (*Pst*DC3000). **(b)** Slight chlorosis (white arrow) after infiltration with the avirulent strain of *P. syringae* pv. *tomato* (*Pst*1065). **(c)** No disease symptoms after infiltration with 10 mM MgCl₂.

(d) to (f) Disease symptoms on Col-0 (wt) leaves, 3 d after vacuum infiltration. **(d)** Necrotic and water soaked leaves (white arrow) of a susceptible interaction after infiltration with the virulent strain of *P. syringae* pv. *tomato* (*Pst*DC3000). **(e)** Slight chlorosis (white arrow) of a resistant interaction after infiltration with the avirulent strain of *P. syringae* pv. *tomato* (*Pst*1065). **(f)** No disease symptoms after infiltration with 10 mM MgCl₂. Bar is equivalent to 20 mm. Representative images from three independent experiments.

(g) Bacterial numbers within Ler (wt) leaves vacuum infiltrated with the (■) virulent (*Pst*DC3000) and the (●) avirulent (*Pst*1065) strain of *P. syringae* pv. *tomato*. **(h)** Bacterial numbers within Col-0 (wt) leaves vacuum infiltrated with the (□) virulent (*Pst*DC3000) and (○) an avirulent (*Pst*1065) strain of *P. syringae* pv. *tomato*. Each data point represents the mean ± s.e.m. from four independent experiments. If error bars are not shown they were smaller than the data symbol.



($p < 0.05$) greater (18 fold) than numbers found following infiltration with the avirulent strain of *P. syringae* pv. *tomato* (Figure 3.7g and h).

Vacuum infiltration of the ABA deficient mutants *aba1-1*, *aba1-3*, *aba2-1* and *aba3-1* and the ABA insensitive mutant *abi1-1* with the virulent or avirulent strain of *P. syringae* pv. *tomato* resulted in interaction phenotypes that were the same as the Ler (wt) and Col-0 (wt) plants, 3 d after infiltration (Figure 3.8a-n). The bacterial numbers within the mutants were also not significantly ($p > 0.05$) different from those found in the wild type plants (Figure 3.8o-q).

The phenotype of ABA deficient and ABA insensitive mutant plants prior to vacuum infiltration was similar to the wild types (Figure 3.9a-g). The concentration of ABA in ABA deficient and ABA insensitive mutant leaves prior to infiltration was not significantly ($p > 0.05$) different from the wild type leaves (Figure 3.9h and i). The inability of the ABA deficient mutants to synthesis ABA as readily as wild type plants was confirmed by measuring the concentration of ABA in leaves 3 h after detachment from roots. At that time point, the concentration of ABA in *aba1-1* and *aba1-3* leaves was significantly ($p < 0.05$) lower (eight fold) than Ler (wt) and *abi1-1* leaves (Figure 3.9j) and *aba2-1* and *aba3-1* were significantly ($p < 0.05$) lower (10 fold) than Col-0 (wt) leaves (Figure 3.9k). The insensitivity of *abi1-1* seed stocks to ABA was confirmed by the ability of the seeds to germinate on MS medium containing 10 μ M ABA (a concentration that inhibited germination of wild type seeds) (data not shown).

Figure 3.8 Disease symptoms and leaf bacterial populations following *P. syringae* pv. *tomato* vacuum infiltration of ABA deficient and ABA insensitive mutants of *Arabidopsis*.

(a) to (g) Necrosis and water soaked leaves (white arrow) of susceptible interactions, 3 d after vacuum infiltration with the virulent strain of *P. syringae* pv. *tomato* (*Pst*DC3000). (a) Ler (wt), (b) ABA deficient mutants *aba1-1* and (c) *aba1-3* and (d) ABA insensitive mutant *abil-1*, (e) Col (wt), (f) ABA deficient mutants *aba2-1* and (g) *aba3-1*.

(h) to (n) Slight chlorosis (white arrow) of resistant interactions, 3 d after vacuum infiltration with the avirulent strain of *P. syringae* pv. *tomato* (*Pst*1065). (h) Ler (wt), (i) *aba1-1*, (j) *aba1-3*, (k) *abil-1*, (l) Col (wt), (m) *aba2-1* and (n) *aba3-1*. Bar is equivalent to 40 mm. Representative images from three independent experiments.

(o) Bacterial numbers within (□) Ler (wt), (○) *aba1-1* and (△) *aba1-3* leaves vacuum infiltrated with the virulent strain of *P. syringae* pv. *tomato* (*Pst*DC3000). (p) Bacterial numbers within (□) Ler (wt) and (■) *abil-1* leaves vacuum infiltrated with a virulent strain of *P. syringae* pv. *tomato* (*Pst*DC3000). (q) Bacterial numbers within (●) Col-0 (wt), (▲) *aba2-1* and (◆) *aba3-1* vacuum infiltrated with the virulent strain of *P. syringae* pv. *tomato* (*Pst*DC3000). Each data point represents the mean \pm s.e.m. from four independent experiments. If error bars are not shown they were smaller than the data symbol.

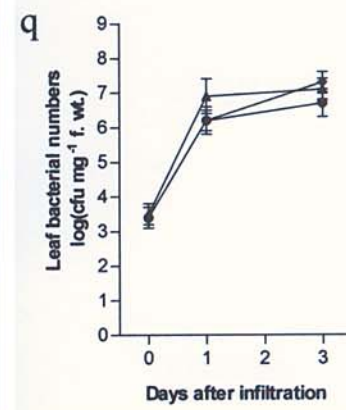
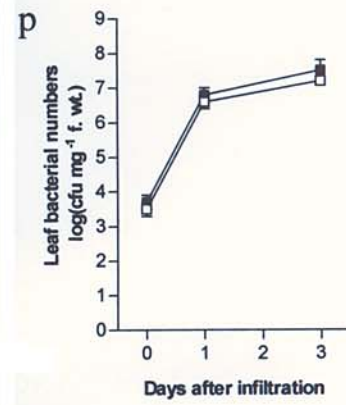
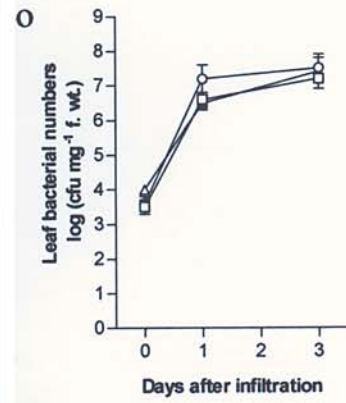
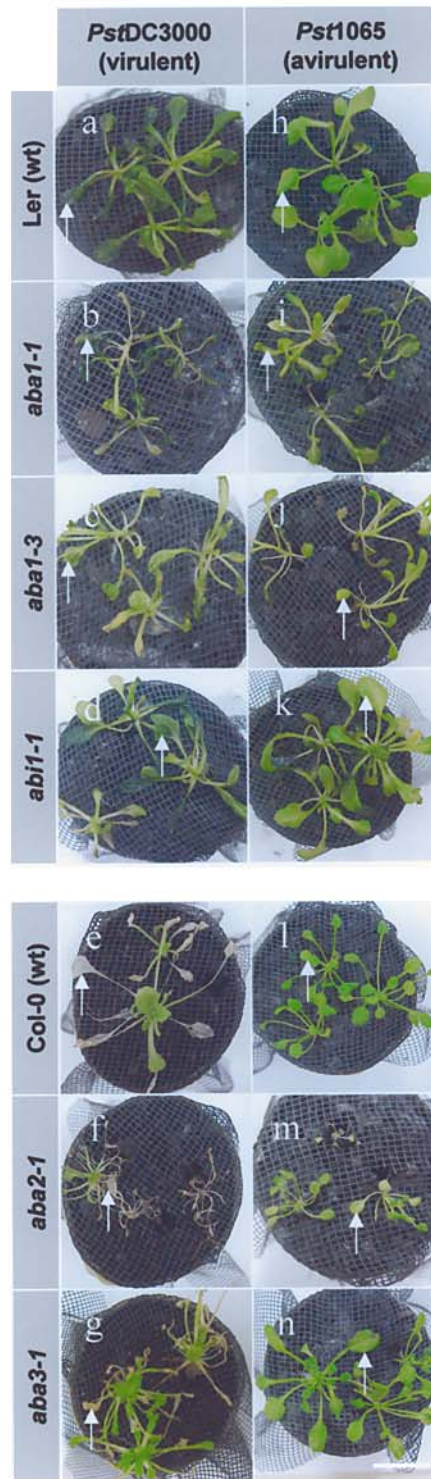
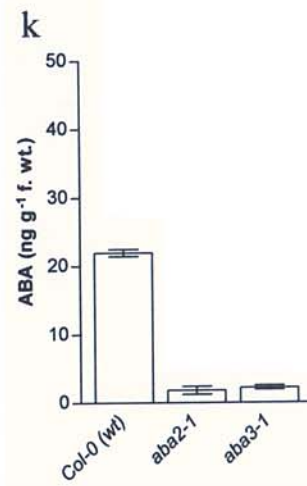
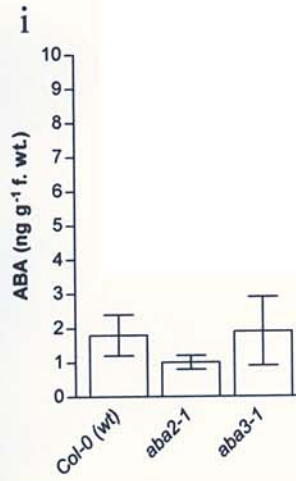
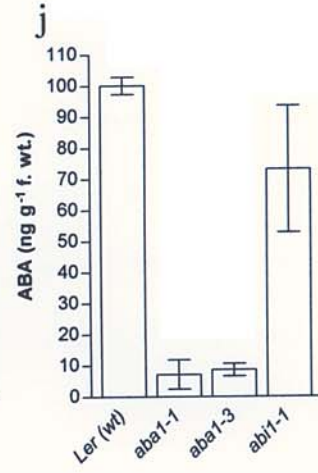
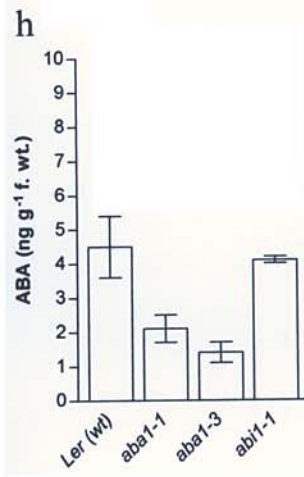


Figure 3.9 Comparison of growth form and endogenous ABA concentrations within Arabidopsis ABA deficient and ABA insensitive mutant leaves.

(a) to (g) Plants 5 wk of age. **(a)** Ler (wt), **(b)** ABA deficient mutants *aba1-1* and **(c)** *aba1-3*, **(d)** ABA insensitive mutant *abil-1*, **(e)** Col-0 (wt), **(f)** ABA deficient mutants *aba2-1* and **(g)** *aba3-1* prior to vacuum infiltration. Bar is equivalent to 20 mm. Representative images from two independent experiments.

(h) Endogenous ABA concentrations within ABA deficient and ABA insensitive mutant leaves of Ler (wt) background and **(i)** ABA deficient mutant leaves of Col-0 (wt) background prior to vacuum infiltration.

(j) Endogenous ABA concentrations within ABA deficient and ABA insensitive mutant leaves of Ler (wt) background and **(k)** ABA deficient mutant leaves of Col-0 (wt) background 3 h after root detachment. Each column represents the mean \pm s.e.m. from two independent experiments.



3.3.5 Comparison of morphological, anatomical and biochemical components in ABA-treated Ler (wt) leaves following syringe infiltration with the avirulent *P. syringae* pv. *tomato* (Pst1065)

3.3.5.1 Development of necrosis in ABA treated leaves following infiltration with the avirulent strain of *P. syringae* pv. *tomato*

Necrosis of leaf cells in large areas of cellular collapse was detected 3 d after syringe infiltration with the virulent strain of *P. syringae* pv. *tomato* (Figure 3.10a-c). In contrast, small clusters of necrotic cells were detected 12 h through to 3 d after infiltration with the avirulent strain of *P. syringae* pv. *tomato* (Figure 3.10d-f). Necrosis of leaf cells was not detected following infiltration with 10 mM MgCl₂ (data not shown). Small clusters of necrotic cells also developed in leaves treated with ABA or 1% (v/v) methanol (control), 12 h after infiltration with the avirulent strain of *P. syringae* pv. *tomato* (Figure 3.11a and d). The necrotic clusters in both treatments remained similar 1 d after infiltration (Figure 3.11b and e). However, the necrosis had increased to encompass large areas of cells in ABA treated leaves 3 d after infiltration (Figure 3.11c and f).

3.3.5.2 H₂O₂ production in leaves treated with ABA following infiltration with an avirulent strain of *P. syringae* pv. *tomato*

After DAB treatment and prior to infiltration, H₂O₂ was only detected in the vascular tissue of leaves (data not shown). Following treatment with 10 mM MgCl₂, DAB detection of H₂O₂ production within leaves was only found at the point of syringe contact up to 4 h after infiltration with 10 mM MgCl₂ (Figure 3.12a and b) but not detected at 8 h (data not shown). Following infiltration with either the virulent or avirulent strain of *P. syringae* pv. *tomato* H₂O₂ was detected throughout the infiltrated region of leaves up to 4 h after infiltration (Figure 3.12c-f), but was

Figure 3.10 Development of necrotic cells in Arabidopsis leaves following syringe infiltration with *P. syringae* pv. *tomato*.

Ler (wt) leaves LTB stained.

(a) to (c) Leaves infiltrated with the virulent strain of *P. syringae* pv. *tomato* (*Pst*DC3000). **(a)** No necrosis of leaf cells 12 h and **(b)** 1 d after infiltration. **(c)**

Necrosis of leaf cells in large areas of cellular collapse (white arrow) 3 d after infiltration. Black arrow: vascular tissue.

(d) to (f) Leaves infiltrated with the avirulent strain of *P. syringae* pv. *tomato* (*Pst*1065). **(d)** Small clusters of necrotic cells (white arrow) 12 h, **(e)** 1 d and **(f)** 3 d

after infiltration. Black arrow: vascular tissue. Bar is equivalent to 150 μ m.

Representative images from three independent experiments.

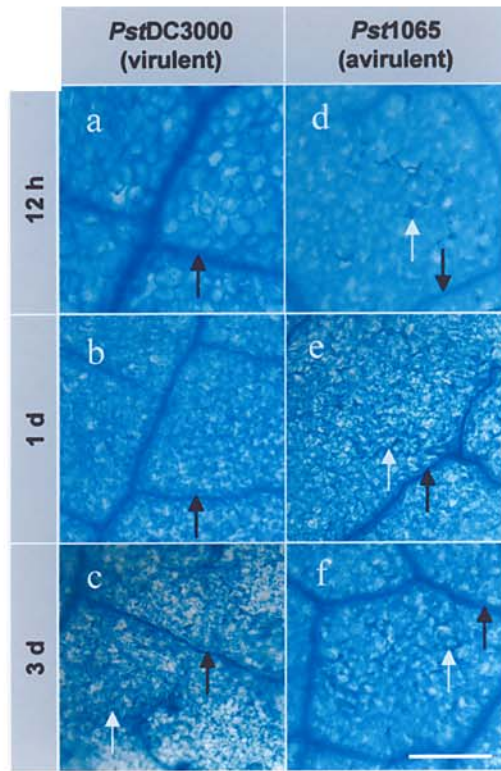


Figure 3.11 Development of necrotic cells in ABA treated Arabidopsis following syringe infiltration with the avirulent strain of *P. syringae* pv. *tomato*.

Ler (wt) leaves LTB stained.

(a) to (c) One percent (v/v) methanol (control) treated leaves infiltrated with the avirulent strain of *P. syringae* pv. *tomato* (*Pst1065*). (a) Small clusters of necrotic cells (white arrow) 12 h, (b) 1 d and (c) 3 d after infiltration. Black arrow: vascular tissue.

(d) to (f) Leaves treated with 100 μ M ABA and then infiltrated with the avirulent strain of *P. syringae* pv. *tomato* (*Pst1065*). (d) Small clusters of necrotic cells (white arrow) 12 h and (e) 1 d after infiltration. (f) Necrosis of leaf cells in large areas of cellular collapse (white arrow) 3 d after infiltration. Black arrow: vascular tissue. Bar is equivalent to 150 μ m. Representative images from three independent experiments.

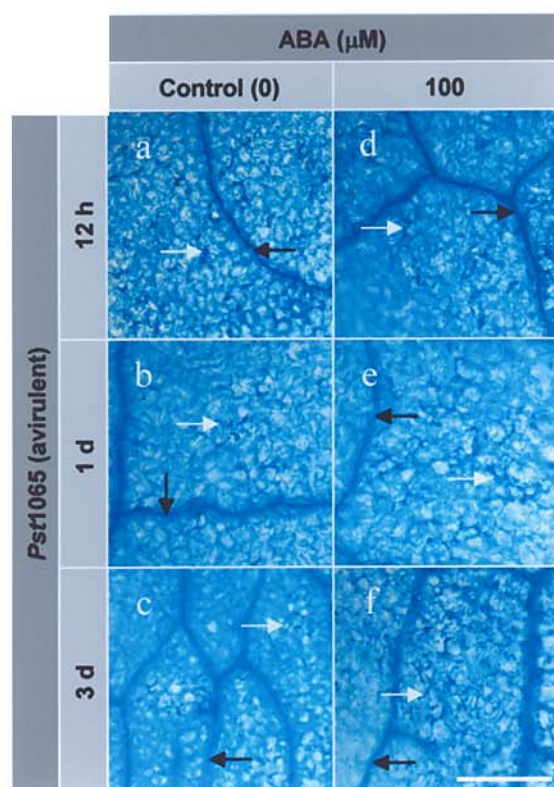


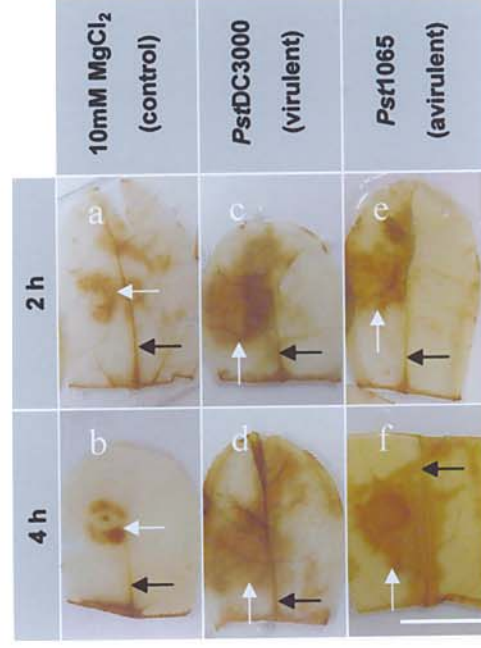
Figure 3.12 DAB detection of H₂O₂ in Arabidopsis leaves following syringe infiltration with *P. syringae* pv. *tomato*.

Ler (wt) leaves were syringe infiltrated on the left side of the midrib. Leaves were cleared of photosynthetic pigments after DAB treatment.

(a) and **(b)** DAB detection of H₂O₂ in leaf cells after infiltration with 10 mM MgCl₂ (control). **(a)** H₂O₂ at the point of syringe contact (white arrow), 2 and **(b)** 4 h after infiltration. Black arrow: H₂O₂ in vascular tissue. Note: DAB polymerisation on the cut edge of the leaf.

(c) and **(d)** DAB detection of H₂O₂ in leaf cells after infiltration with the virulent strain of *P. syringae* pv. *tomato* (*Pst*DC3000). **(c)** H₂O₂ detected throughout the infiltrated region of leaves (white arrow) 2 and **(d)** 4 h after infiltration. Black arrow: H₂O₂ in vascular tissue. Note: DAB polymerisation on the cut edge of the leaf.

(e) to **(f)** DAB detection of H₂O₂ in leaf cells after infiltration with the avirulent strain of *P. syringae* pv. *tomato* (*Pst*1065). **(e)** H₂O₂ detected throughout the infiltrated region of leaves (white arrow) 2 and **(f)** 4 h after infiltration. Black arrow: H₂O₂ in vascular tissue. Note: DAB polymerisation on the cut edge of the leaf. Bar is equivalent to 5mm. Representative images from two independent experiments.



restricted to the point of syringe contact 8 h after infiltration (data not shown). A similar temporal and spatial pattern of H₂O₂ production was also detected within leaves treated with ABA or 1% (v/v) methanol followed by infiltration with the avirulent strain (Figure 3.13a-d).

3.3.5.3 Lignin accumulation in leaves treated with ABA following infiltration with the avirulent strain of *P. syringae* pv. *tomato*

Lignin was detected by Phl / HCl stain in the vascular tissue of leaves prior to infiltration (data not shown). Lignin did not accumulate in leaves 3 d after infiltration with 10 mM MgCl₂ or the virulent strain of *P. syringae* pv. *tomato* (Figure 3.14a and c). However, lignin accumulated in small clusters of leaf cells 3 d after infiltration with the avirulent strain of *P. syringae* pv. *tomato* (Figure 3.14b). Phenolics were also detected by TB0 stain in small clusters of leaf cells 3 d after avirulent infiltration (data not shown). Suberin was not detected by SBB stain within the vascular tissue or in association with avirulent infiltrations (data not shown). The wall bound TGA derivatives extracted from leaves were therefore attributed to lignin accumulation. Three days after infiltration of leaves with the virulent strain of *P. syringae* pv. *tomato* the accumulation of wall bound TGA derivatives was not significantly ($p>0.05$) different from the 10 mM MgCl₂ infiltrations (Figure 3.14d). In contrast, 3 d after infiltration with the avirulent strain of *P. syringae* pv. *tomato* the accumulation of wall bound TGA derivatives was significantly ($p<0.05$) greater (2.6 fold) than that found in the control (Figure 3.14d).

Three days after infiltration with the avirulent strain of *P. syringae* pv. *tomato* of leaves treated with ABA lignin was not detected in areas of cellular collapse. In contrast, small clusters of cells accumulated lignin in control leaves (Figure 3.15a and b). The accumulation of wall bound TGA derivatives 3 d after infiltration of 100

Figure 3.13 DAB detection of H₂O₂ in ABA treated Arabidopsis following syringe infiltration with the avirulent strain of *P. syringae* pv. *tomato*.

Ler (wt) leaves were syringe infiltrated on the left side of the midrib. Leaves were cleared of photosynthetic pigments after DAB treatment.

(a) and **(b)** DAB detection of H₂O₂ in 1% (v/v) methanol (control) treated leaves after infiltration with the avirulent strain of *P. syringae* pv. *tomato* (*Pst1065*). **(a)** H₂O₂ detected throughout the infiltrated region of leaves (white arrow) 2 and **(b)** 4 h after infiltration. Black arrow: H₂O₂ in vascular tissue. Note: DAB polymerisation on the cut edge of the leaf.

(c) and **(d)** DAB detection of H₂O₂ in 100 µM ABA treated leaves after infiltration with the avirulent strain of *P. syringae* pv. *tomato* (*Pst1065*). **(c)** H₂O₂ detected throughout the infiltrated region of leaves (white arrow) 2 and **(d)** 4 h after infiltration. Black arrow: H₂O₂ in vascular tissue. Note: DAB polymerisation on the cut edge of the leaf. Bar is equivalent to 5 mm. Representative images from two independent experiments.

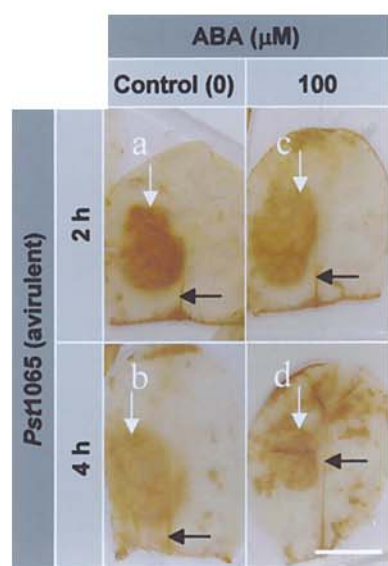
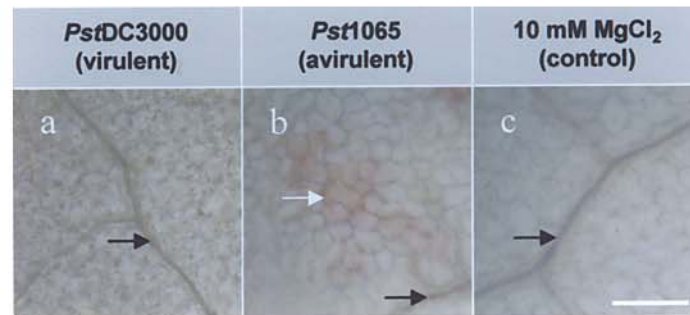


Figure 3.14 Detection of lignin deposition in Arabidopsis leaves following syringe infiltration with *P. syringae* pv. *tomato*.

(a) to (c) Ler (wt) leaves stained with PhI / HCl, 3 d after infiltration.

(a) No lignin accumulation following infiltration with the virulent strain of *P. syringae* pv. *tomato* (*Pst*DC3000). **(b)** A cluster of cells that accumulated lignin in the cell walls (white arrow) following infiltration with the avirulent strain of *P. syringae* pv. *tomato* (*Pst*1065). **(c)** No lignin accumulation following infiltration with 10 mM MgCl₂ (control). Black arrow: lignin in vascular tissue. Bar is equivalent to 250 µm. Representative images from three independent experiments.

(d) Wall bound TGA derivatives extracted from Ler (wt) leaves 3 d after syringe infiltration with the virulent (*Pst*DC3000) and avirulent strain of *P. syringae* pv. *tomato* (*Pst*1065) and 10 mM MgCl₂ (control). Each column represents the mean ± s.e.m. from four independent experiments.



d

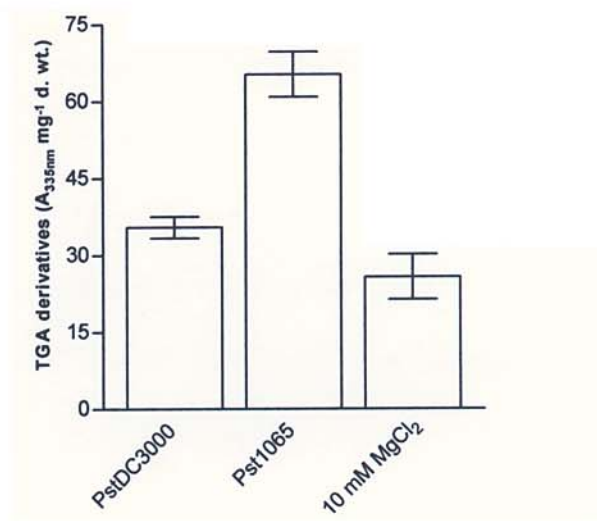


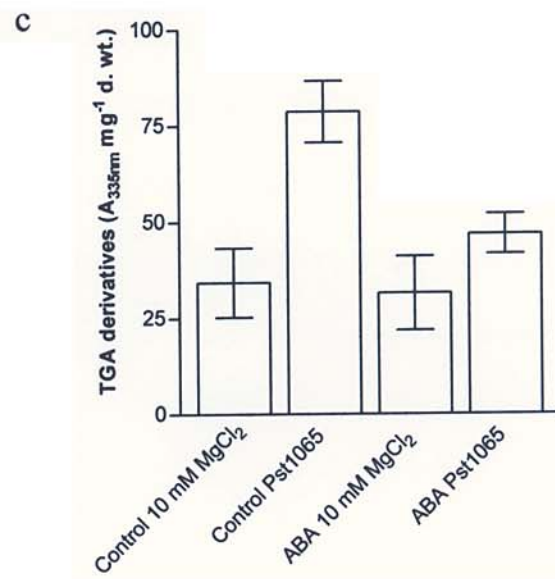
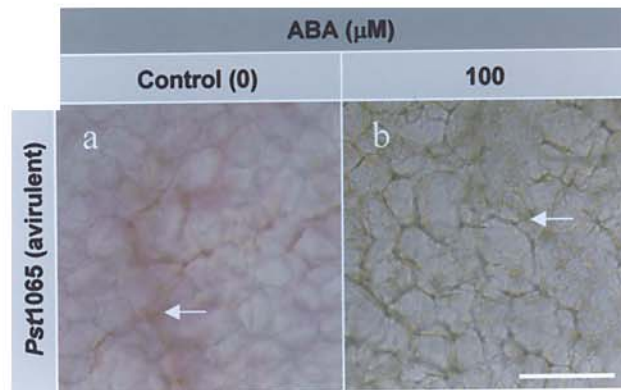
Figure 3.15 Detection of lignin deposition in ABA treated Arabidopsis leaves following syringe infiltration with the avirulent strain of *P. syringae* pv. *tomato*.

Ler (wt) leaves stained with PhI / HCl, 3 d after infiltration with the avirulent strain of *P. syringae* pv. *tomato* (*Pst1065*).

(a) A cluster of cells accumulated lignin in their cell walls (white arrow) following infiltration in leaves treated with 1% (v/v) methanol (control). (b) No lignin accumulation detected in areas of cellular collapse (white arrow) following infiltration in leaves treated with 100 μ M ABA. Bar is equivalent to 100 μ m.

Representative images representative from three independent experiments.

(c) Wall bound TGA derivatives extracted from 1% (v/v) methanol or 100 μ M ABA treated Ler (wt) leaves 3 d after syringe infiltration with 10 mM MgCl₂ (control) or the avirulent strain of *P. syringae* pv. *tomato* (*Pst1065*). Each column represents the mean \pm s.e.m. from three independent experiments.



μ M ABA treated leaves was also a significantly ($p < 0.05$) less than that in controls, in similarity to the wall bound TGA derivatives of 10 mM $MgCl_2$ infiltrations (Figure 3.15c).

3.3.5.4 Callose accumulation in leaves treated with ABA following infiltration with the avirulent strain of *P. syringae* pv. *tomato*

Prior to syringe infiltration of leaves, callose was detected by AB stain within vascular tissue and at the base of trichomes (data not shown). Three days after infiltration of leaves with avirulent or virulent strains of *P. syringae* pv. *tomato* callose was deposited extensively throughout cells in the infiltrated region of the leaves (Figure 3.16a and b). In the control callose was present in small cell wall depositions in scattered cells 3 d after treatment (Figure 3.16c). Callose was also deposited extensively in both ABA and control treated leaves 3 d after infiltration with an avirulent strain of *P. syringae* pv. *tomato* (Figure 3.16d and e).

3.3.5.5 Accumulation of *AtPALI* mRNA transcripts in ABA treated leaves following infiltration with the avirulent strain of *P. syringae* pv. *tomato*

Six hours after infiltration of leaves with the avirulent strain of *P. syringae* pv. *tomato* the abundance of *AtPALI* mRNA transcripts was 12% greater than infiltration with the virulent strain of *P. syringae* pv. *tomato* or the control treatment (Figure 3.17a). Six hours after infiltration with the avirulent strain of *P. syringae* pv. *tomato* of leaves treated with ABA, the abundance of *AtPALI* transcripts was 17% less than that in control treated leaves (Figure 3.17b).

3.3.5.6 SA accumulation in leaves treated with ABA followed by infiltration with the avirulent strain of *P. syringae* pv. *tomato*

Free SA accumulated in leaves 1 and 3 d after infiltration with the virulent or an avirulent strain of *P. syringae* pv. *tomato* to concentrations that were

Figure 3.16 Callose deposition in Arabidopsis leaves following syringe infiltration with *P. syringae* pv. *tomato*.

Ler (wt) leaves stained with AB, 3 d after infiltration.

(a) Callose deposited extensively throughout cells (white arrow) in the infiltrated region of the leaves following infiltration with the virulent (*Pst*DC3000) or (b) an avirulent (*Pst*1065) strain of *P. syringae* pv. *tomato*. (c) Callose was deposited as small cell wall depositions in scattered cells (white arrow) following infiltration with 10 mM MgCl₂ (control). Black arrow: callose in vascular tissue.

(d) Callose deposited extensively throughout cells (white arrow) in the infiltrated region of leaves treated with 1% (v/v) methanol (control) or (e) 100 μM ABA following infiltration with the avirulent strain of *P. syringae* pv. *tomato* (*Pst*1065). Black arrow: callose in vascular tissue. Bar is equivalent to 200 μm. Representative images from three independent experiments.

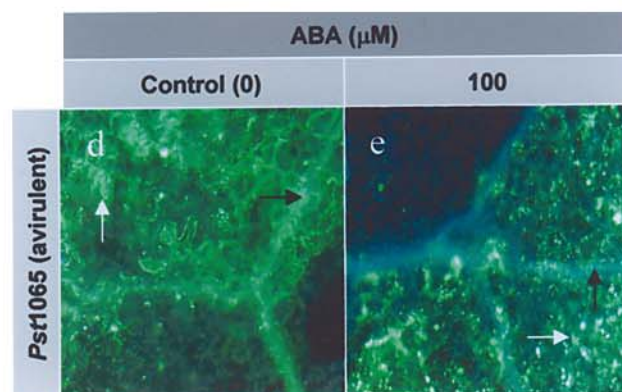
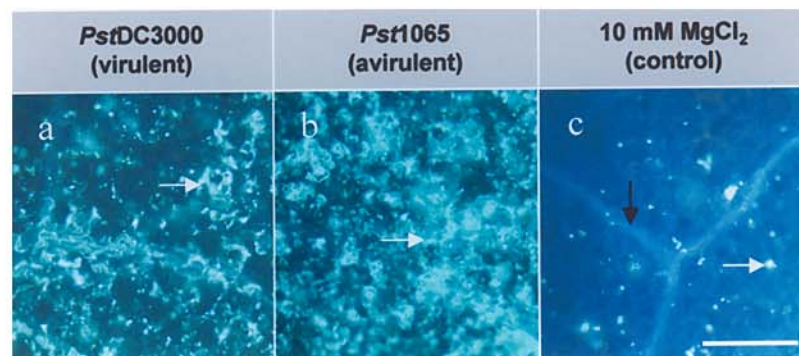


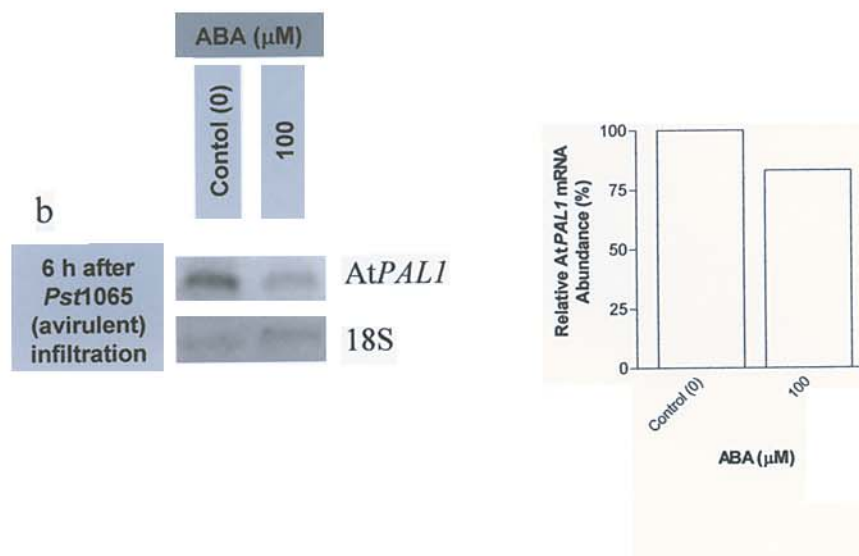
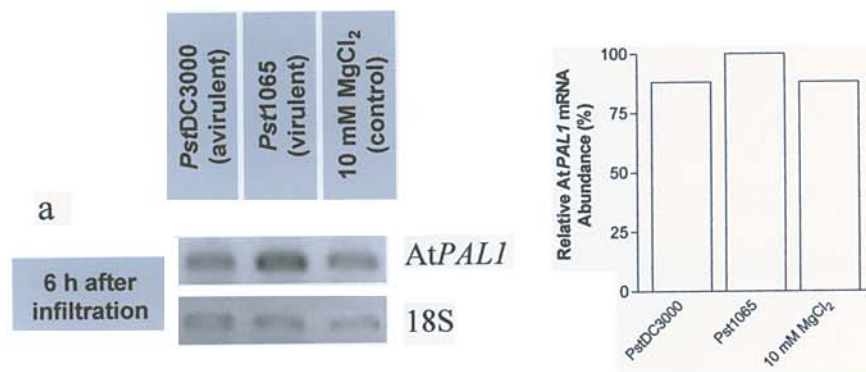
Figure 3.17 Abundance of *AtPAL1* mRNA transcripts in Arabidopsis leaves following syringe infiltration with *P. syringae* pv. *tomato*.

(a) to (d) Negative images of EtBr stained 1% (w/v) agarose gels containing the products from simultaneous *AtPAL1* (20 cycles) and 18S (26 cycles) RT-PCR reactions. Accompanied by a figure that shows the equalised, relative abundance of *AtPAL1* from each gel. Each RT-PCR was conducted on total RNA extracted from Ler (wt) leaves.

(a) Six hours after infiltration with the virulent (*Pst*DC3000) or avirulent strain (*Pst*1065) of *P. syringae* pv. *tomato*.

(b) Six hours after infiltration with the avirulent strain of *P. syringae* pv. *tomato* (*Pst*1065) of leaves treated with 1% (v/v) methanol (control) or 100 μ M ABA.

Representative image from two independent experiments.



significantly greater ($p < 0.05$) (four fold) than the control (Figure 3.18a). Conjugated SA accumulated in the same leaves to concentrations that were significantly greater ($p < 0.05$) (three fold) 1 d after infiltration and seven fold greater 3 d after infiltration (Figure 3.18b). Free SA accumulated in 100 μ M ABA and 1% (v/v) methanol treated leaves to concentrations that were not significantly ($p > 0.05$) different 1 and 3 d after infiltration with the avirulent strain of *P. syringae* pv. *tomato* (Figure 3.18c). In contrast, conjugated SA accumulated in ABA treated leaves to a concentration that was significantly ($p < 0.05$) less than the controls, 3 d after infiltration with avirulent strain (Figure 3.18d).

3.3.5.7 Accumulation of *AtPR-1* mRNA transcripts in ABA treated leaves following infiltration with the avirulent strain of *P. syringae* pv. *tomato*

The abundance of *AtPR-1* transcripts within leaves 3 d after infiltration with the virulent or avirulent strain of *P. syringae* pv. *tomato* were at least 5% greater than control infiltrations (Figure 3.19a). The abundance of *AtPR-1* transcripts in control treated leaves 3 d after infiltration with the avirulent strain of *P. syringae* pv. *tomato* was 6% greater than ABA treated leaves (Figure 3.19b).

3.4 Discussion

In chapter 2, ABA was identified as a regulator of the outcome of the interactions of *Arabidopsis* with the Oomycete, *Peronospora parasitica* (Pers. ex Fr.) Fr.. In the present chapter, elevation of endogenous concentrations of ABA concentrations by exogenous addition of ABA or simulated drought stress treatment, compromised the normally resistant interactions with an avirulent strain of the bacterium, *P. syringae* pv. *tomato*. Raised ABA concentrations correlated with a reduction in the accumulation of defence components associated with the phenylpropanoid pathway and resulted in a susceptible phenotype (Table 3.1). In

Figure 3.18 SA accumulation in Arabidopsis leaves following syringe infiltration with *P. syringae* pv. *tomato*.

(a) and (b) SA concentrations in Ler (wt) leaves after infiltration with the virulent (*Pst*DC3000) or avirulent (*Pst*1065) strain of *P. syringae* pv. *tomato* or 10 mM MgCl₂ (control), (□)1 and (■) 3 d after infiltration.

(a) Free SA.

(b) Conjugated SA.

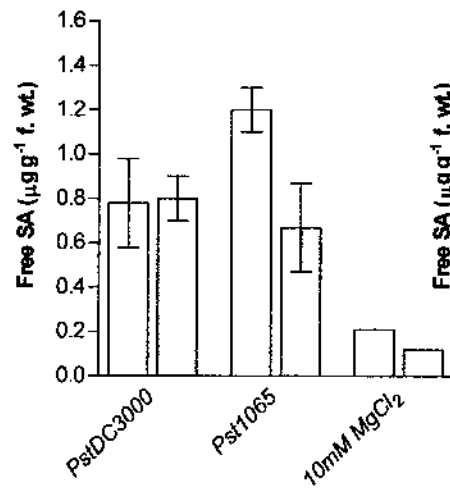
(c) to (d) SA concentrations of Ler (wt) leaves treated with 1% (v/v) methanol (control) or 100 μM ABA followed by infiltration with the avirulent strain of *P. syringae* pv. *tomato* (*Pst*1065), (□)1 and (■) 3 d after infiltration.

(c) Free SA.

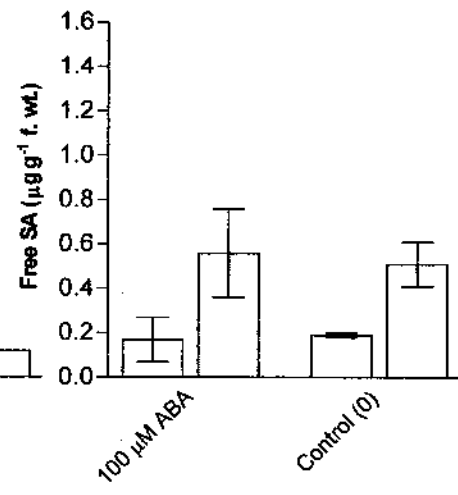
(d) Conjugated SA.

Each column represents the mean \pm s.e.m. from three independent experiments (except 1 d after infiltration concentrations that are from two independent experiments).

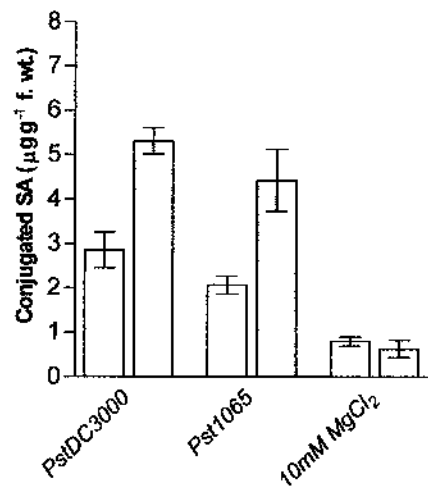
a



c



b



d

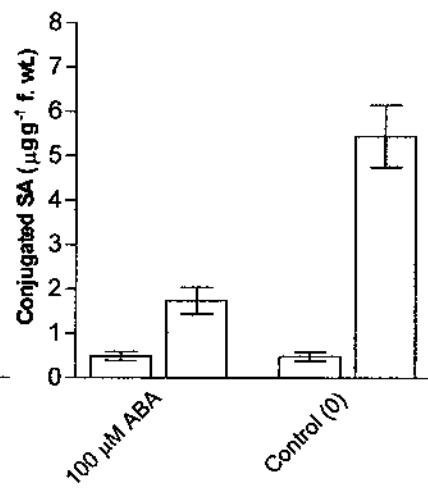


Figure 3.19 Abundance of *AtPR-1* mRNA transcripts in *Arabidopsis* leaves following syringe infiltration with *P. syringae* pv. *tomato*.

(a) and (b) Negative images of EtBr stained 1% (w/v) agarose gels containing the products from simultaneous *AtPR-1* (20 cycles) and 18S (26 cycles) RT-PCR reactions. Accompanied by a figure that shows the equalised, relative abundance of *AtPR-1* from each gel. Each RT-PCR was conducted on total RNA extracted from Ler (wt) leaves.

(a) Three days after infiltration with the virulent (*Pst*DC3000) and avirulent strain (*Pst*1065) of *P. syringae* pv. *tomato*.

(b) Three days after infiltration with the avirulent strain of *P. syringae* pv. *tomato* (*Pst*1065) of 1% (v/v) methanol (control) or 100 μ M ABA treated leaves.

Representative image from two independent experiments.

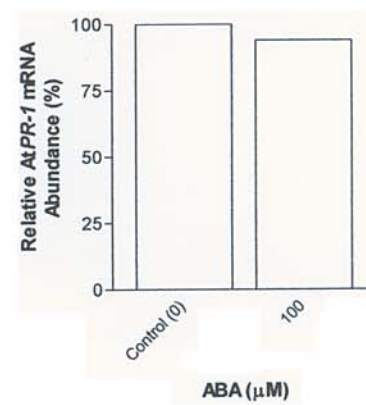
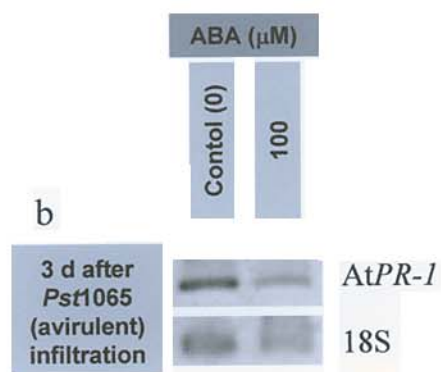
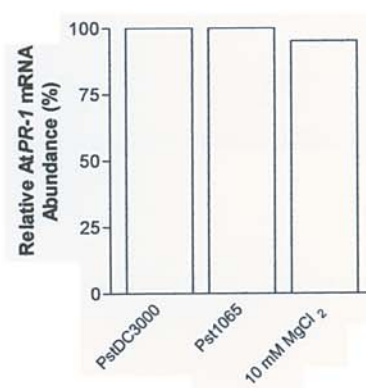
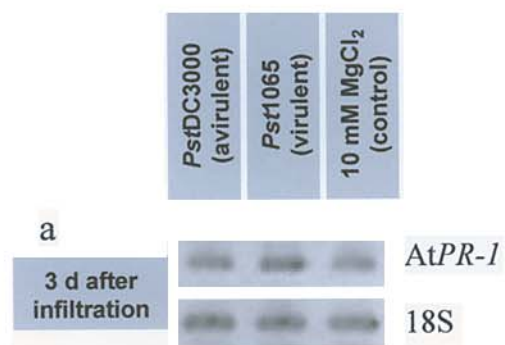


Table 3.1 The effect of ABA treatment on Arabidopsis defence components in leaves following syringe infiltration with the avirulent strain of *P. syringae* pv. *tomato*.

Arabidopsis ^a	Treatment ^b	<i>P. syringae</i> pv. <i>tomato</i> ^c	Interaction ^d	HR ^e	H ₂ O ₂ ^f	Lignin ^g	Callose ^h	AtPALI ⁱ	SA ^j	AtPR-I ^k
Ler (wt)	None	<i>Pst</i> DC3000 (virulent)	Susceptible	A	P	L - none	P	L	H	H
	1% (v/v) methanol (control)	<i>Pst</i> 1065 (avirulent)	Resistant	P	P	H - cluster	P	H	H	H
	100 µM ABA	<i>Pst</i> 1065 (avirulent)	Susceptible?	P	P	L - none	P	L	L	L

^a Arabidopsis ecotype. ^b Root uptake treatment solution for 20 h. ^c *P. syringae* pv. *tomato* strain. ^d Interaction phenotype (3 d after infiltration): Resistant; necrosis at the site of infiltration, low bacterial numbers. Susceptible; spreading necrosis and chlorosis, high bacterial numbers. Susceptible?; spreading chlorosis, high bacterial numbers. ^e Necrotic HR cells (12 h after infiltration) and ^f H₂O₂ production (4 h after infiltration): absent (A) or present (P). ^g Lignin accumulation (3 d after infiltration): TGA derivatives (A_{333nm} mg⁻¹ d. wt.) <55 low (L) or >55 (H) and PhI / HCl stained as in cell cluster or none at the site of infiltration. ^h Callose deposition (3 d after infiltration): present (P) throughout infiltrated regions. ⁱ AtPALI (6 h after infiltration), ^j SA (3 d after infiltration) and ^k AtPR-I (3 d after infiltration): low (L) or high (H). Red text denotes a change in a defence component induced by ABA treatment.

particular, high endogenous ABA concentrations reduced transcripts of the key entry point enzyme to the phenylpropanoid pathway, PAL1, the cell wall strengthening phenylpropanoid-derived compound, lignin, the defence related hormone, SA and transcripts of the SA-associated pathogenesis-related gene, *PR-1*.

Previously, soybean (*Glycine max* (L.) Merr.) leaves that were treated with ABA prior to inoculation with an avirulent race of the hemibiotrophic Oomycete *Phytophthora sojae* Kauf. and Gerd., caused a concentration-dependent increase in susceptibility (McDonald and Cahill, 1999). This effect of ABA also extends to the susceptible interactions of necrotrophic fungi, as shown for example by an increase in lesion spreading in the interactions of *Botrytis cinerea* Pers.:Fr with tomato (*Lycopersicon esculentum* Mill.) (Audenaert *et al.*, 2002). In the current study, the susceptibility of *Arabidopsis* leaves to an avirulent strain of the biotrophic bacterium *P. syringae* pv. *tomato* following treatment of plants with ABA, adds further support to the increasing body of data that show ABA is a key regulator. Importantly this has now been shown for several plant and pathogen combinations from a variety of kingdoms and pathogenic habits.

The rapid accumulation of *AtPAL1* transcripts and lignin in *Arabidopsis* leaves following infiltration with an avirulent strain of *P. syringae* pv. *tomato* have both been correlated with RPS2 mediated resistance (Davis *et al.*, 1991; Lee *et al.*, 2001). The necessity for PAL and lignin accumulation in the resistance of *Arabidopsis* to biotrophic pathogens was previously shown by specific inhibitor studies. AIP (2-aminoindan-2-phosphonic acid) inhibition of PAL activity and OH-PAS (*N* (*O*-hydroxyphenyl) sulfinamoyl-*tert*iobutyl acetate) inhibition of lignin biosynthesis caused a shift toward susceptibility, following inoculation with a virulent isolate of *P. parasitica* (Mauch-Mani and Slusarenko, 1996). In chapter 2,

the *Arabidopsis* ABA deficient mutant *aba1-1* [impaired in functional zeaxanthin epoxidase (Rock and Zeevaart, 1991)] had lower endogenous ABA concentrations than wild type plants but had increased accumulation of *AtPAL1* transcripts and lignin that correlated with a shift toward resistance, following infiltration with an virulent isolate of *P. parasitica*. In the present study, *AtPAL1* activity and lignin deposition were reduced in ABA treated leaves following infiltration with an avirulent strain of *P. syringae* pv. *tomato* and correlated with a shift toward susceptibility. These observations therefore show negative regulation by ABA of the phenylpropanoid pathway at the level of PAL transcription and subsequent suppression of lignin accumulation in *Arabidopsis* during interactions with biotrophic pathogens.

The accumulation of SA and *AtPR-1* transcripts (an indicator of SA-dependent defence) to similar concentrations in *Arabidopsis* leaves following infiltration with either a virulent or an avirulent (*AvrRpt2* expressing) strain of *P. syringae* pv. *tomato* as observed in the current study, has previously been documented (Cameron *et al.*, 1999). However, the necessity for accumulation of SA in RPS2 mediated resistance to *P. syringae* pv. *tomato* has been shown by the susceptibility that is induced in transgenic NahG plants (expressing the enzyme, salicylate hydroxylase that inactivates SA) following infiltration with an avirulent (*avrRpt2* expressing) strain of *P. syringae* pv. *tomato* (Rairdan and Delaney, 2002). In the current study, ABA treatment of *Arabidopsis* plants reduced the accumulation of SA and *AtPR-1* transcripts in leaves following infiltration with an avirulent strain of *P. syringae* pv. *tomato* and induced a shift towards susceptibility. The accumulation of SA in plants has been attributed to both phenylpropanoid pathway dependent (PAL) and independent (isochorismate synthase) biosynthesis

(Wildermuth *et al.*, 2001; Dixon *et al.*, 2002). The reduction in SA concentration and subsequent *AtPR-1* transcript accumulation found in the current study, therefore suggests negative regulation by ABA was via the phenylpropanoid pathway.

In chapter 2, *aba1-1* leaves were found to have lower endogenous concentrations of ABA than wild type plants accumulated H₂O₂ and the development a HR-like necrosis following inoculation with a virulent isolate of *P. parasitica*. However, in the current study elevated endogenous ABA concentrations in *Arabidopsis* leaves following root uptake of ABA did not alter the accumulation of H₂O₂ or the development of HR after infiltration with an avirulent strain of *P. syringae* pv. *tomato*. This was unexpected but is in accordance with a previously soybean study in which treatment with ABA prior to inoculation with an avirulent race of *P. sojae*, did not alter the development of a HR and pathogen spread was similar to a susceptible interaction (Mohr and Cahill, 2001). It has also been observed in NahG *Arabidopsis* plants that a HR developed following infiltration with an avirulent (*avrRpt2* expressing) strain of *P. syringae* pv. *tomato*, despite a deficiency in SA that compromised RPS2-mediated resistance (Gaffney *et al.*, 1993). Therefore the development of a HR in gene-for-gene mediated resistance is not suppressed by treatment with ABA and its development may be an important component of resistance but alone is insufficient to limit pathogen spread.

Imposition of simulated drought stress on *Arabidopsis* roots was an effective alternative for inducing increased endogenous ABA concentrations in leaves. Inoculation of these leaves with an avirulent strain of *P. syringae* pv. *tomato* induced susceptibility, confirmed by an increase in bacterial populations, in what is normally a resistant interaction. Increased susceptibility induced by drought stress had previously been shown in other plant / pathogen interactions, for example, in

Parthenocissus quinquefolia (L.) Planch. vines infected with *Xylella fastidiosa* Wells, the causal agent of leaf scorch (McElrone *et al.*, 2001) and in *Phaseolus vulgaris* (L.) infected with *Macrophomina phaseolina* (Tassi) Goid., the causal agent of charcoal rot (Mayek-Perez *et al.*, 2002). The results of the current study suggest that the susceptibility induced by drought stress may be due, in part, to an ABA effect.

Previously, norflurazon treatment of soybeans induced a reduction in endogenous ABA concentrations and decreased susceptibility to a virulent race of *P. sojae* (Mohr and Cahill, 2001). In the present study application of norflurazon and a structurally different phytoene desaturase inhibitor, fluridone (Bartels and Watson, 1978), did not reduce endogenous ABA concentrations or susceptibility to a virulent strain of *P. syringae* pv. *tomato*. As found in chapter 2, photobleaching of inflorescence stalks indicated that the plants had taken up the chemicals,. The inability of norflurazon and fluridone to reduce endogenous ABA in Arabidopsis plants compared with the reductions found in soybean, may be due to the higher basal concentrations of ABA in soybeans (Mohr and Cahill, 2001).

In chapter 2, ABA deficient mutants of Arabidopsis were more resistant to virulent isolates of *P. parasitica* than wild type plants. In the present study, ABA deficient mutants were as susceptible as wild type plants following vacuum infiltration with a virulent strain of *P. syringae* pv. *tomato*. Further investigation revealed that the humid conditions required to successfully grow the ABA deficient mutants without ABA supplementation had reduced the concentration of ABA in wild type plants to concentrations similar to ABA deficient mutants. In chapter 2, the concentration of ABA was significantly higher in wild type plants than ABA deficient mutants. The Arabidopsis plants in both studies were grown by similar

techniques, but in the present study the plants were at least 3 wk older at the time of infiltration. The variation in age of plants in both studies could account for the lack of variation in ABA concentration between wild type plants and ABA deficient mutants in the older plants of the current study and therefore explain the similar susceptibility to a virulent strain of *P. syringae* pv. *tomato*.

The Arabidopsis ABA insensitive mutant *abil-1* (impaired in a 2C class protein serine / threonine phosphatase) plants have a reduced responsiveness to ABA concentrations in vegetative tissues (Leung *et al.*, 1997). In the current study *abil-1* leaves were as resistant or susceptible following infiltration with avirulent or virulent strains of *P. syringae* pv. *tomato* respectively, as wild type plants. In chapter 2, Arabidopsis ABA insensitive mutants also had similar resistant or susceptible interactions as wild type plants following inoculation with avirulent or virulent isolates of *P. parasitica*. The ABA signal transduction pathway that involves ABI1-1 is therefore unlikely to be involved in the Arabidopsis resistance or susceptibility to biotrophic pathogens.

The present study was the first to detail a regulatory role for ABA in plant / bacterial pathogen interactions. In particular, two defence mechanisms negatively regulated by ABA were identified, 1) the phenylpropanoid pathway (especially lignin accumulation) and 2) SA-dependent defence. However, ABA may regulate other defence components not identified in the current study, that in conjunction with the two identified mechanisms, contribute to ABA induced plant susceptibility to an avirulent bacterial pathogen. An advantage of studying ABA regulation in Arabidopsis / pathogen interactions is the availability of commercial genome arrays. The microarrays will be utilised in chapter 4 to analysis global changes in gene expression and identify further ABA regulated defence mechanisms following

infiltration of ABA treated Arabidopsis with an avirulent strain of *P. syringae* pv. *tomato*.